UNITED STATES DEPARTMENT OF COMMERCE
DANIEL C. ROPER, Secretary
NATIONAL BUREAU OF STANDARDS
Lyman J. Briggs, Director

✦

Journal of Research

of the

National Bureau of Standards

✦

Volume 21, No. 3
September 1938

[Published with approval of the Director of the Budget]

UNITED STATES
GOVERNMENT PRINTING OFFICE
WASHINGTON : 1938

For sale by the Superintendent of Documents, Washington, D. C. - - - - - - Price 30 cents
$3.50 per year on subscription

The prices of the separate Research Papers appearing in this JOURNAL are given on the front cover page. If 100 or more copies of any separate are ordered, a discount of 25 percent is allowed. Those who desire copies of separate Research Papers should send their orders and remittances without delay to the Superintendent of Documents, U. S. Government Printing Office, Washington, D. C. This will aid him to determine the number of copies to be printed for sale. Research Papers are not printed from electrotypes, and usually no more reprints can be had when the first and only printing is exhausted.

U. S. Department of Commerce National Bureau of Standards

RESEARCH PAPER RP1129

Part of Journal of Research of the National Bureau of Standards, Volume 21, September 1938

OPTICAL AND DIMENSIONAL CHANGES WHICH ACCOMPANY THE FREEZING AND MELTING OF HEVEA RUBBER.

By W. Harold Smith and Charles Proffer Saylor

ABSTRACT

The opacity of "frozen" rubber results from crystallization of the rubber hydrocarbons. At temperatures between −15° and −35° C rubber is known to freeze in a few hours. The rubber of *Hevea brasiliensis* and its sol and gel fractions were frozen at about −25° C and maintained at that temperature for periods of 2 weeks to 3 months. Microtome sections were prepared and examined at controlled temperatures under a polarizing microscope.

When unstrained rubber was studied in this way, each section appeared to be composed entirely of irregular, strongly birefringent, crystalline particles, exhibiting no systematic orientation with respect to each other. The crystalline rubber usually melted between +5° and +16° C, a range which was similar to that observed previously with discrete crystals of rubber which had been prepared from solution. With the frozen specimens, however, the temperatures through which melting occurred were not the same in different pieces of frozen rubber, even when they had been prepared from the same material and frozen simultaneously. The crystals in adjacent microtome sections cut from any piece of frozen rubber melted alike, but crystals in sections from widely separated parts of the same piece sometimes exhibited real differences.

When rubber was frozen while strained, crystalline groups tended to be oriented with their high refractive indices parallel to axes of elongation. A curious consequence of this was observed in strips of rubber which were stretched and then frozen. As freezing progressed, the continuing orientation of rubber molecules caused the strips to elongate about 4 percent beyond the length previously attained by the stretching. The melting temperatures of strained, frozen rubber did not greatly differ from those of unstrained rubber, although they may have been slightly lower.

When rubber was frozen under pressure, the melting points of its crystals were higher than those determined without pressure, melting not being complete below 33° C. Vulcanized rubber did not crystallize at the temperatures used to produce crystals in unvulcanized rubber, but when a lightly vulcanized rubber was stretched before being subjected to low temperatures, notable amounts of freezing occurred.

CONTENTS

	Page
I. Introduction	258
II. Preparing, sectioning, and examining frozen rubber	259
III. Melting behavior of sections of frozen rubber	261
1. Unvulcanized specimens	261
2. Specimens partially vulcanized by Peachey process	263
IV. Melting behavior of thin films of frozen rubber	263
V. Effect of stress on the freezing of rubber	264
1. Compression	264
2. Extension	265
VI. Crystallinity of frozen and stretched rubber	267
VII. References	268

I. INTRODUCTION

At suitable low temperatures, unvulcanized rubber loses its elasticity and becomes hard and opaque. Similar changes frequently occur in baled rubber, which has been tightly compressed before shipment. It is said to be frozen or "boardy." The phenomenon has been studied by many investigators who have determined changes of volume [1] [1], softening temperatures [2], the effects of increasing time of storage at low temperatures [2], the influence of pressure during freezing [3, 4], and changes in heat capacity and entropy [5]. These effects have generally been ascribed to a form of crystallization, and X-ray diffraction powder patterns indicate that crystals are present in frozen rubber [6].

When total rubber is stretched, there are changes of volume and of heat content such as attend crystallization. With X-rays a crystal fiber pattern is obtained. It and the powder pattern obtained with frozen, compact rubber have been shown to indicate similar spacings and are assumed to be caused by the same type of crystal, [7] the differences being ascribed to conditions of orientation.

Dilute solutions of rubber hydrocarbon in ethyl ether yield small crystals of the hydrocarbon when they are subjected to temperatures between −35° and −60° C for several hours.[2] The optical properties and melting points of these crystals and their X-ray diffraction patterns [7] indicate their identity with the crystals in stretched and frozen rubber. Under the best conditions the crystals appear in spherulitic groupings, the individual needles in each spherulite having optical properties that closely approach those of a uniaxial crystal with negative elongation.[3] The crystals of sol rubber which we obtained,[4] melted between 9.5° and 11.0° C. Crystals of gel rubber [4] melted between −2° and 14° C, but the melting ranges within this interval were not the same for all samples. Numerous observations have repeatedly confirmed the data. About 90 percent of the rubber in solution may be obtained as birefringent material at −65° C. Temperatures between −40° and −50° C have been preferred, however, because better crystals are obtained in that range.

Thus crystalline rubber has been prepared in fundamentally different ways—by sustained low temperature, by stretching,[5] by compression, and by separation from solution at low temperatures. It

[1] Figures in brackets indicate the literature references at the end of this paper.

[2] The methods of purifying and of fractionating rubber hydrocarbon used in this work and of obtaining discrete crystals from solution have been discussed in this Journal, BS J. Research **10**, 479 (1933) RP544; **13**, 453 (1934) RP719.

[3] It is not improbable that the crystals are in fact biaxial, although, under the difficult conditions of observation, differences between β and γ, normal to the long axis of the needles, have not been detected.

[4] In the dark, in the absence of oxygen, rubber hydrocarbon can be separated into fractions which are soluble and insoluble in ethyl ether. Ether was used as a medium of separation in earlier work. A separation has been made with petroleum ether, chloroform, and with other solvents by different investigators. Whether the same molecular species exist in the two fractions when different solvents are used is not known. In accordance with common usage, the fractions separated with ether are here called sol and gel. The use of these terms does not imply that the sol does not form true solutions. The gel when dissolved may not have the same molecular structure as in latex or as in unmilled crude rubber. Presumably it is insoluble because it has a higher molecular weight than the sol, or a different structure. It is separated from the sol by its insolubility in the absence of light, and in the presence of natural antioxidants which normally protect crude Hevea rubber from oxidation. Light accelerates solvent action. When it is absent the gel remains undissolved for months. Of the structure of undissolved gel little is known. It may have weak cross-linkages connecting molecules which are similar to those in the sol. If that structure exists, the linkages are readily destroyed by light and air. It may possess strong cohesive forces, which are related to the existence of molecules of very long chains. By the breaking of the chains into smaller units these forces would decrease and the hydrocarbon become soluble.

[5] By the application of the term "crystalline" to stretched rubber, nothing is implied except that the atoms assume some form of orderly, spatial arrangement which produces optical effects and X-ray patterns which do not differ in general characteristics from those produced by ordinary types of crystals.

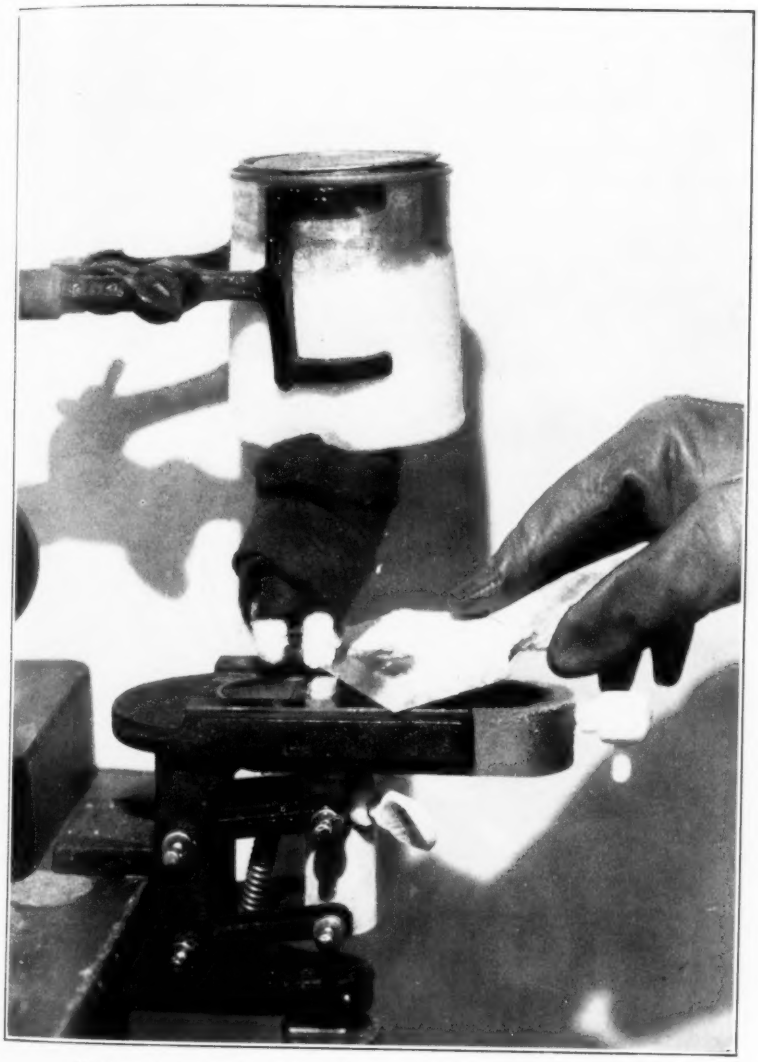

FIGURE 1.—*Apparatus for slicing frozen rubber hydrocarbon.*

The sample, held in the jaws of the microtome, is surrounded by cold acetone in which are chunks of solid carbon dioxide. From the tin can two streams of carbon dioxide vapor descend upon the surface of the sample and the slice after it is cut. The chisel-form knife is used on account of its rigidity.

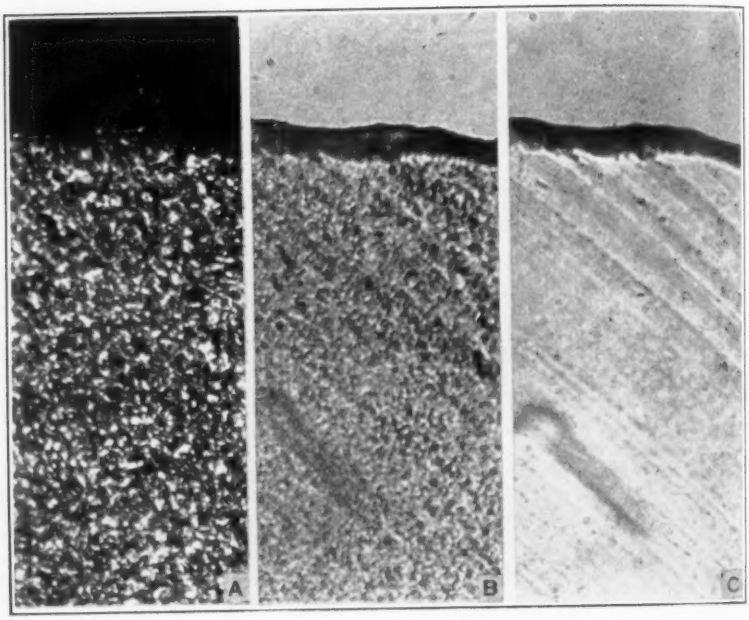

FIGURE 3.—*Photomicrographs of sliced total rubber hydrocarbon.*

A, view near the edge of a slice of frozen rubber. Temperature about 0° C. Crossed nicols. ×250. All brightness in the field is caused by the birefringence of crystal grains; *B*, same conditions except that polarizer has been removed. Random orientation of birefringent particles causes boundary effects by which crystal grains are seen superimposed upon faint streaks caused by the microtome blade; and *C*, sample at about 15° C. Polarizer removed. Crystals have melted and the grain boundaries between them have disappeared. Streaks caused by the microtome blade are relatively prominent. Between crossed nicols the entire field is black.

has not been clear whether, in each case, the crystals represented the same solid phase. Since we had previously used the polarizing microscope to determine the behavior of crystalline rubber grown from solution, we decided to extend the observations to frozen and stretched rubbers. By making microtome sections of frozen rubber, and its frozen sol and gel fractions, it was possible to determine some optical properties; and by observing the disappearance of birefrigence as temperatures rose, to determine melting points by a technic similar to that which had been used with crystals grown from solution.

II. PREPARING, SECTIONING, AND EXAMINING FROZEN RUBBER

The greater part of the work described in this communication was performed upon rubber hydrocarbon purified and separated into ether-soluble and ether-insoluble fractions by the methods previously described. The total purified but unseparated hydrocarbon, or its fractions, in the form of chunks 0.5 to 1 cm on a side, were subjected to a temperature of −25° C for periods of 2 weeks to 3 months. At that temperature oxidation is suppressed. At the end of such periods the pieces had acquired the hardness and turbidity that is associated with the frozen state.

To obtain sections, the chunks of rubber were held directly between the jaws of a Spencer table microtome and slices made with a chisel-form microtome blade. In the first experiments the sectioning was performed out-of-doors on days when the temperature was −10° C or lower. Such days were not common, however, and there was evidence that even these temperatures were not adequately low. In consequence, the accessories illustrated in figure 1 were adopted and operations transferred to the laboratory. The steel pin which normally supports the clamp was replaced by a pin of vulcanized fiber. The trough was cemented to the bottom of the clamp. It was filled with acetone and maintained at approximately −70° C by adding small pieces of solid carbon dioxide. The can, filled with solid carbon dioxide, had two outlet tubes through which the cold vapors of carbon dioxide emerged, one being directly above the specimen and the other above the position at which the knife stopped after the section had been cut. The microtome blade and all accessory apparatus, brushes, tweezers, etc., were kept surrounded by solid carbon dioxide until the moment when they were to be used.

When all was in readiness, the sample previously held in a Dewar flask with cold acetone was transferred to the clamp. There it was largely immersed in cold acetone and was directly under the stream of cold carbon dioxide. A dozen or more slices were made to prepare a suitable surface and then the critical sections were made—as thin as the behavior of the sample would permit—each section being washed with a brush into the acetone as soon as it was cut. The heat capacity of the knife was such that its temperature did not rise appreciably during the cutting. Occasionally when slicing was difficult, it was thought expedient to interrupt the proceedings and rechill the knife. These sections and the acetone in which they were immersed were then poured into another vessel in which the low temperature could more easily be maintained until needed.

For microscopic study, sections were selected that were as uniform and undistorted as possible. One of them would be grasped with a pair of tweezers and by a quick movement transferred to a vessel containing an aqueous solution of calcium chloride at about −20° C to remove acetone. From this it was transferred to a similar solution in another vessel, placed upon a microscope cover glass, and then covered with another cover glass. The two cover glasses were grasped by the edge with another pair of tweezers and transferred to the wire support of the cold stage illustrated in figure 2.[6] Here the sections were studied under the microscope.

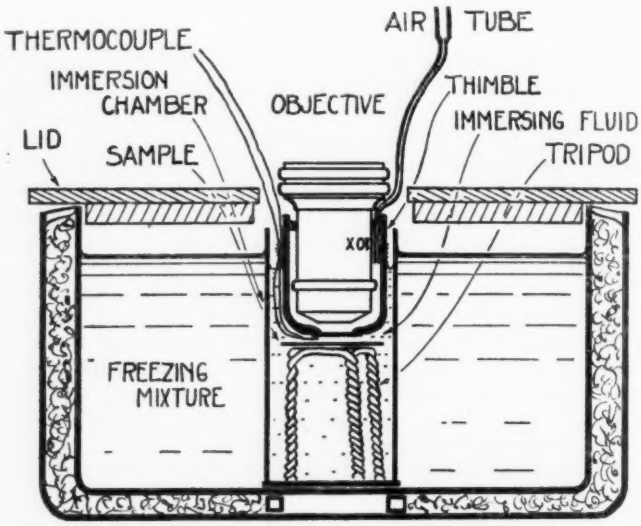

FIGURE 2.—*The simple cold stage.*

Two crystallizing dishes of slightly different sizes were chosen. Except for windows at the center of the bottom, the space between the dishes has been stuffed with rock-wool and the surfaces of the dishes silvered. The dishes are filled with a freezing mixture. Above the windows rests the immersion chamber made from a glass tube to the lower end of which is cemented a glass plate. This contains immersing fluid and a tripod of bent wire upon which the sample rests. The microscope objective dips into the immersing fluid, but is protected by a thimble made from a piece of constricted glass tubing, to the ground lower end of which is cemented a small cover glass. The thermocouple is held in place by being tied with thread to the thimble. The air tube of drawn copper tubing conducts a very slow stream of well-dried air into the space between the objective and the thimble and prevents the formation of frost. The entire apparatus rests upon the stage of a petrographic microscope.

In general, sections were easily cut. They could never be made as thin as desired because of a tendency to crumple, and a few specimens were so hard that successful cutting was difficult, but in most instances it was much like cutting across the end grain of a soft wood. It was vitally important, however, that the temperature be kept very low at all times. Otherwise, the outside of the sample would regain its rubberiness and sectioning become impossible. A warning was conveyed when the fresh slice adhered to the edge of the frozen block.

Sections made by the foregoing process were generally about 50μ thick. When viewed between crossed nicols they had a fine granular appearance, the individual granules being equidimensional and varying in diameter between approximately 5μ and 20μ. A photomicrograph is reproduced in figure 3 (A). It is plain, therefore, that despite

[6] This stage and its equipment have been described in J. Research NBS **13**, 453 (1934) RP719.

the effort to secure sections as thin as possible, their thickness still was several times the diameter of a particle. In consequence, complete extinction of any part was uncommon. Instead, the granules had high-order polarization colors, the order in each granule changing with the synchronous rotation of the crossed nicols, as the vibration direction of the first and last particles on any optical path became parallel to the axes of the nicols. Boundaries between adjacent granules were darkened by refraction effects. The entire preparation, by being a complex mixture of small granules of high-order colors and occasional granules in the position of extinction, all separated by dark borders, produced between crossed nicols a general effect of grayness.

When the analyzer was removed, strong refraction effects at the borders persisted, but the interference colors in each granule disappeared. The section still looked very granular, but no noteworthy changes occurred during rotation of the polarizer.

Thus, both under crossed nicols and with the analyzer removed, the slices had properties consistent with a section composed of many small crystals, strongly birefringent.

III. MELTING BEHAVIOR OF SECTIONS OF FROZEN RUBBER

1. UNVULCANIZED SPECIMENS

In general, at temperatures well below the melting point of their crystals, sections which had been prepared from unstrained compact rubber crystallized at sustained low temperatures, exhibited no other birefringence than the heterogeneous birefringence of numerous contiguous granules. At places, however, where the microtome knife had entered a pore in the rubber, then at the edges, or where the section had crumpled slightly, there was an oriented birefringence that had a definite relation to the direction of cutting. This birefringence was similar to that which was previously noted [7] with crystals of sol rubber grown from a solution. Such crystals yielded plastically and acquired a new and strong birefringence when they were deformed under the microscope.

In the present work, it was noted that this phenomenon could be greatly reduced if slicing was performed at very low temperatures. The earlier experiments in the sectioning of frozen rubber, undertaken on cold days, out-of-doors, showed the effect rather prominently. In the later work indoors at lower temperatures, well below the melting point of the crystals, the rubber did not yield plastically and there was no oriented birefringence. Defects in the cutting edge tended to cause flow and hence new anisotropy. Such effects, however, were not common and did not affect the granular crystallinity.

After the appearance of a slice had been well observed, residual pieces of ice were removed from the freezing mixture, and by passing an electric current through a coiled resistance wire immersed in the bath, the temperature was caused to rise slowly. It was always difficult to determine the precise temperature at which melting of the crystals commenced. Since, except for changes in birefringence, there was no evidence of the melting process until melting was nearly over, and since the birefringence itself had complex causes, it was necessary to observe minutely the first changes of the interference colors. Nevertheless, it is certain that in nearly all cases some melting occurred

[7] See footnote 2.

at temperatures slightly below the first changes that were noted. During melting, as long as the interference colors were those of superimposed birefracting granules and, therefore, composed of interference colors of high order, the changes were difficult to observe and analyze, but as melting neared its end, the polarization colors became much brighter, the transparency of the slice increased rapidly, and refraction effects at the interfaces between granules decreased. Finally, all birefringence related to the granules disappeared and genuine melting of the crystalline rubber was considered complete. Photomicrographs of a melting sequence are reproduced in figure 3. At this point some feeble birefringence that was related to the physical history of the sample persisted. The manner in which slices curled and wrinkled after the disappearance of granular birefringence indicated the persistence of strains. Distortions of the rubber, by the act of forming the original piece or of sectioning, showed as a general feeble birefringence. Often this did not disappear until well above the melting point (judged by loss of crystallinity) or until there was increasing mobility of the rubber, which is ordinarily so viscous that individual molecules are slow to change their relative positions.

In columns 2 and 3 of table 1 is presented a summary of the melting ranges of ether-soluble, ether-insoluble, and total rubber hydrocarbons as determined upon slices made from frozen compact samples.

The temperature ranges within which the frozen specimens melted are far from the same. The upper and lower limits vary, as well as the ranges of temperatures, and the data offer nothing which distinguishes total, sol, and gel rubber. Some specimens began to melt at 4.5° and others at 14°. In one specimen, melting was complete at 8.5° and in another at 15.6°. The temperatures do not agree precisely with those found for unstrained crystals of rubber as grown from ether solutions, principally in the particular that the ranges are greater and the reproducibility is less.

TABLE 1.—*Temperatures between which melting occurred*

Specimens sliced outdoors at about −10° C	Specimens sliced indoors at about −60° C	Specimens on cover glasses
SOL		
°C	°C	°C
+9.8 to +12.1 (44.5)*	+12.1 to +15.3 (40.7)	+12.1 to +15.0.
	+6.0 to +8.5	+14.0 to +15.6.
	+5.7 to +13.7	
GEL		
+5.7 to +15.3 (>20)	+10.6 to +15.8 (18.8)	+6.5 to +13.
+5.7 to +13.8 (>21.7)	−5.5 to +13.1	+5.7 to +15.3.
	+4.5 to +14.5	+14.0 to +15.1.
		+13.5 to +14.9.
		+11.1 to +12.2.
TOTAL		
+8.8 to +15.3 (37.3)	+11.6 to +14.4 (17.3)	
	+9.5 to +13.5	
	+4.5 to +10.5	

* Temperatures in parentheses are those at which birefringence of strain disappeared. The birefringences of strain and crystallinity originate in dissimilar causes and, in most cases, are easily differentiated under the microscope.

There were irregularities in the melting ranges of different specimens of frozen rubber, although they were prepared from the same material and were frozen simultaneously. Adjacent microtome sections, cut from any specimen of frozen rubber melted alike, but sections from widely separated parts sometimes exhibited real differences. In one experiment an oblong piece of purified total rubber was cut in two parts which were approximately of equal size, and cubical. The two parts were placed in separate bottles and frozen side by side. Samples were sliced from the sides which had been formed when the specimen was cut (*B* and *C* in table 2), and from the sides opposite to them (*A* and *D* in table 2). The data given in table 2 were obtained.

TABLE 2.—*Melting ranges of samples sliced from an oblong block*

Sample	First changes	Region of maximum change	Last persistence of granular birefringence
	°C	°C	°C
A	5.0	6.2 to 8.1	9.8
B	4.0	4.5 to 6.9	7.7
C	4.0	4.5 to 6.8	7.6
D	4.1	4.4 to 7.0	7.8
A (repeat)	5.3	5.7 to 8.1	9.0

2. SPECIMENS PARTIALLY VULCANIZED BY PEACHEY PROCESS

To compare the behavior at low temperatures of unvulcanized and vulcanized rubber, a specimen was surface-cured by the Peachey process. In this method active sulfur is produced at room temperature by the interaction of sulfur dioxide and hydrogen sulfide. The specimen was kept at −25° C for several weeks, sectioned, and a photomicrograph between crossed nicols was made. (See fig. 4.) The inner or unvulcanized rubber has crystallized; the outer layers of vulcanized rubber are unchanged except at the edges, which are birefringent, the effect, it was at first supposed, of free sulfur. The edges however, lost their birefringence at temperatures slightly lower than those at which this occurred in the middle of the specimen. The surface therefore, consisted of unvulcanized rubber and not free sulfur. During the vulcanization process, sulfur dioxide probably diffused from the surface before hydrogen sulfide was applied.

IV. MELTING BEHAVIOR OF THIN FILMS OF FROZEN RUBBER

As an alternative method of observing the optical properties that appear with the freezing of rubber hydrocarbon, solutions of the forms of the hydrocarbon in ethyl ether (see footnote 4) were allowed to evaporate upon circular microscope cover glasses. By this means, very thin films were produced. As with the bulk samples, freezing was brought about at a temperature of about −25° C during 2 weeks, after which the originally transparent films were noticeably murky. They were immersed in a solution of aqueous calcium chloride at about −25° C, transferred to the cold-stage apparatus and examined between crossed nicols. The general appearance of these samples is represented by the finely grained portions of figure 5 and was very similar to that of most of the frozen and sliced samples.

When samples frozen from films deposited upon cover glasses were allowed to melt, their behavior was the same as that of sliced rubber, except that there were no birefringences caused by strain that persisted above the temperature of true melting. The melting points of these samples are given in column 4 of table 1. They do not differ significantly from those determined from sections of the bulk specimens.

In several samples of sol rubber prepared as films upon cover glasses, there were groups of striking spherulitic clusters. A photomicrograph is reproduced in figure 5. Since it was thought that this might indicate a partial recrystallization of the fine-grained portions, the sample was kept for 2 months at −25° C and examined, and then for 1 month at 0° C, with the hope that recrystallization would be accelerated. Another photomicrograph was made at the end of the 3 months. Since no differences could be observed in prints made before and after that period, it was evident that no growth had occurred. When the sample was allowed to melt, the rubber film was found to be much thinner at the region of the spherulites. The departure from a uniformly granular appearance, therefore, was caused by fewer nuclei which had formed per unit of area, and because the extent of each crystal in the plane of the film had been correspondingly larger.

The similar properties of frozen rubber in slices and of frozen thin films deposited from solution on cover glasses established the following points: No important changes in the material were caused by slicing. Solution of total, sol, and gel rubber hydrocarbon had not modified the manner of their freezing or the characteristics of the frozen material.

V. EFFECT OF STRESS ON THE FREEZING OF RUBBER

1. COMPRESSION

There is a form of boardy rubber which is observed at times in bales of crude rubber that have been tightly compressed before shipment. This is of interest because it usually persists in the frozen state at ordinary room temperatures or slightly above them, and in this respect is similar to rubber which was frozen for 8 years by van Rossem, and which melted at 37° to 38° C. No crystalline rubber with such melting characteristics has been observed in this laboratory, but the following experiment was performed with the object of producing it. A specimen of gel rubber was used, since in earlier work it had been shown that gel rubber is more resistant to an impressed force than sol. It was placed between two aluminum plates, about 6 mm thick, which were forced together as closely as possible by wing bolts, and immediately subjected to a temperature of −25° C. After 6 months, the specimen was sliced parallel to the axis of compression and examined. The slice had a marked directional birefringence with much extinction when the nicols were parallel and perpendicular to the compression axis. The direction of the highest index of refraction was normal to the direction of compression. Superimposed upon this directed birefringence there was a granular birefringence that tended to be parallel to it. By compression, the rubber molecules were oriented to positions which were approximately maintained during crystallization.

Both forms of birefringence disappeared in the temperature range 10.6° to 11.1° C. A birefringence, which, from its position, was no doubt related to the stresses of cutting, slowly disappeared with rising temperature but persisted up to 57.5° C.

FIGURE 4.—*Strip of total rubber, vulcanized, frozen and sliced.*

Crossed nicols. ×25.

A strip of rubber was vulcanized by the Peachey process, and then frozen. In the center where the vulcanizing gases failed to penetrate, the rubber has crystallized in the usual way. In two zones on each side of the center zone, where vulcanization was most complete, there has been no crystallization. In thin films along the surface from which it is supposed that the sulfur dioxide diffused before application of hydrogen sulfide, vulcanization has not been sufficiently complete to prevent freezing.

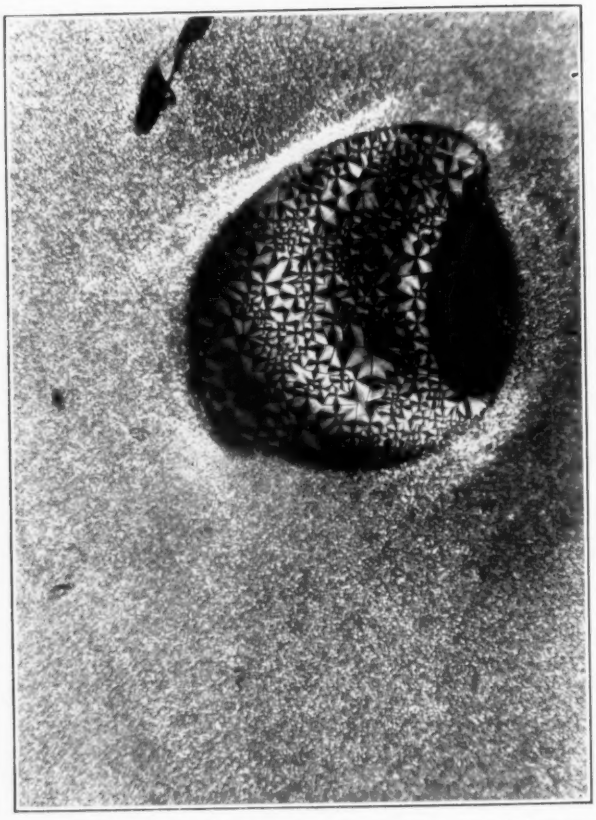

FIGURE 5.—*Sol rubber deposited on cover glass and frozen.*

Crossed nicols. ×75.

Fine grained portions represents the usual appearance of such samples. The marked spherulitic tendency has occurred in a region where the film of rubber was thinner so that fewer crystal nuclei formed per unit of area.

Another slice was cut from the frozen material, at a direction 90 degrees from that at which the first slice was made. In this slice, also, the direction of highest index of refraction was normal to the direction of compression. There was no evidence in either slice of granular, crystalline rubber which persisted above room temperature.

Between aluminum plates the effects were more largely those of distortion than compression. To restrict conditions so that the effects would be primarily those of compression, the following experiment was conducted. A sample of total rubber about 1 cm^3 in volume was placed in a hole 1 cm square in a steel block. Steel pistons which closely fitted the cavity were placed above and below the specimen, and the whole was compressed to about 1,000 atmospheres between the jaws of a 6-inch screw clamp. After remaining at −25° C for 2 weeks the specimen was examined. A cubical block of rubber had been formed. It was very hard and exceedingly difficult to slice. Incipient melting was observed at 6.9° C, but the birefringence of the crystalline rubber had not all disappeared until 33° to 34° C. was reached. It was difficult to determine the temperature more exactly as there was sufficient birefringence of strain to obscure that of the granules. This birefringence persisted to 41.3° C. The result is in accord with observations by others [2] of the melting of crude rubber frozen for several years without compression or for several weeks under it.

2. EXTENSION

All available evidence indicates that the molecules of rubber are very long. In the course of some observations which were made to test the orientation of birefringent colors by directed strain, a curious effect was observed that probably had its origin in this excessive magnitude of one dimension [8]. For this work strips of crude rubber about 5 mm wide and 2 mm thick were used. They were stretched different amounts and nailed to a board. The elongations varied between 20 percent and the point at which rubber greatly resists further extension. The stretched samples were placed in a cabinet at −25° C. During a few hours, they increased in length about 4 percent, with the exception of specimens stretched to the point at which further extension was greatly resisted. With them the secondary extension was feeble. The strips rose to form an arc between the points of attachment. The secondary extension was observed with smoked sheet, pale crepe, milled pale crepe, and with smoked sheet that had been swelled slightly by benzene, to remove strains or orientation caused by processing and from which the benzene was subsequently evaporated. The elongation does not occur with unstretched rubber. Stretched vulcanized rubber bands increased in length slightly when kept for several days at −25° C. This is interpreted as an instance in which stretching has fostered the freezing even of a vulcanized rubber. Samples of the product from the reaction between dichloroethyl ether and sodium polysulfide, a Thiokol, also exhibited a secondary extension after 2 weeks at −25° C, whether tested in the unvulcanized or the vulcanized condition.

The piece of smoked sheet that had been swelled with benzene, and from which the benzene had evaporated before the stretching and freezing experiment, was allowed to remain at −25° C for 2 weeks. It was then sliced, and the sections observed microscopically. They were smooth and very strongly birefringent, the direction of highest

index being parallel to the axis of elongation. The multitude of birefringent granules usually observed with the sections of frozen rubber was not present. When the temperature was allowed to rise, slight changes in the degree of double refractions were first observed at −2° C. At +3° C melting (judged by changes in birefringence) was proceeding rapidly, and at +6° C, after a marked deformation caused by the retraction of the stretched piece, it was complete.

The secondary elongation of stretched rubber may occur at approximately 0° C and does not require freezing temperatures as low as −25° C. It always disappears, however, on warming to about 10° C and the rubber resumes its previously stretched condition. This indicates that the elongation is associated with crystallization. The following explanation is suggested.

When stretched or compressed, rubber is forced to flow, its molecules are oriented parallel to the direction of elongation, and when freezing begins a crystal axis is already established. As crystallization proceeds, molecules enter the spacing, the rubber hardens, and presently when a tendency to elongate is asserted, the stresses that produced stretching are neutralized. Then, as more molecules move into the crystalline arrangement, the spacings at right angles to the stretch become less, the long directions of the molecules become more strictly parallel to the axis of stretch, and the strip elongates. Stretched rubber contracts when heated, the well-known Gough-Joule effect. The density of rubber which is chilled while stretched is higher than that of rubber which is chilled without stretching [9, 10] and since the chilling of the stretched rubber is accompanied by an elongation, it is necessarily accompanied by a lateral contraction and a decrease of volume.

When rubber is stretched or compressed there appears to be a movement of whole, or parts of, molecules by compulsion. When a strain orients the molecules so that they are approximately parallel to each other, the movement permits an adjustment of positions so that the rigid spacings necessary for an X-ray diffraction fiber pattern are possible. When stretched, the highest refractive index and, when compressed, the lowest index is parallel to the direction of the applied force. An increased index is an indication either of changed spacing or of the orientation of molecules so that their long directions are parallel to the increased index. In the case of rubber, it is evident that the latter phenomenon predominates.

The conditions of melting of stressed and frozen rubber are briefly summarized in table 3.

TABLE 3.—*Temperature of melting of specimens frozen under stress*

Kind of rubber	Mode of applying stress	Conditions of freezing	Temperature of melting
			°C
Gel	Compressed between aluminum plates	6 months at −25° C	10.6 to 11.1.
Total	1,000 atm applied with piston	2 weeks at −25° C	6.9 to 33 or 34.
Crude	Stretched 20 percent (secondary increase in length occurred).	2 weeks at −25° C	3 to 6.[a]

[a] Some indications of incipient melting appeared as low as −2° C.

VI. CRYSTALLINITY OF FROZEN AND STRETCHED RUBBER

The granular birefringence of a frozen specimen makes it appear that crystallization has gone far toward completion, but determinations of the density of frozen rubber, as reported in the literature, indicate that rubber when frozen for comparatively short periods of several weeks may be incompletely crystallized. This fact may be related to the varying melting points of frozen specimens prepared under similar conditions. The density of amorphous rubber is approximately 0.92, whereas that of frozen, unstretched rubber has been reported by several investigators as about 0.95. When stretched and frozen, that is, under conditions which are more favorable to the growth of crystals than when rubber is frozen unstretched, the density increases, and the highest value reported for rubber so treated 0.965, was obtained by Kirchhof [9] and was duplicated by Lotmar and Meyer [10]. These authors have calculated from X-ray data that the density of completely crystallized rubber should be 1.02, if there are eight isoprene groups in the monoclinic unit cell. Assuming that 1.02 represents the density of rubber which is completely crystallized, the approximate amount crystallized in frozen rubber would be 30 percent and in stretched frozen rubber 45 percent.

When a block of rubber crystallizes the medium in which crystallization occurs is, of course, the rubber itself. The ease with which crystallization is initiated is surprising, in view of the low fluidity of this medium. It is probably quickly retarded because chilling must lower appreciably the mobility of molecules, which are admitted to be large. Then too, the mobility necessary for the intimate alignment of molecules in a crystal lattice must be quickly diminished as parts of very long molecules enter into crystalline structures and ultimately impede all further movement. For these reasons, it was hoped that crystallization from a solution of ethyl ether, a medium more mobile than rubber, would induce the maximum number of molecular species to become crystalline. This has not been the case, since when this method is used there is no evidence of crystals which exist unchanged at 25° C or higher. (See footnote 2.) Our present knowledge of the crystallinity of rubber appears to be far from complete, and deductions drawn from it, therefore, seem subject to reserve.

No doubt exists about the crystallinity of many complex organic compounds, albumin and some vitamins, for example, but there is a curious reluctance by many scientific authors to concede the crystallinity of rubber. The word crystal is frequently used in quotation marks when rubber is discussed, or it is indicated that its use is justified because others have employed it. However, rubber assumes a crystalline state with great facility. This is accomplished merely by stretching it, and its crystallinity is confirmed by the X-ray diffraction patterns of stretched and frozen rubber, which indicate the same structure in each. Studies by Thiessen and Wittstadt [11] indicate that crystallization during stretching is influenced by pressure, and that it may be reconciled with the normal process of crystallization which is accompanied by the formation and growth of nuclei.

The superficial characteristic of a crystal, that which attracts the eye, is external symmetry, the regularity and planarity of the bounding surfaces. This external symmetry is only an indication, however,

of a more fundamental symmetry according to which its atoms and molecules are arranged. Crystallinity is defined most rationally in terms of those properties which bring about the symmetry of surfaces. A certain minimum number of atoms or molecules grouped together in a definite pattern is a unit cell. It is the smallest part of a crystal that can contain all spacings and orientations that characterize the crystal, as a whole. In an ideal or perfect crystal every part would consist of elements like the unit cell, all strictly parallel to each other and displaced with respect to each other by distances that are precise multiples of the length of a side. From this there results an anisotropy of physical properties. The orderly arrangement causes the diffracted energy of X-rays to follow, by interference, definite paths. With these criteria, crystallized rubber is in complete accord. It has been repeatedly demonstrated that rubber when crystalline produces a characteristic diffraction pattern, which cannot be caused by liquid crystals, as these do not form X-ray crystal patterns.

Usually the unit cell of a crystal contains several molecules. In some substances there are repeated atomic groupings within the molecule. Since these groupings may respond to X-rays as though they were molecules which compose a unit cell, it may happen that the unit cell is much smaller than a single molecule. In rubber the molecule varies in size, but is long and by some evidence, usually over 500 times as large as the unit cell. Consequently, a rubber molecule may possibly be crystalline in one part and amorphous in another. Perhaps it may simultaneously belong to several different crystalline particles and several groups of amorphous matter. Certainly the crystallinity of rubber is of an unusual type and differs profoundly from that of a substance like sodium chloride. But each yields a characteristic X-ray diffraction pattern.

VII. REFERENCES

[1] N. Bekkedahl, J. Research NBS **13,** 411 (1934) RP717.
[2] A. van Rossem and J. Lotichius, Kautschuk. **5,** 2 (1929).
[3] M. Krōger, Gummi-Ztg. **40,** 782 (1926).
[4] C. M. Carson, Ind. Eng. Chem. **23,** 691 (1931).
[5] N. Bekkedahl, J. Research NBS **15,** 503 (1935) RP844.
[6] E. A. Hauser and P. Rosbaud, Kautschuk. **3,** 17 (1927).
[7] G. L. Clark, E. Wolthuis, and W. Harold Smith, J. Research NBS **19,** 479 (1937) RP1039.
[8] W. Harold Smith and Charles Proffer Saylor, Science **85,** 204 (1937).
[9] F. Kirchhof, Kautschuk. **2,** 155 (1926).
[10] W. Lotmar and K. H. Meyer, Monatsh. **69,** 115 (1936).
[11] P. A. Thiessen and W. Wittstadt, Z. physik. Chem. **29** [B], No. 8, 359 (1935).

WASHINGTON, May 13, 1938.

U. S. DEPARTMENT OF COMMERCE NATIONAL BUREAU OF STANDARDS

RESEARCH PAPER RP1130

Part of Journal of Research of the National Bureau of Standards, Volume 21, September 1938

STRENGTH OF A RIVETED STEEL RIGID FRAME HAVING STRAIGHT FLANGES

By Ambrose H. Stang, Martin Greenspan, and William R. Osgood

ABSTRACT

The distribution of stress in and near the knee of a riveted steel rigid-frame specimen having straight flanges was investigated both experimentally and theoretically for various conditions of loading. The theory developed for the distribution of stress in the knee gave stresses which agreed within the experimental error with those obtained experimentally. Reinforcing the outer corner was shown to have little effect on the stress distribution in the frame. The maximum load that could be sustained by the specimen was determined.

CONTENTS

	Page
I. Introduction	269
II. Rigid-frame specimen	270
1. Description of the specimen	270
2. Tensile properties of the material	270
III. Testing procedure	272
IV. Measured stresses	272
V. Theory for web of knee	294
VI. Theoretical stresses	295
VII. Greatest stresses	308
1. The legs	308
2. The knee web	308
(a) Greatest normal stress	308
(b) Greatest shearing stress	309
VIII. Maximum load	310
IX. Conclusions	310
X. Appendix—Stresses from strain data	311
XI. References	312

I. INTRODUCTION

A rigid frame is a portion of a structure in which ends of component members are connected in such a way as to prevent relative rotation of the ends at the connection. Steel rigid frames are usually built up from plates and angles, like a plate girder.

Rigid frames are being increasingly used in the construction of bridges, warehouses, auditoriums, etc. [1] [1] The fundamental reason for the increasing use of rigid frames is their economy. General sturdiness and ease of maintenance are other advantages. An example of recent rigid-frame construction is shown in figure 1.

A rigid frame is analyzed much like an arch, either two-hinged or fixed, depending upon the conditions at the foundations [2, 3]. How-

[1] Figures in brackets indicate the references at the end of this paper.

ever, ordinary methods of design do not apply to a knee, or junction of two members, because of the abrupt change in direction of the members at this point. The stresses in rigid frames have been estimated by photoelastic methods [4, 5, 6]. The strains in reinforced-concrete frames have been determined by the use of strain gages [6]. However, no numerical values for the stresses in a steel rigid frame were found in the literature.

The American Institute of Steel Construction, through its chief engineer, F. H. Frankland, approached the National Bureau of Standards with a program of research on the stress distribution in steel rigid frames. The work was authorized in April and begun in July 1935. The Institute arranged to secure three frames and cooperated by maintaining a research associate at the Bureau and by publishing 10 progress reports during the course of the investigation.

This paper gives the results of the tests on a steel rigid-frame specimen donated by the Bethlehem Steel Co. Tests on other steel frames will be reported in later papers. The distribution of stress in the specimen was determined both experimentally and theoretically. The experimental work consisted in loading the specimen and measuring the strains on a sufficiently large number of gage lines to determine the state of strain, from which the state of stress could be determined by standard methods. The theoretical work was undertaken at the suggestion of H. D. Hussey of the American Bridge Co., who cooperated effectively and made an extensive independent study of this important problem. Many valuable suggestions were received from F. H. Frankland, chief engineer of the Institute, and from the Institute's Committee on Technical Research, consisting of Jonathan Jones, chairman, H. G. Balcom, O. E. Hovey, H. D. Hussey, J. R. Lambert, Aubrey Weymouth, and F. H. Frankland (ex officio).

II. RIGID-FRAME SPECIMEN

1. DESCRIPTION OF THE SPECIMEN

The rigid-frame specimen is shown in figure 2. It was fabricated from steel plates and angles joined by riveting. The weight as determined by the Bethlehem Steel Co. was 3,610 lb. The lower leg and the knee were fabricated as a unit. The upper leg was spliced to the knee at the inner flange angles of the lower leg. It was intended that the inner flange angles of the upper leg abut on those of the lower leg at the inner corner of the knee, but actually there was some lack of bearing (leaving a maximum clearance of $\frac{1}{32}$ in.). There was also some lack of bearing at the inner corner of the knee between the ends of the lower-leg stiffener angles and the outstanding legs of the inner flange angles of the lower leg. The outer corner of the knee was built so that it could be reinforced by a gusset on each side secured by turned bolts in reamed holes.

The rigid-frame specimen is shown in the testing machine in figure 3.

2. TENSILE PROPERTIES OF THE MATERIAL

Samples were taken from the flange angles and web plates before fabrication, and marked *AR*, *AL*, *C*, etc., for identification, as shown in figure 2. The tensile properties of the material were determined from coupons machined from these samples. The coupons were ASTM 8-in.-gage-length tensile specimens for plates, shapes, and

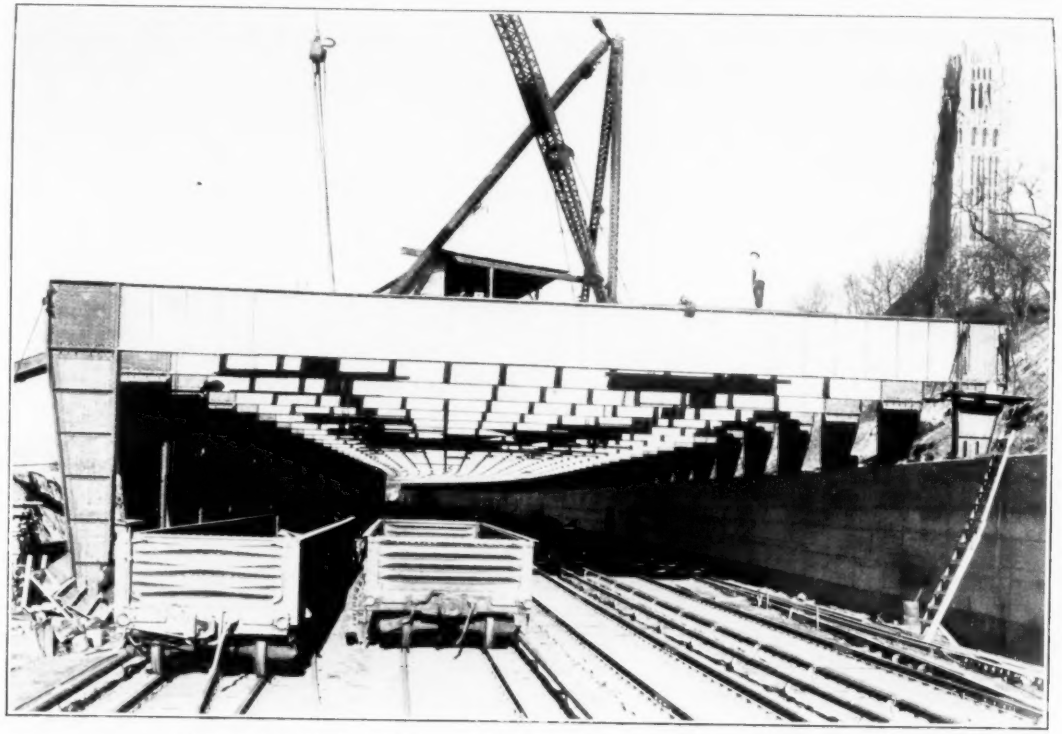

FIGURE 1.—*Steel rigid frames, West Side Improvement, New York City.*

Approximately 12,000 tons of structural steel, comprising 397 frames, were involved in this development.

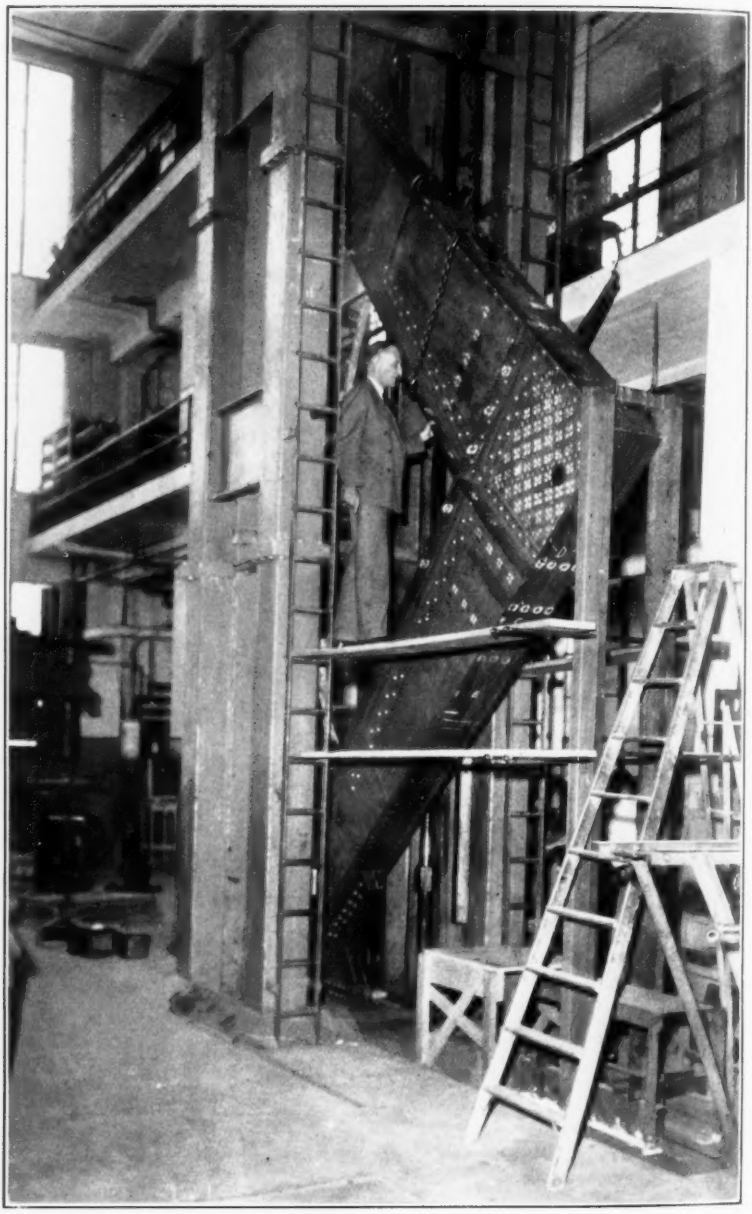

FIGURE 3.—*Rigid-frame specimen in the testing machine.*

flats [7]. The width of the coupons at the reduced section was 1.5 in., and the thickness was that of the material as rolled.

The coupons were tested in a screw-driven, beam-and-poise testing machine having a capacity of 100 kips [2]. The speed of the movable platen of the testing machine was 0.008 in./min until the extensometer was removed from the coupon. Thereafter the speed of the movable platen was 0.4 in./min.

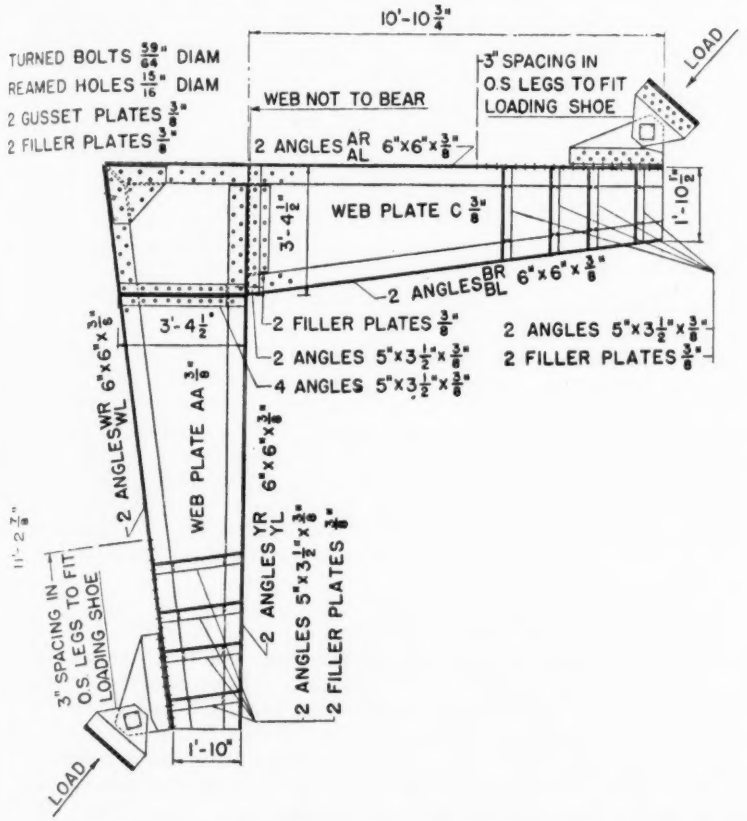

FIGURE 2.—*Dimensions of the rigid-frame specimen and location of the coupons.*

The strains were determined by means of a Ewing extensometer of 8-in. gage length. One division on the scale of this instrument corresponds to a strain of 0.000025. Readings were estimated to 0.1 division.

The yield point was determined by the drop-of-beam method. Young's modulus of elasticity and the proportional limit were determined from difference curves [8].

The tensile properties of the material are given in table 1.

[2] 1 kip=1,000 lb.

TABLE 1.—*Tensile properties of the material*

Coupon No.	Coupon from—		Thickness	Young's modulus of elasticity	Proportional limit	Yield point	Tensile strength	Elongation in 8 in.	Reduction of area	
	Angle	Plate								
			in.	*kips/in.²*	*kips/in.²*	*kips/in.²*	*kips/in.²*	%	%	
1	*AR*		0.380	28,300	23	38.3	60.8	29.0		60
2	*AL*		.384	29,100	22	36.7	56.6	28.7		60
3	*BR*		.387	28,000	26	38.9	62.6	27.9		56
4	*BL*		.386	29,900	21	37.4	57.0	28.5		61
5	*WR*		.372	28,500	15	37.0	58.1	27.7		55
6	*WR*		.379	29,600	18	35.9	57.6	26.2		63
7	*WL*		.371	28,300	15	37.4	58.2	26.0		57
8	*WL*		.376	28,000	19	36.6	58.0	25.3		57
9	*YR, YL*[*]		.371	29,200	15	38.4	61.6	28.4		57
10	*YR, YL*[*]		.377	27,900	19	37.2	60.9	26.6		60
11		*AA*	.373	29,000	10	34.9	58.5	24.0		59
12		*AA*	.376	27,400	21	37.6	64.8	31.0		55
13		*C*	.376	28,300	10	33.2	55.0	30.2		63
14		*C*	.372	28,400	16	40.3	70.1	26.3		49
	Average			28,600						

[*] Angles *YR* and *YL* were from the same piece.

III. TESTING PROCEDURE

The rigid-frame specimen was loaded in a vertical, screw-driven, beam-and-poise testing machine having a capacity of 600 kips. The load was applied through two pin-connected shoes, shown in figure 2, one attached to each leg of the frame. Different load lines could be obtained by bolting the shoes to the legs in different positions. Five different tests were made with the load acting along the lines indicated in figure 4. In test 1 the gussets, one of which is shown in figures 2, 4, and 5, were bolted to the outer corner of the knee. In tests 2, 3, 4, and 5 the gussets were removed, and the bolts through the angles replaced.

Strain-gage readings were taken at "rosettes", as shown in figure 4, with Whittemore strain gages having gage lengths of 2 in. One division on the dial of the strain gage corresponds to a strain of 0.00005. Readings were estimated to 0.1 division. Each rosette consisted of four gage lines intersecting at a point and inclined at 45° to one another. Each rosette shown on the webs in figure 4 represents two rosettes, one on either side of the specimen; and each rosette shown on the angles represents six rosettes, two on the outside and one on the inside of the outstanding leg of each angle.

The specimen is shown in the testing machine for test 1 in figure 3. Strain-gage readings were taken at compressive loads of 5 kips and 80 kips. In test 1 all the strain-gage readings at the load of 5 kips were taken before the specimen was subjected to a higher compressive load. The results of test 1 indicated, however, that preloading of the specimen was desirable, and in the subsequent tests a compressive load of 82 kips was applied and released five times before strain-gage readings were taken.

IV. MEASURED STRESSES

Stresses computed from the strain-gage readings will be called measured stresses. These stresses were computed from the strains due to the 75-kip increase in load by the methods outlined in the

FIGURE 5.—*Test 1. Knee of the rigid-frame specimen.*

UNIV OF MICH.

Appendix (case 1).[3] The strains in corresponding gage lines on opposite sides of the webs of the specimen were averaged and the average values used in the computations. In the case of the outstanding legs of the flange angles the strains in corresponding gage lines of the six rosettes were averaged and the average values used in the computations. The magnitudes and directions of the principal stresses and of the maximum shearing stress at each rosette were computed.

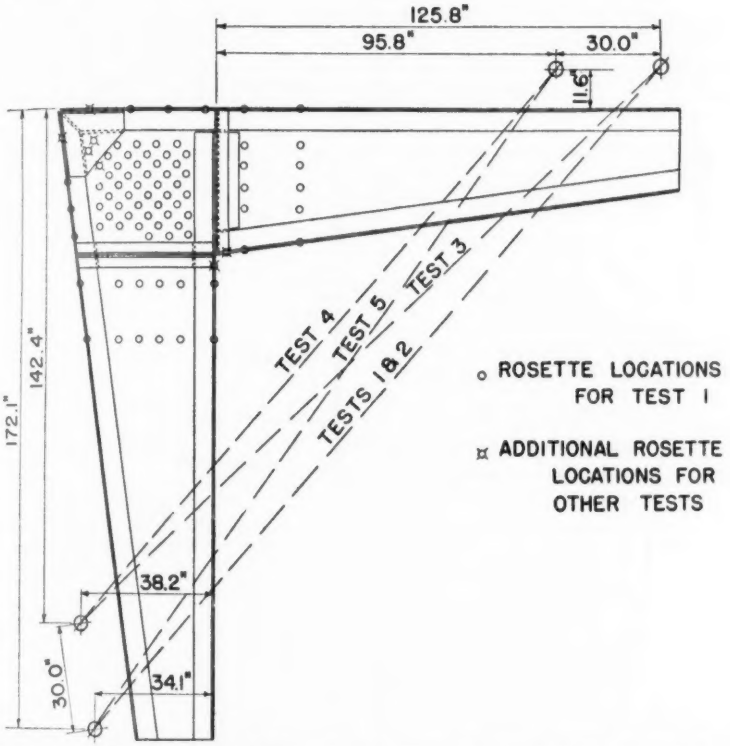

FIGURE 4.—*Load lines and location of the rosettes for strain-gage readings.*

The results of these computations are shown for test 1 in figures 6 to 9, inclusive. Figure 6 is a contour chart of maximum principal stress. Each contour line is a locus of points of equal maximum principal stress in the plane of stress. The contour lines show only the magnitudes of the stress. The directions of the contour lines are not the directions of the maximum principal stresses. The contour lines do not give the values of the stresses in the stiffeners. Similar contour charts of minimum principal stress and of maximum shearing stress are shown in figures 7 and 8, respectively, except that the contour lines of maximum shearing stress in figure 8 were drawn for the three-dimensional state of stress. At any point at which the

[3] The greatest deviation of any value of the modulus of elasticity from the average value was about 4.5 percent (table 1). The average value was used for computing the stresses, because it was estimated that the error in the strain-gage readings was greater than 4.5 percent.

principal stresses in the plane of stress are of the same sign, the maximum shearing stress occurs in planes at 45° to the plane of stress and is equal to one-half the numerically larger of these principal stresses. The magnitudes and directions of the principal stresses in the plane of stress are shown in figure 9.

The results of tests 2, 3, 4, and 5, are shown in the same way in figures 10 to 25, inclusive.

Comparison of the results of test 1, figures 6, 7, 8, and 9, with those of test 2, figures 10, 11, 12, and 13, shows that the gussets at the outer corner had little effect on the stress distribution. The stresses at the outer corner were very small. The measured stresses for test 2 are in general somewhat less than those for test 1. As has been pointed out, the strain-gage readings at the load of 5 kips for test 1

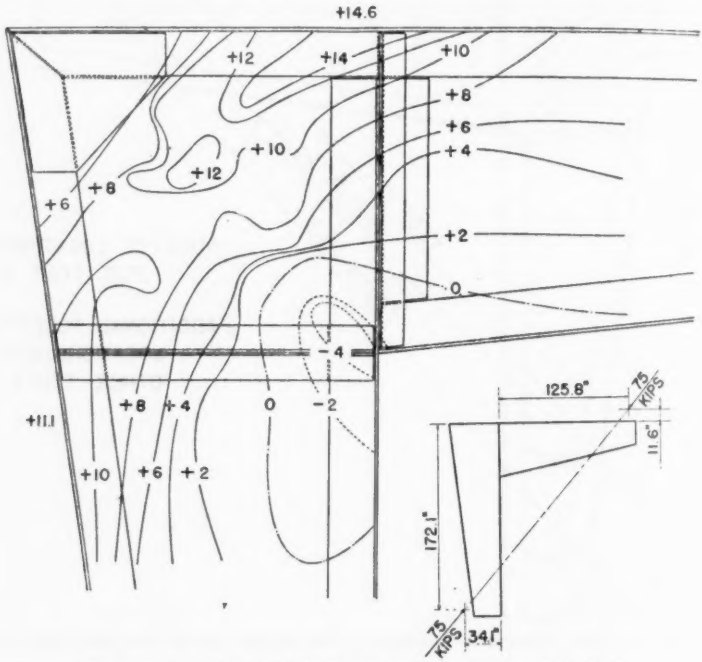

FIGURE 6.—*Test 1. Maximum principal stress, kips/in².*

were taken before the frame was subjected to a higher load. From the tensile properties of the material, given in table 1, it is seen that the proportional limit was exceeded in some places in test 1. It is probable that the loading of test 1 and the repeated loadings before test 2 brought the material in the frame to a more nearly elastic condition for test 2 than for test 1, and that the initial, low proportional limits were increased by the cold work of the material. The strains would then be less for a given load and the measured stresses smaller than those for the initial inelastic condition.

The influence of the position of the load line on the stress distribution is evident from a comparison of the results for tests 2, 3, 4, and 5. All other conditions were the same for these tests.

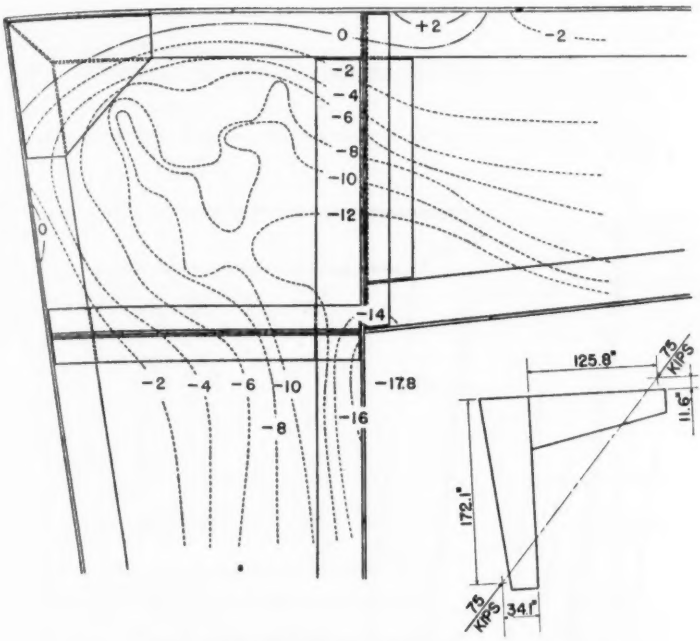

FIGURE 7.—*Test 1. Minimum principal stress, kips/in².*

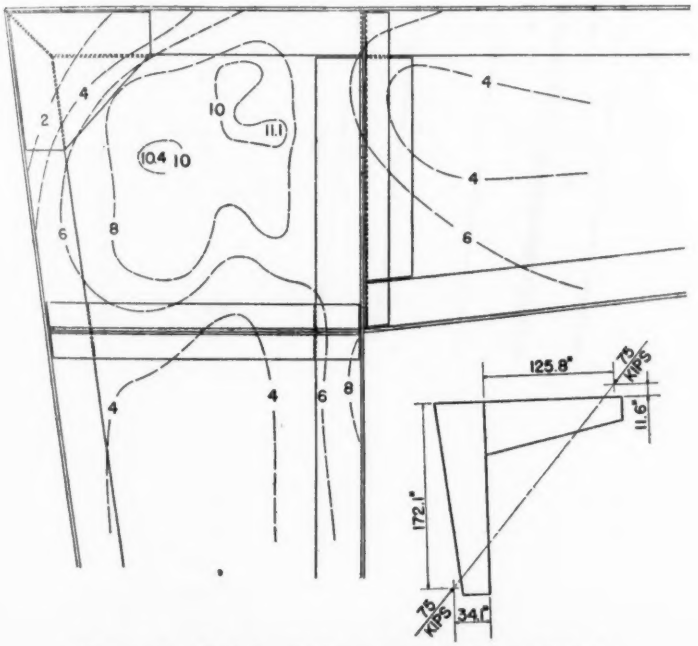

FIGURE 8.—*Test 1. Maximum shearing stress, kips/in².*

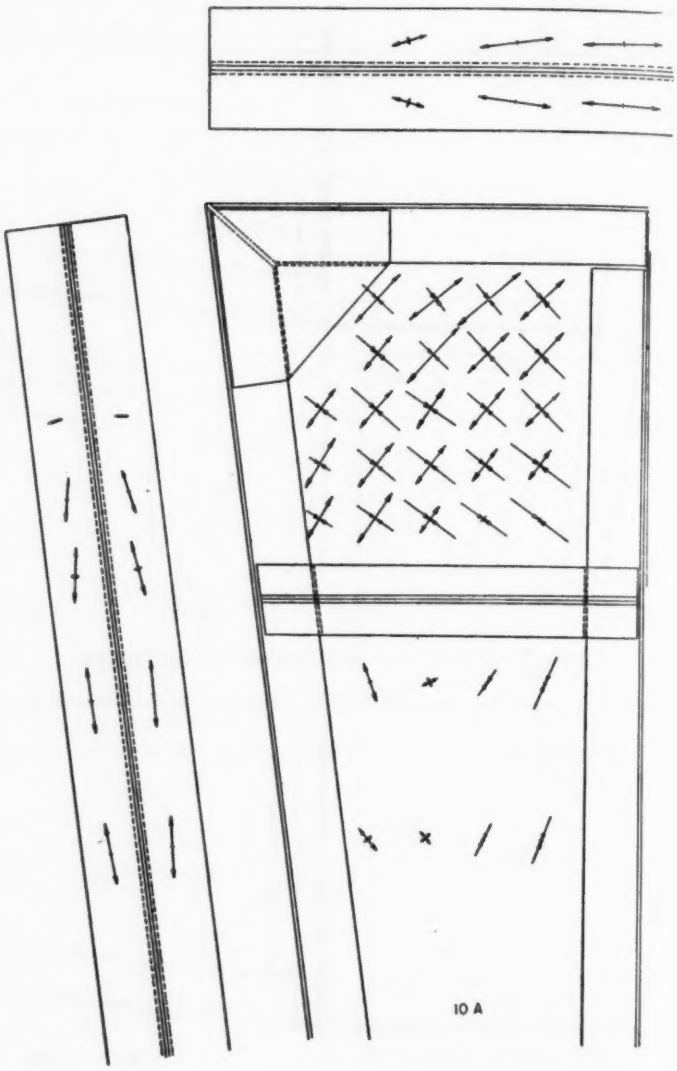
10 A

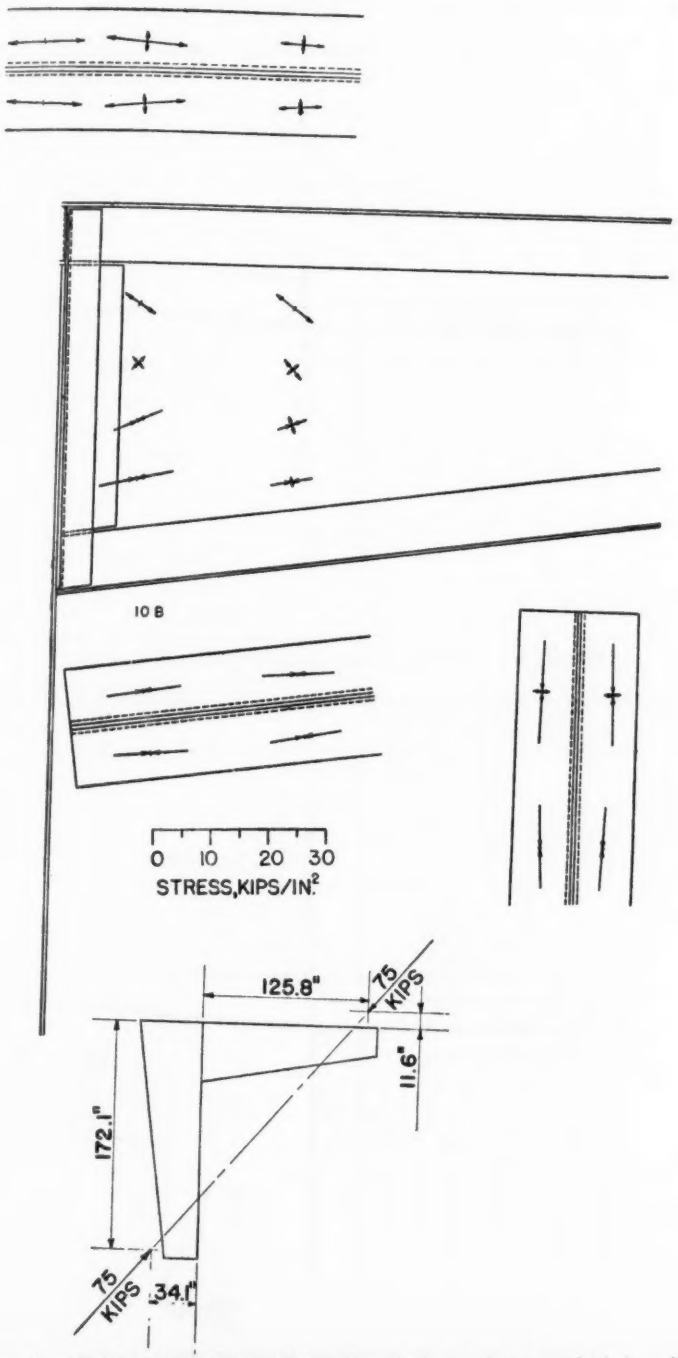

FIGURE 9.—*Test 1. Magnitude and direction of the maximum and of the minimum principal stresses, kips/in².*

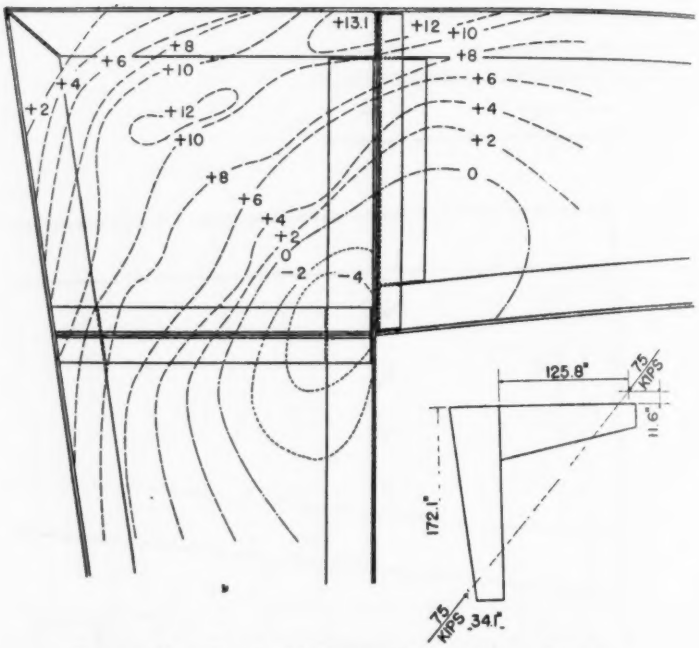

FIGURE 10.—*Test 2. Maximum principal stress, kips/in².*

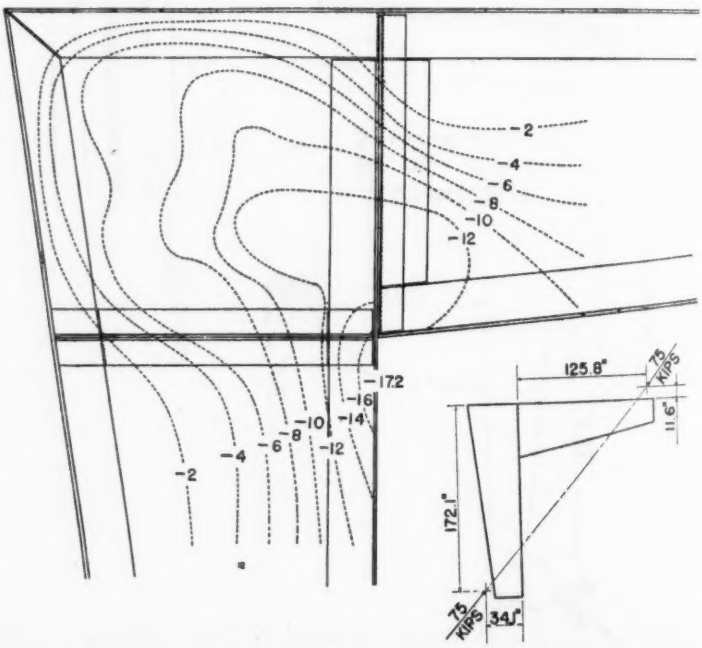

FIGURE 11.—*Test 2. Minimum principal stress, kips/in².*

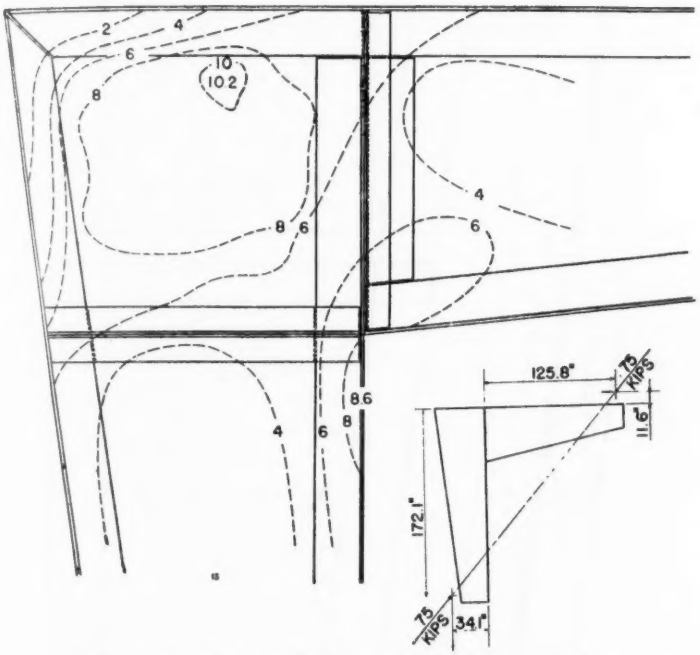

FIGURE 12.—*Test 2. Maximum shearing stress, kips/in².*

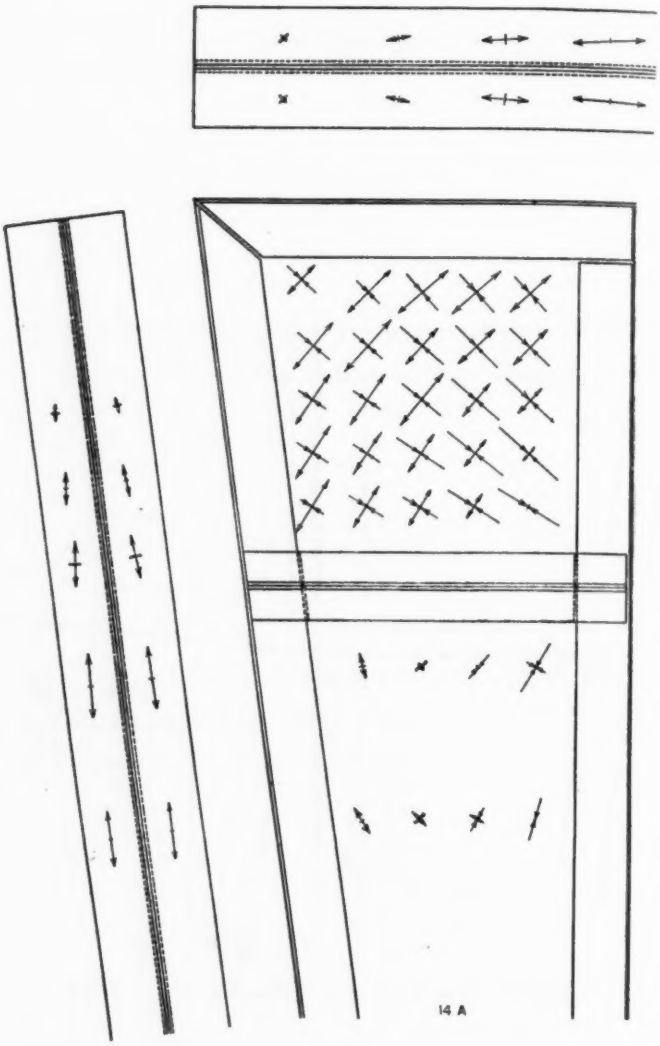
14 A

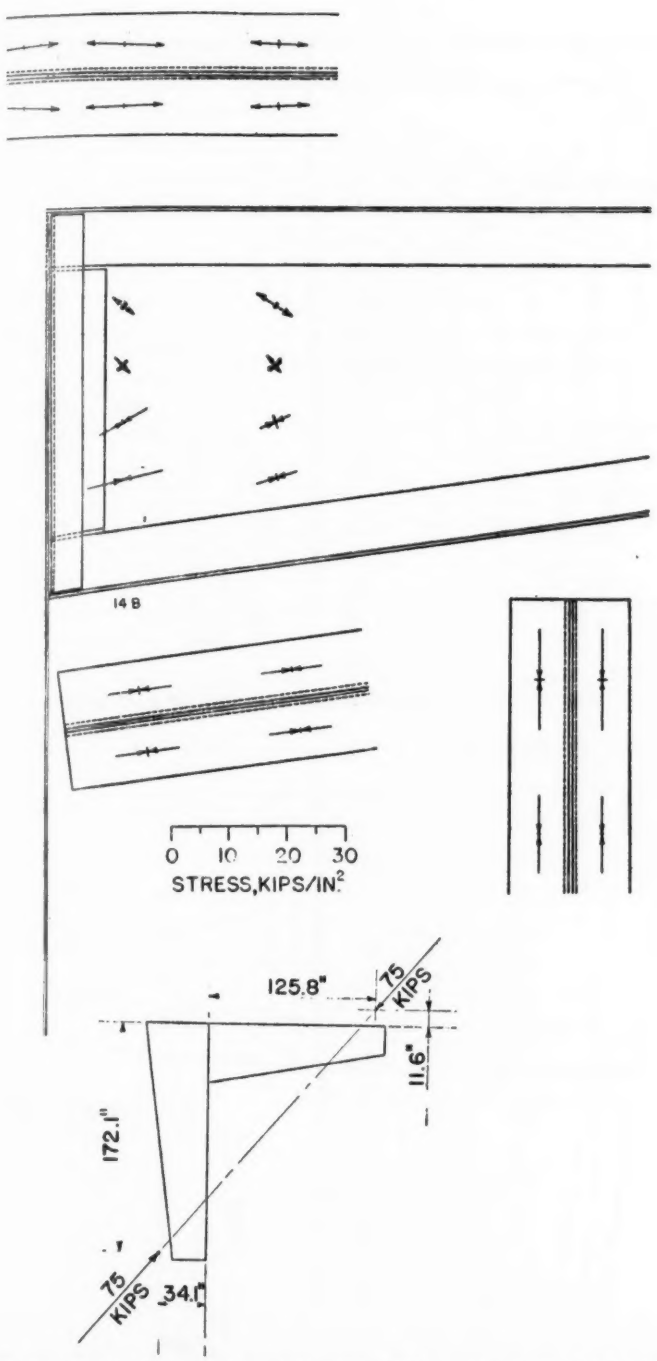

FIGURE 13.—*Test 2. Magnitude and direction of the maximum and of the minimum principal stresses, kips/in².*

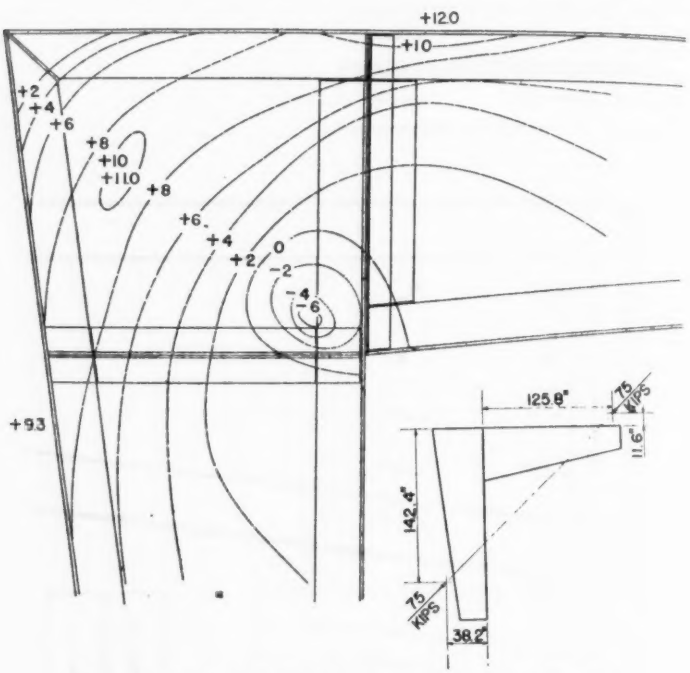

FIGURE 14.—*Test 3. Maximum principal stress, kips/in².*

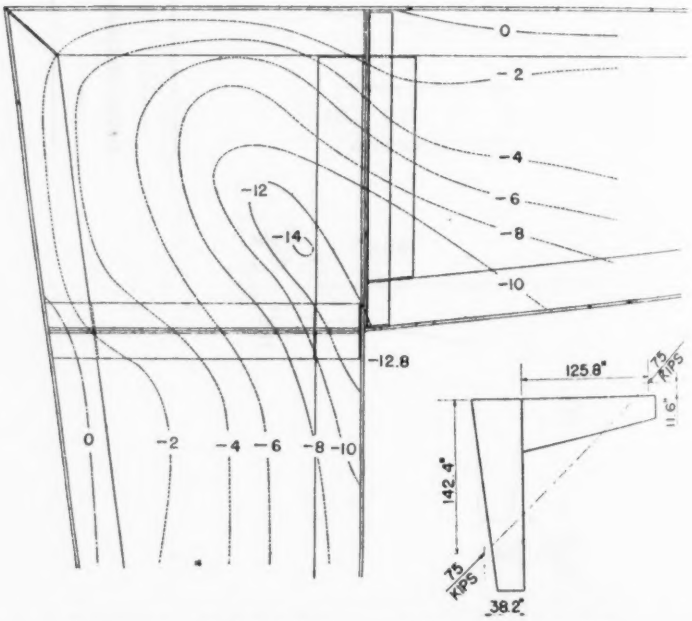

FIGURE 15.—*Test 3. Minimum principal stress, kips/in².*

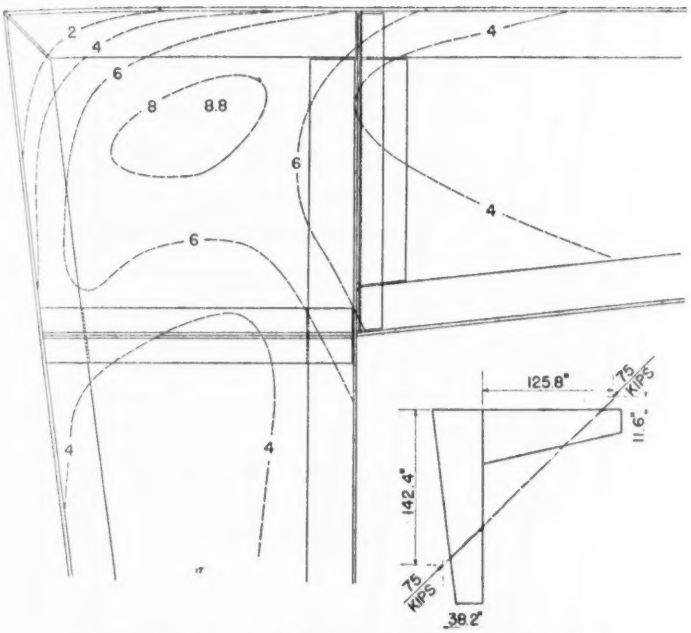

FIGURE 16.—*Test 3. Maximum shearing stress, kips/in².*

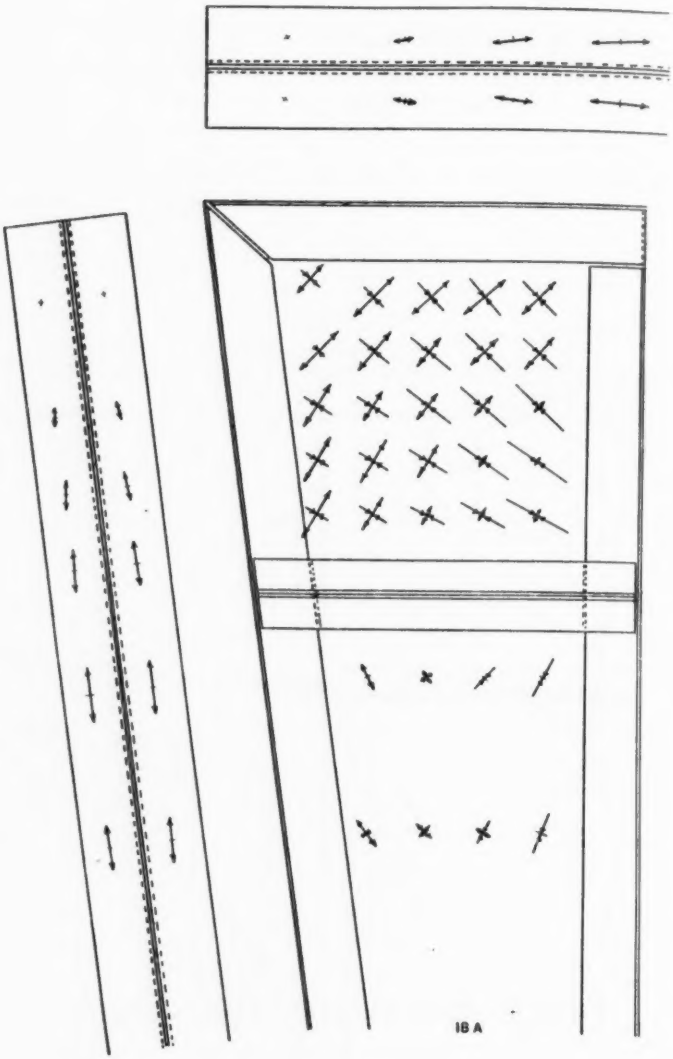
IB A

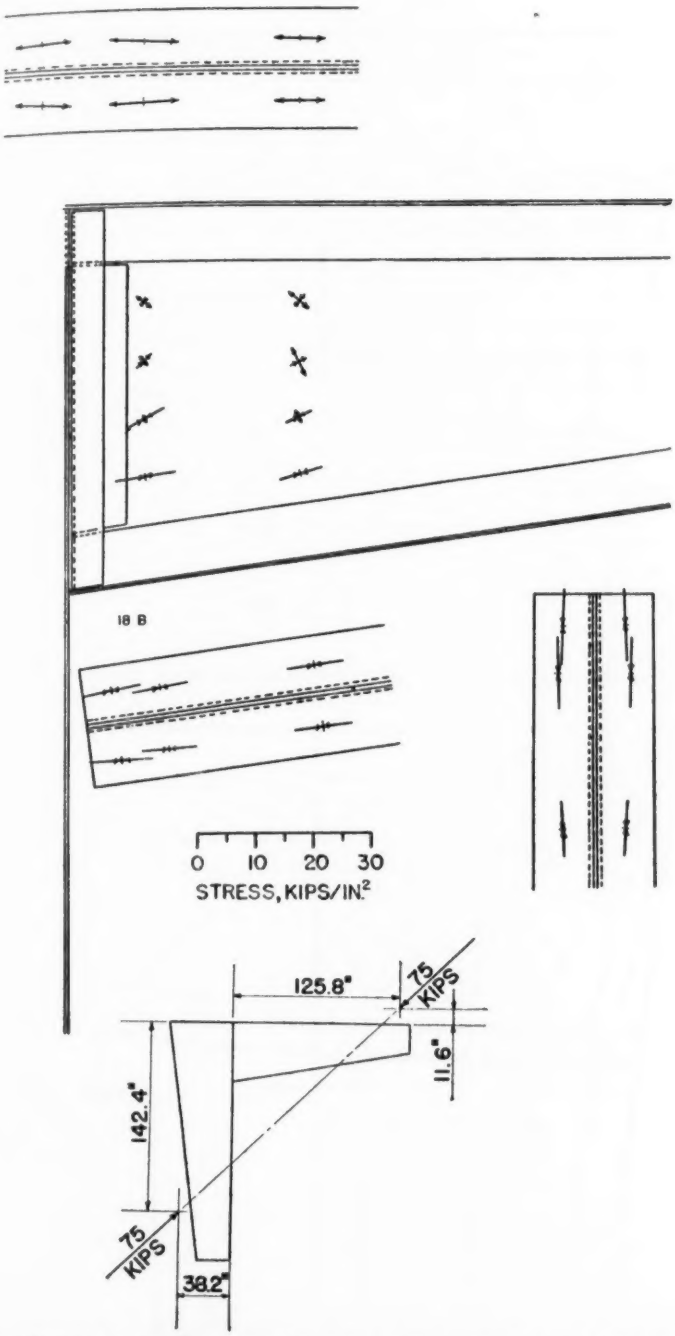

FIGURE 17.—*Test 3. Magnitude and direction of the maximum and of the minimum principal stresses, kips/in².*

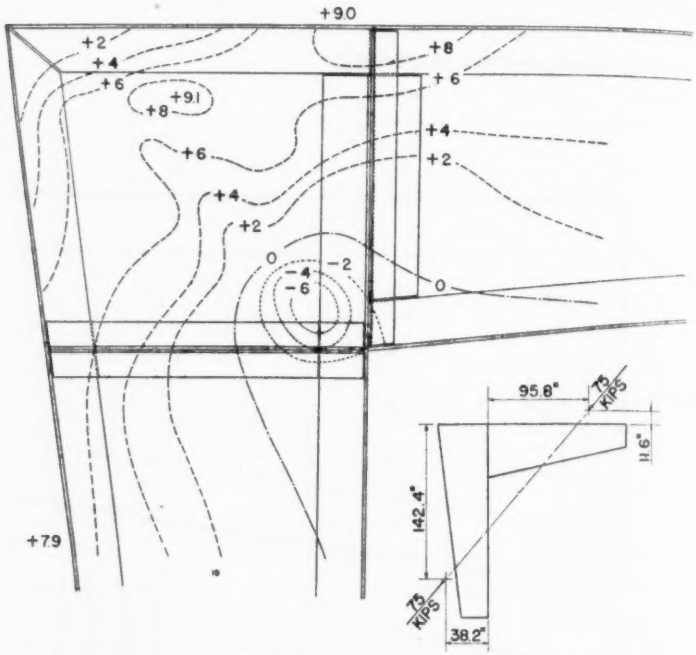

FIGURE 18.—*Test 4. Maximum principal stress, kips/in².*

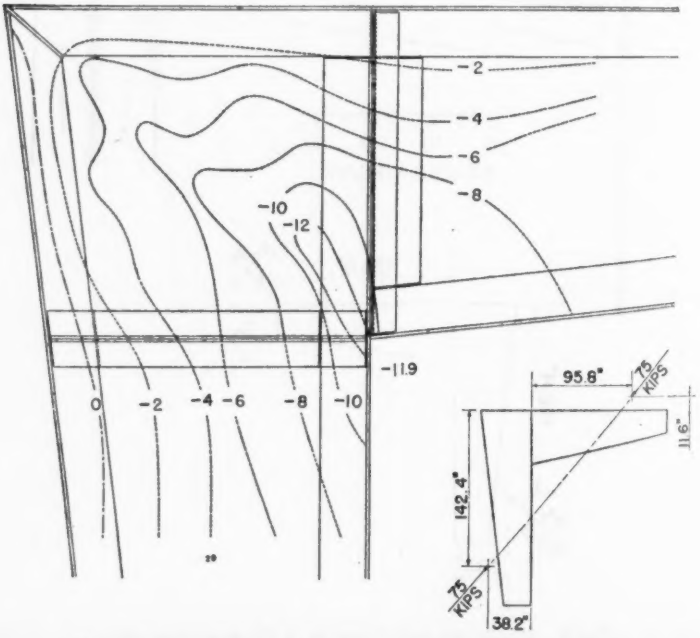

FIGURE 19.—*Test 4. Minimum principal stress, kips/in².*

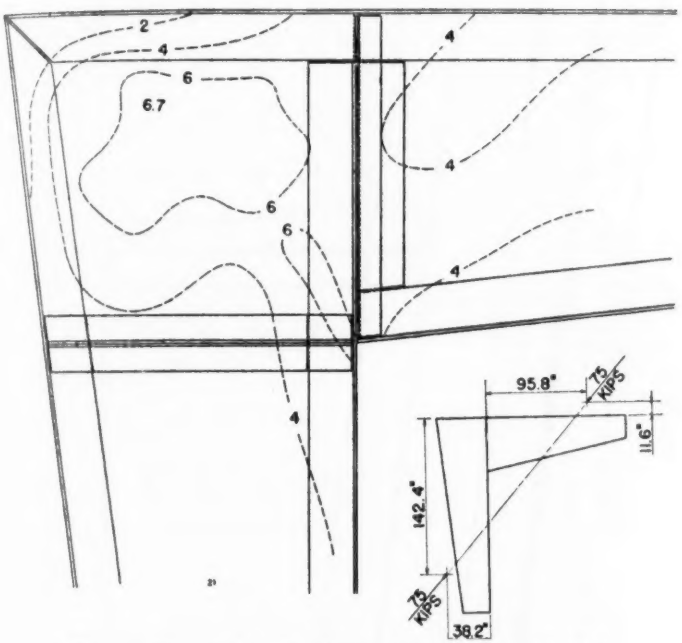

FIGURE 20.—*Test 4. Maximum shearing stress, kips/in².*

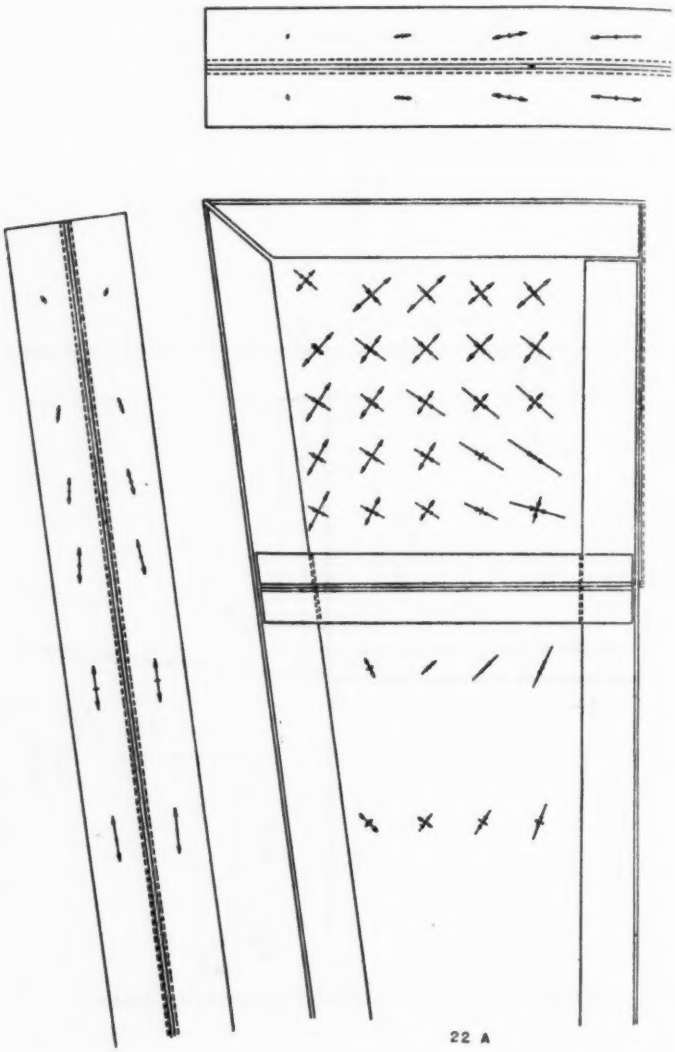
22 A

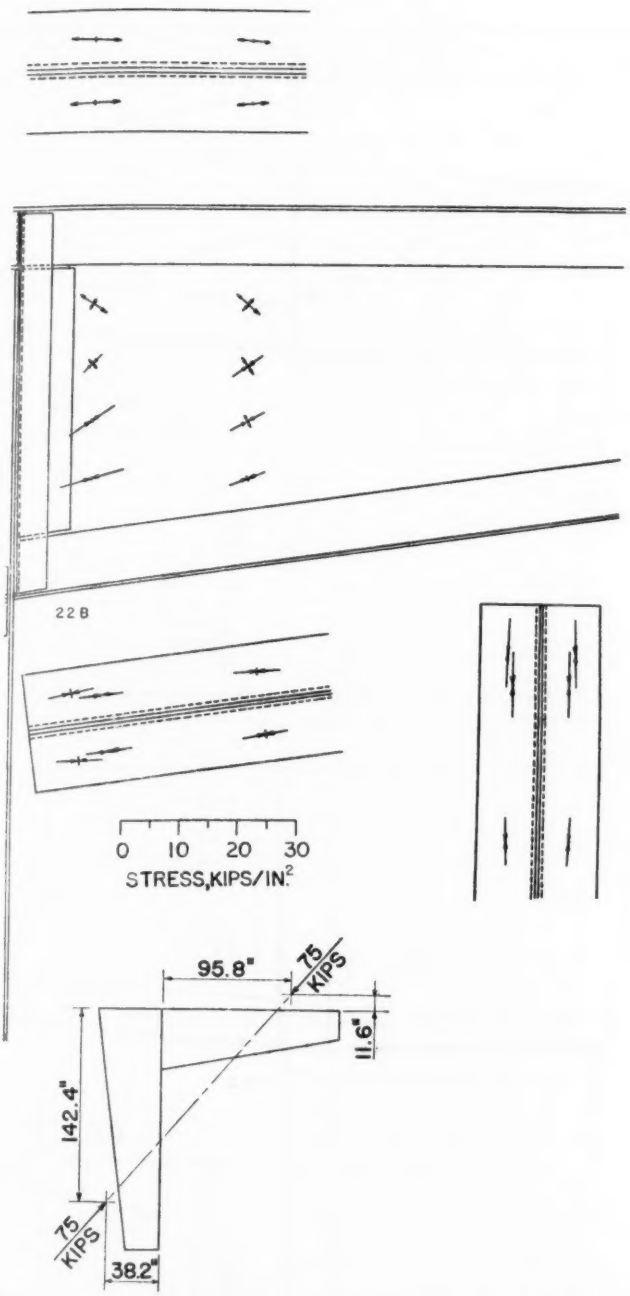

FIGURE 21.—*Test 4. Magnitude and direction of the maximum and of the minimum principal stresses, kips/in².*

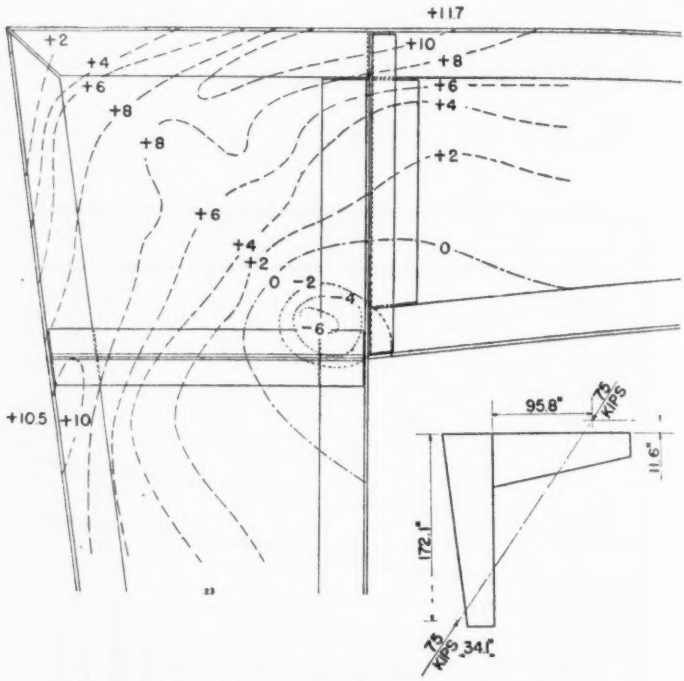

FIGURE 22.—*Test 5. Maximum principal stress, kips/in².*

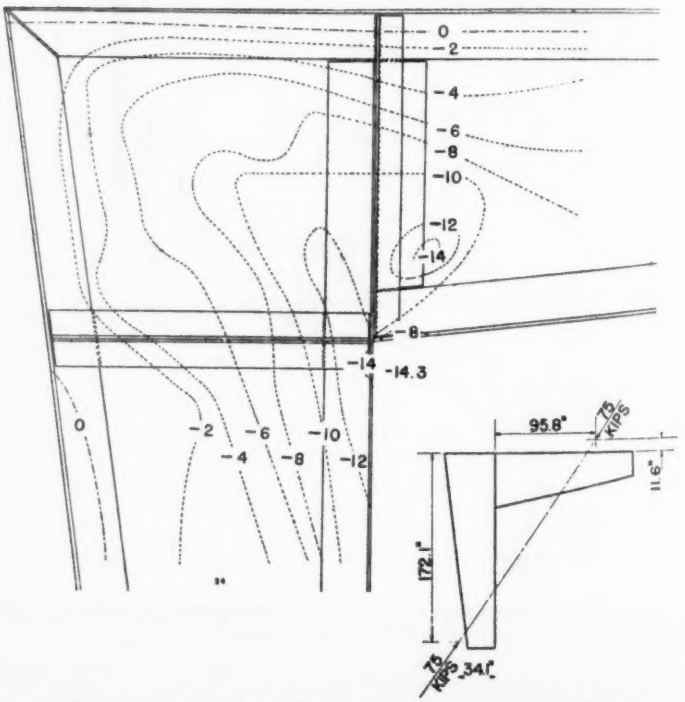

FIGURE 23.—*Test 5. Minimum principal stress, kips/in².*

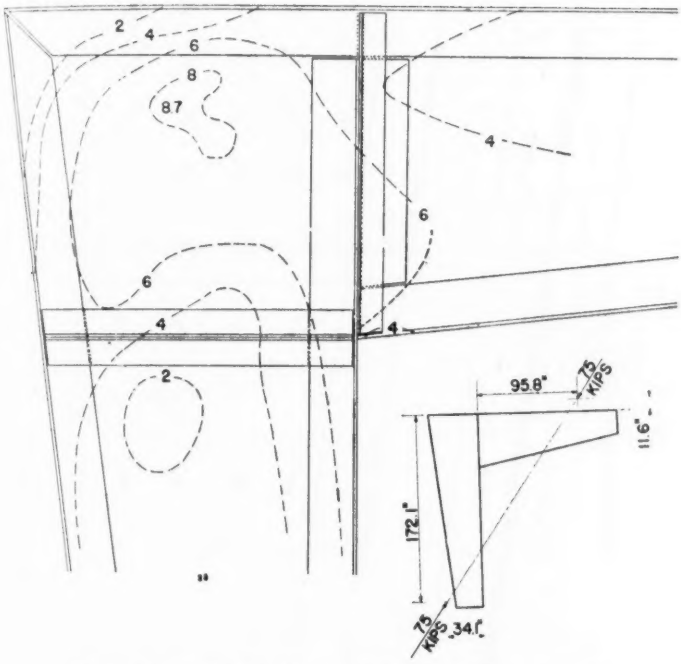

FIGURE 24.—*Test 5. Maximum shearing stress, kips/in².*

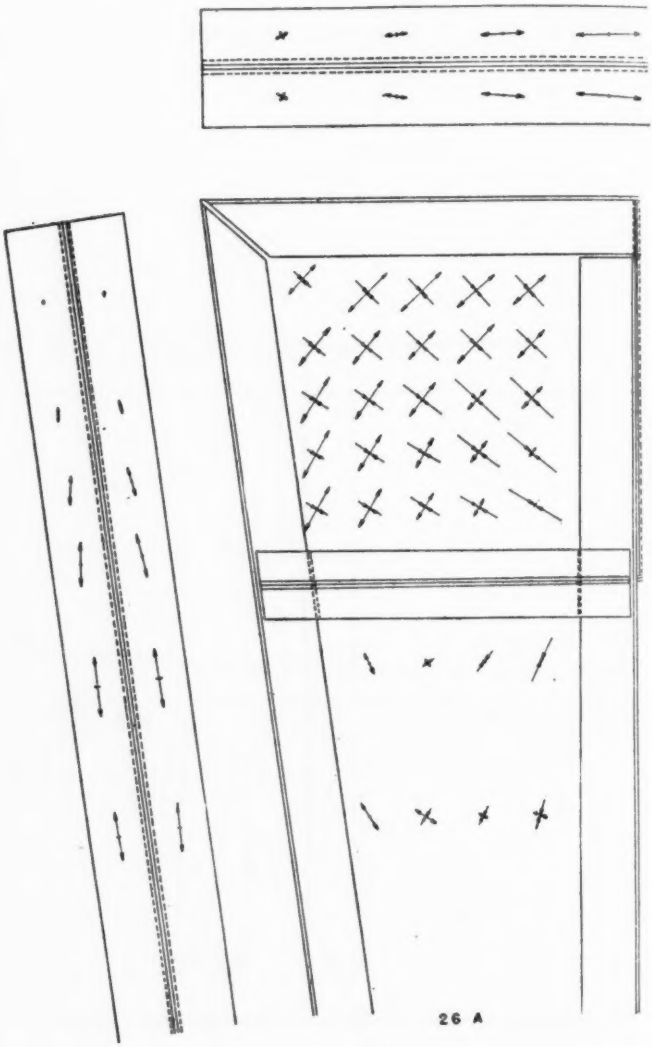
26 A

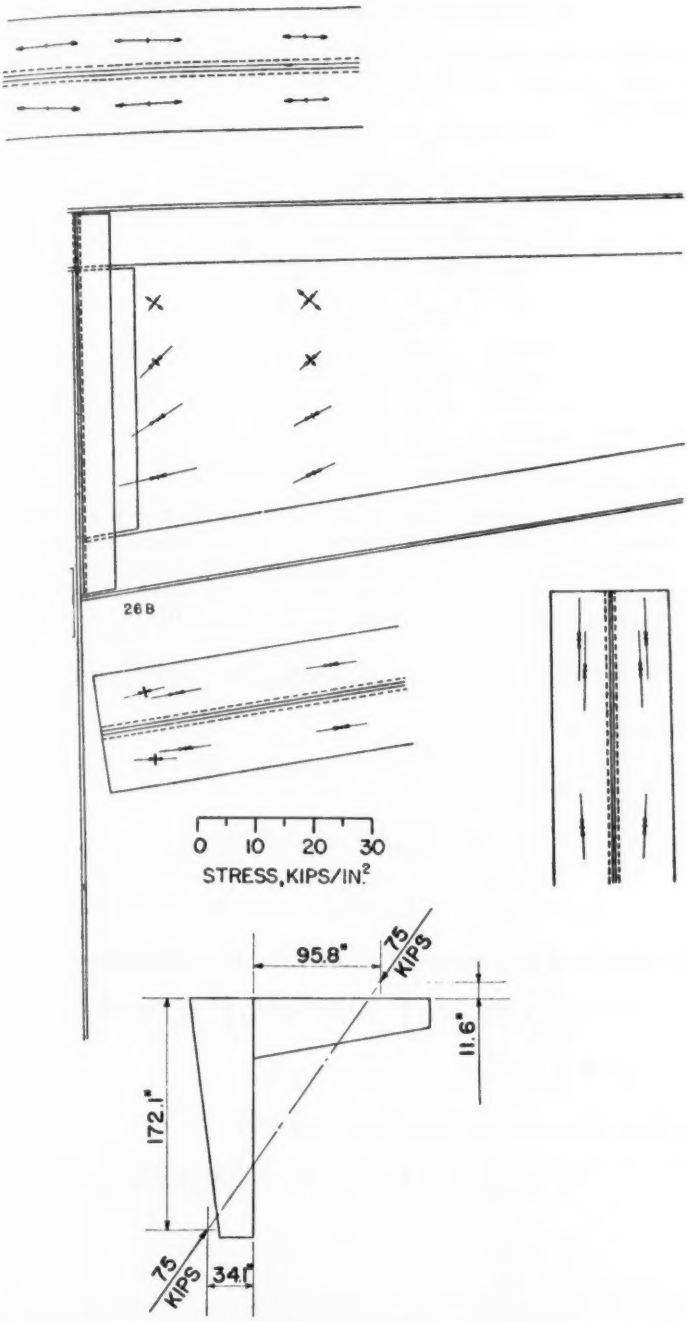

FIGURE 25.—*Test 5. Magnitude and direction of the maximum and of the minimum principal stresses, kips/in².*

V. THEORY FOR WEB OF KNEE[4]

Consider a flat rectangular plate of uniform thickness t, loaded by forces and couples, as shown in figure 26. For equilibrium it is required that

$$M_x - a(2F_{xy}+F_y) = M_y - b(2F_{yx}+F_x). \tag{1}$$

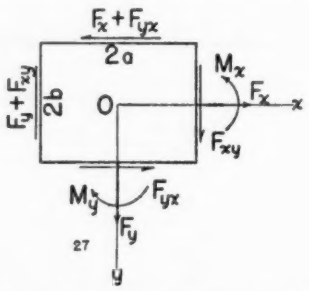

FIGURE 26.—*Loads on rectangular plate.*

It is desired to determine the state of stress in the plate under the assumptions that the normal stresses σ_x and σ_y along the boundaries $x=a$ and $y=b$, respectively, are uniformly varying, and along the boundaries $x=-a$ and $y=-b$ are everywhere zero. Such a state of stress may be derived from the stress function [10]

$$\phi = b_2xy + \frac{1}{6}(3c_3+d_4y)(a+x)y^2 + \frac{1}{6}(3b_3+b_4x)(b+y)x^2.$$

The stresses are

$$\sigma_x = \frac{\partial^2\phi}{\partial y^2} = (c_3+d_4y)(a+x), \tag{2}$$

$$\sigma_y = \frac{\partial^2\phi}{\partial x^2} = (b_3+b_4x)(b+y), \tag{3}$$

$$\tau_{xy} = -\frac{\partial^2\phi}{\partial x\partial y} = -\left(b_2+b_3x+c_3y+\frac{1}{2}b_4x^2+\frac{1}{2}d_4y^2\right). \tag{4}$$

The constants may be determined from the conditions:

$$x=a, \int_{-b}^{b}\sigma_x t\,dy = F_x, \int_{-b}^{b}\sigma_x ty\,dy = M_x, \int_{-b}^{b}\tau_{xy}t\,dy = F_{xy};$$

$$y=b, \int_{-a}^{a}\sigma_y t\,dx = F_y, \int_{-a}^{a}\sigma_y tx\,dx = M_y.$$

By making use of these conditions, one finds

$$\left.\begin{aligned} b_2 &= \frac{1}{4abt}\left[M_x - a(2F_{xy}+F_y) - \frac{3}{2}(M_x+M_y)\right], \\ b_3 &= \frac{F_y}{4abt}, \qquad c_3 = \frac{F_x}{4abt}, \\ b_4 &= \frac{3M_y}{4a^3bt}, \qquad d_4 = \frac{3M_x}{4ab^3t}. \end{aligned}\right\} \tag{5}$$

[4] Since this theory was developed at the National Bureau of Standards, another was published in Germany [9].

Insertion in eq 2, 3, and 4 of the values found for the constants gives for the stresses

$$\sigma_x=\frac{1}{4abt}\left(F_x+\frac{3M_x}{b^2}y\right)(a+x), \tag{6}$$

$$\sigma_y=\frac{1}{4abt}\left(F_y+\frac{3M_y}{a^2}x\right)(b+y), \tag{7}$$

$$\tau_{xy}=-\frac{1}{4abt}\left[M_x-a(2F_{xy}+F_y)+F_yx+F_xy -\frac{3}{2}M_y\left(1-\frac{x^2}{a^2}\right)-\frac{3}{2}M_x\left(1-\frac{y^2}{b^2}\right)\right], \tag{8}$$

in which the forces and moments satisfy eq 1. It may be noted that along $x=a$ and $y=b$, σ_x and σ_y, respectively, since they vary uniformly, are distributed in the same way as in a beam subjected to combined axial and flexural loading. For other values of x and y these stresses fall off linearly. Along these edges ($x=a$, $y=b$) also the shearing stress represented by the last two terms in eq 8 varies parabolically, as in a beam in which the shearing force on a cross section has the value $M_x/(2a)$ or $M_y/(2b)$, respectively.

VI. THEORETICAL STRESSES

In applying the theory to the web plate at the knee of a rigid frame it is necessary first to isolate the portion of the web plate which is to be considered. If a flange is regarded as consisting of the two angles and a part of the web plate between them, figure 27, and if the stress in the flange is assumed to be uniformly distributed over the cross section, it is reasonable to take the boundary of the isolated portion of the web plate at the centroid of the cross-sectional area

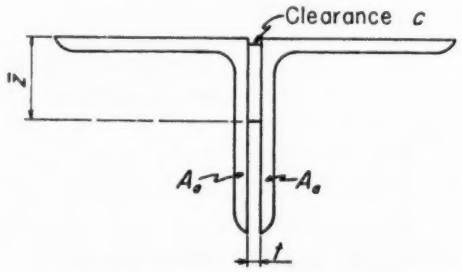

FIGURE 27.—*Cross section of flange.*

of the flange. That is, the boundary in question would be determined from the equation (Fig. 27)

$$2A_az_a+\frac{t}{2}(\bar{z}^2-c^2)=\left[2A_a+t(\bar{z}-c)\right]\bar{z}, \tag{9}$$

where $\bar{z}$ is the distance from the back of the angles to the centroid of the angles and the part of the web plate between the centroid and

the outside edge, z_a is the distance from the back of the angles to the centroid of the angles, and the other quantities are indicated clearly in figure 27. In most cases arising in practice, it would be sufficiently accurate to take the centroid of the flange as at the centroid of the two angles ($\bar{z}=z_a$).

The forces and couples acting on the isolated portion of the web plate are shown in figure 28 for a load with horizontal and vertical components H and V acting on the rigid frame as indicated. α and γ are the proportions of V and the bending moment, respectively, which are carried by each flange of the lower leg at the edge $y=b$. If a flange is not wholly continuous at the knee, it will transmit stress only partially across the discontinuous section and will also upset the assumed linear distribution of normal stress at the boundary, as in the case of the lower flange of the specimen tested. This condition can be approximated by the theory by taking the forces and couples as shown at the right in figure 28. κ and λ are the proportions

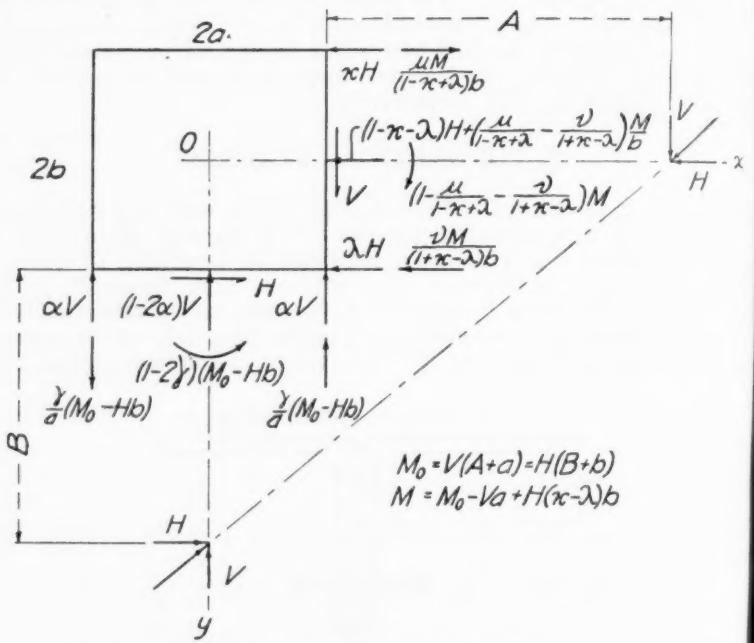

FIGURE 28.—*Resultant loads on knee web.*

of H, and μ and ν are the proportions of the bending moment which are carried by the outer and the inner flange, respectively, of the upper leg at the boundary $x=a$. If there had been no discontinuity, κ would equal λ and μ would equal ν. It is assumed that the flanges carry no transverse shear. In terms of the forces and couples shown in figure 28 those shown in figure 26 become

$$\left.\begin{aligned} F_x &= -(1-\kappa-\lambda)H-\left(\frac{\mu}{1-\kappa+\lambda}-\frac{\nu}{1+\kappa-\lambda}\right)\frac{M}{b}, \\ F_y &= -(1-2\alpha)V, \\ F_{xy} &= V-\alpha V-\frac{\gamma}{a}(M_0-Hb), \\ F_{yx} &= H-\lambda H-\frac{\nu M}{(1+\kappa-\lambda)b}, \\ M_x &= -\left(1-\frac{\mu}{1-\kappa+\lambda}-\frac{\nu}{1+\kappa-\lambda}\right)M, \\ M_y &= -(1-2\gamma)(M_0-Hb). \end{aligned}\right\} \tag{10}$$

In applying the theory to the knee of the rigid-frame specimen tested, $\bar{z}$ was computed for the two 6- by 6- by ⅜-in. angles and part of the included ⅜-in. plate from the equation

$$2(4.36)(1.64)+\frac{3}{16}\left(\bar{z}^2-\frac{1}{16}\right)=\left[2(4.36)+\frac{3}{8}\left(\bar{z}-\frac{1}{4}\right)\right]\bar{z}$$

and found to be $\bar{z}=1.60$ in. The depth of both the upper and the lower leg of the frame immediately adjacent to the knee was 40½ in., and the dimensions of the isolated portion of the web plate at the knee were taken as $2a=2b=40.5-2(1.60)=37.3$ in., that is,

$$a=b=18.65 \text{ in.} \tag{11}$$

α and γ were obtained from the relations

$$\left.\begin{aligned} \alpha &= \frac{A_f}{2A_f+A_w}=\frac{9.23}{32.44}=.285, \\ \gamma &= \frac{I_f}{2I_f+I_w}=\frac{3209}{8040}=.399, \end{aligned}\right\} \tag{12}$$

where A_f is the cross-sectional area of one flange, A_w is the cross-sectional area of the web, I_f is the moment of inertia of the cross-sectional area of one flange with respect to a centroidal axis perpendicular to the web, and I_w is the moment of inertia of the cross-sectional area of the web with respect to the same axis. In computing κ, λ, μ, and ν, the outstanding legs of the inner flange angles were neglected because of the lack of bearing at the knee. This consideration resulted in an unsymmetrical cross section with centroid 2.93 in. above the axis of x, figure 28. κ, λ, μ, and ν were obtained from the relations

$$\left.\begin{aligned} \kappa &= \frac{A_o}{A_o+A_i+kA_w}=\frac{9.23}{26.82}=.344, \\ \lambda &= \frac{A_i}{A_o+A_i+kA_w}=\frac{5.01}{26.82}=.187, \\ \mu &= \frac{I_o}{I_o+I_i+kI_w}=\frac{2280}{6179}=.369, \\ \nu &= \frac{I_i}{I_o+I_i+kI_w}=\frac{2331}{6179}=.377, \end{aligned}\right\} \tag{13}$$

where A_o, A_i, and A_w are the cross-sectional areas of the outer flange, the inner flange, and the web, respectively, I_o, I_i, and I_w are the moments of inertia of the cross-sectional areas of the outer flange, the inner flange, and the web, respectively, with respect to a centroidal axis perpendicular to the web, and k is the relative stiffness of the splice compared to that of the solid plate. A value of $k=0.9$ was arbitrarily assumed in the computations of eq 10. A value of $k=0$ would correspond to a gap in the web, that is, all of the bending moment and axial load would be transmitted through the flanges. A value of $k=1$ would correspond to a solid web, that is, the bending moment and axial load would be transmitted as in an ordinary beam.

With the values of $a=b$, α, γ, κ, λ, μ, and ν given in eq 11, 12, and 13, eq 10 and 6, 7, and 8 were solved for the stresses for the four cases of loading corresponding to tests 2, 3, 4, and 5. The values of the measured stresses and of the theoretical stresses are shown in figures 29, 30, 31, and 32. The measured stresses are given by the arrows and the theoretical stresses by the curves.

The theoretical stresses in the legs were computed from the ordinary beam theory for a beam subjected to combined axial and flexural loading. According to this theory, the normal stress at any point of a cross section is given by

$$\sigma_n=\frac{P}{A}+\frac{Ml}{I}, \tag{14}$$

where l is the distance of the point from the centroidal axis of the cross section perpendicular to the plane of bending, measured positive toward the outer flange; A is the area of the cross section; I is the moment of inertia of the cross section with respect to the centroidal axis; P is the component of load normal to the cross section, positive when it produces tension; and M is the bending moment at the cross section, positive when it produces tension on the outer side of the centroidal axis.

The shearing stress at a distance l from the centroidal axis is given by

$$\tau=\frac{FQ}{Ip}, \tag{15}$$

where F is the total transverse shear on the section, positive when the portion of the leg between the section and the outer end tends to slide in the direction of the other leg; p is the width of the section at l; and Q is the moment about the centroidal axis of the area of the portion of the section between l and the extreme fiber.

In the ordinary beam theory the normal stress on any plane perpendicular to the cross section is zero.

In computing the stresses by formulas 14 and 15, the sections were taken perpendicular to the outer flange of the upper leg and the inner flange of the lower leg. The sections were taken as symmetrical about a point midway between the extreme fibers, the obliquity of one flange to the section being neglected. The gross section was used in the computations [11].

The agreement between the theoretical and measured stresses in the lower leg is very close, especially for the normal stresses. In the upper

leg near the knee very high normal stresses were developed in the web, and correspondingly low ones in the flange. This is undoubtedly due to the lack of bearing of the inner (compression) angles at the inner corner, explained in section II. These high stresses extend into the web of the knee and undoubtedly account for a considerable part of the discrepancy between the measured stresses and the theoretical stresses, for the assumptions of the theory concerning the loading of the edges of the plate are not fulfilled. The agreement between the theoretical and measured shearing stresses in the web of the knee is very close, and the shearing stresses seem to have been very little affected by the lack of bearing of the compression angles at the inner corner.

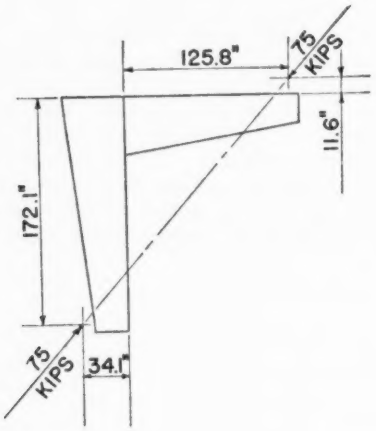
125.8"
75 KIPS
11.6"
172.1"
75 KIPS
34.1"

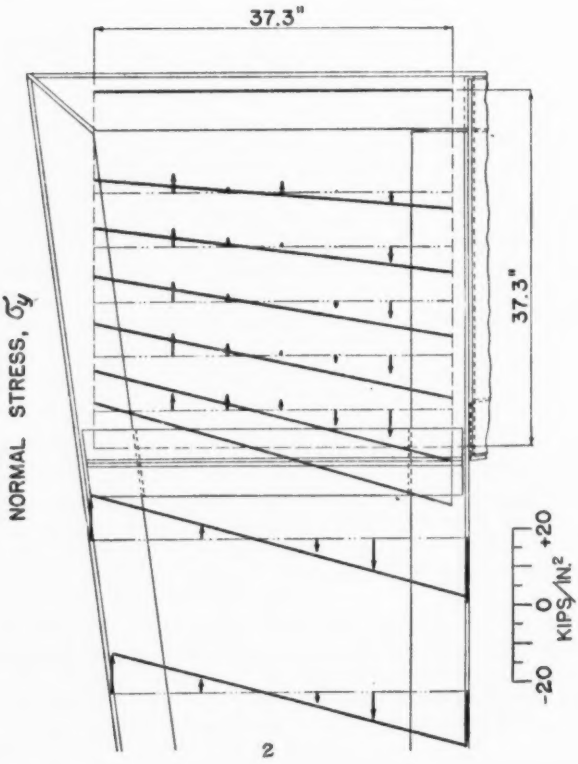
37.3"
37.3"
NORMAL STRESS, σ_y
-20
0
+20
KIPS/IN.²
2

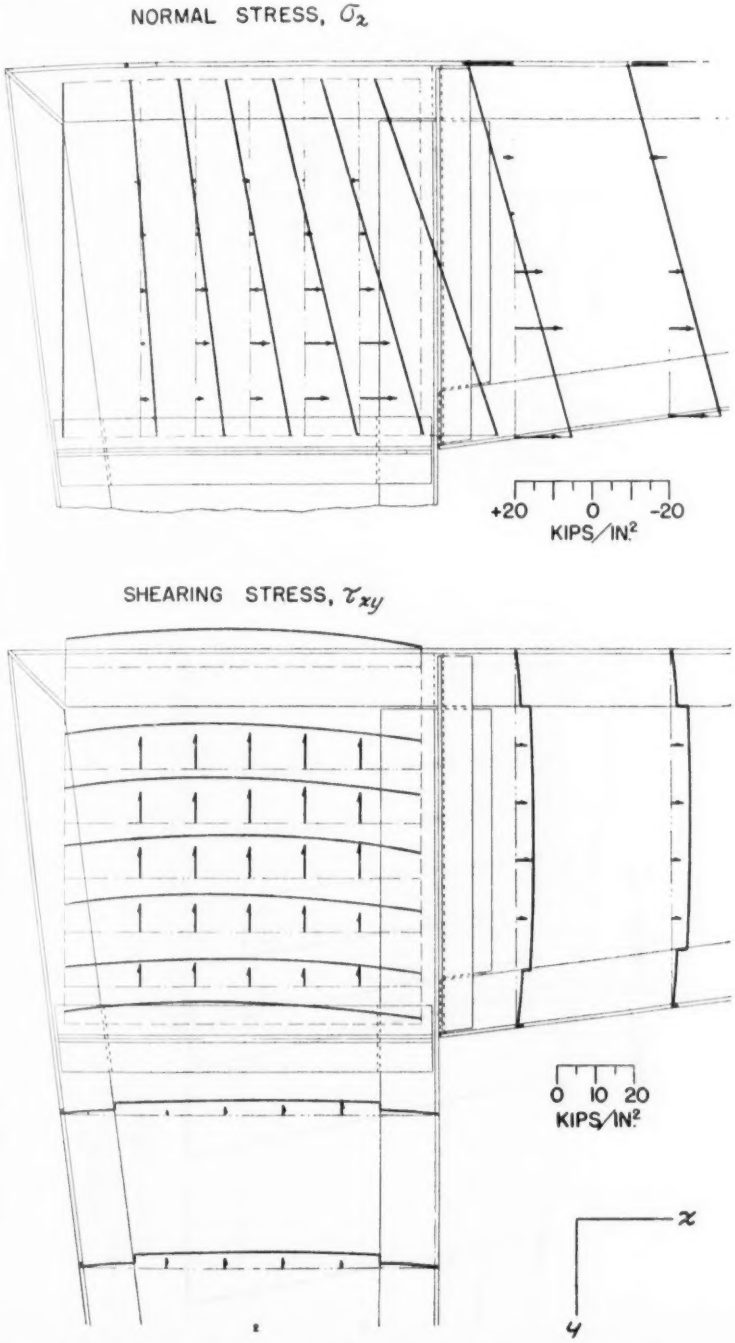

FIGURE 29.—*Test 2. Theoretical stresses and measured stresses.*
The curves represent theoretical, and the arrows measured, stresses.

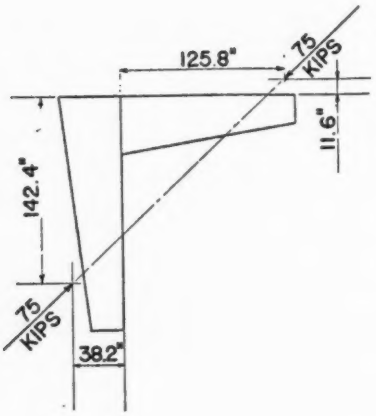
125.8"
75 KIPS
11.6"
142.4"
75 KIPS
38.2"

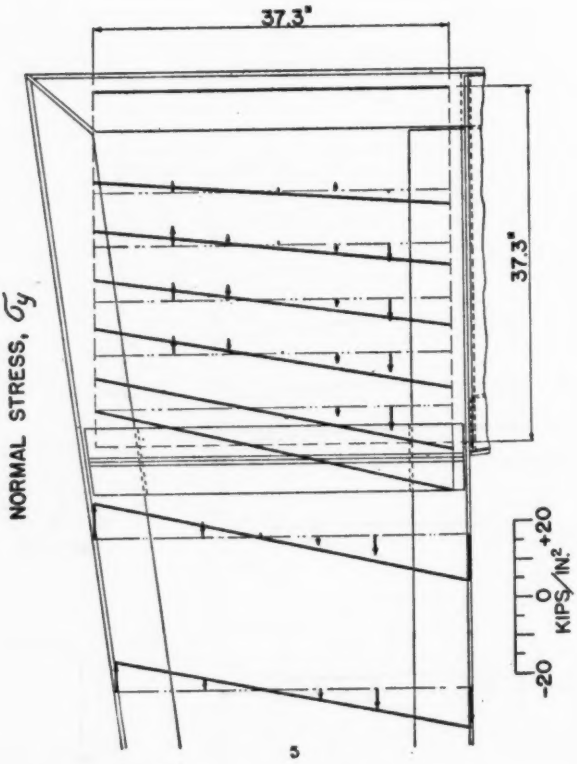
37.3"
37.3"
NORMAL STRESS, σ_y
-20
0
+20
KIPS/IN.²

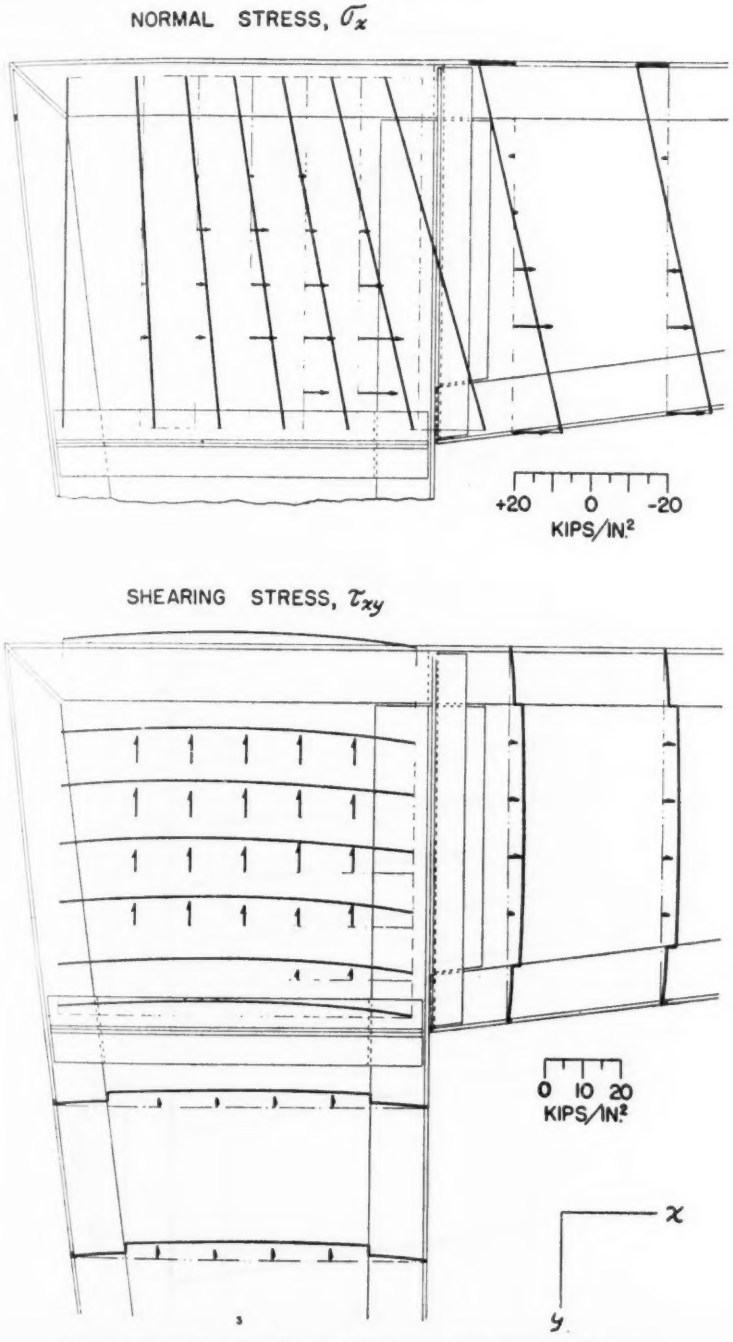

FIGURE 30.—*Test 3. Theoretical stresses and measured stresses.*
The curves represent theoretical, and the arrows measured, stresses.

87595—38——4

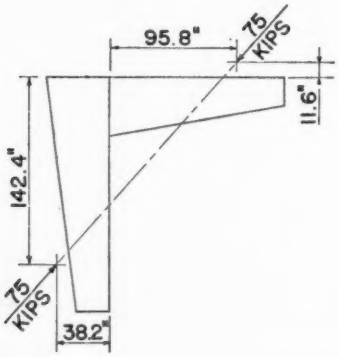
95.8"
75 KIPS
11.6"
142.4"
75 KIPS
38.2"

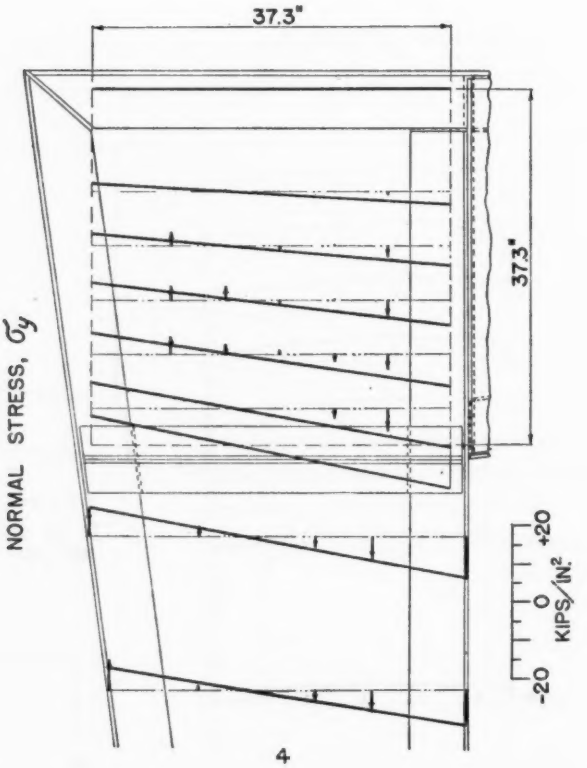
37.3"
37.3"
NORMAL STRESS, σ_y
+20
0
-20
KIPS/IN.²
4

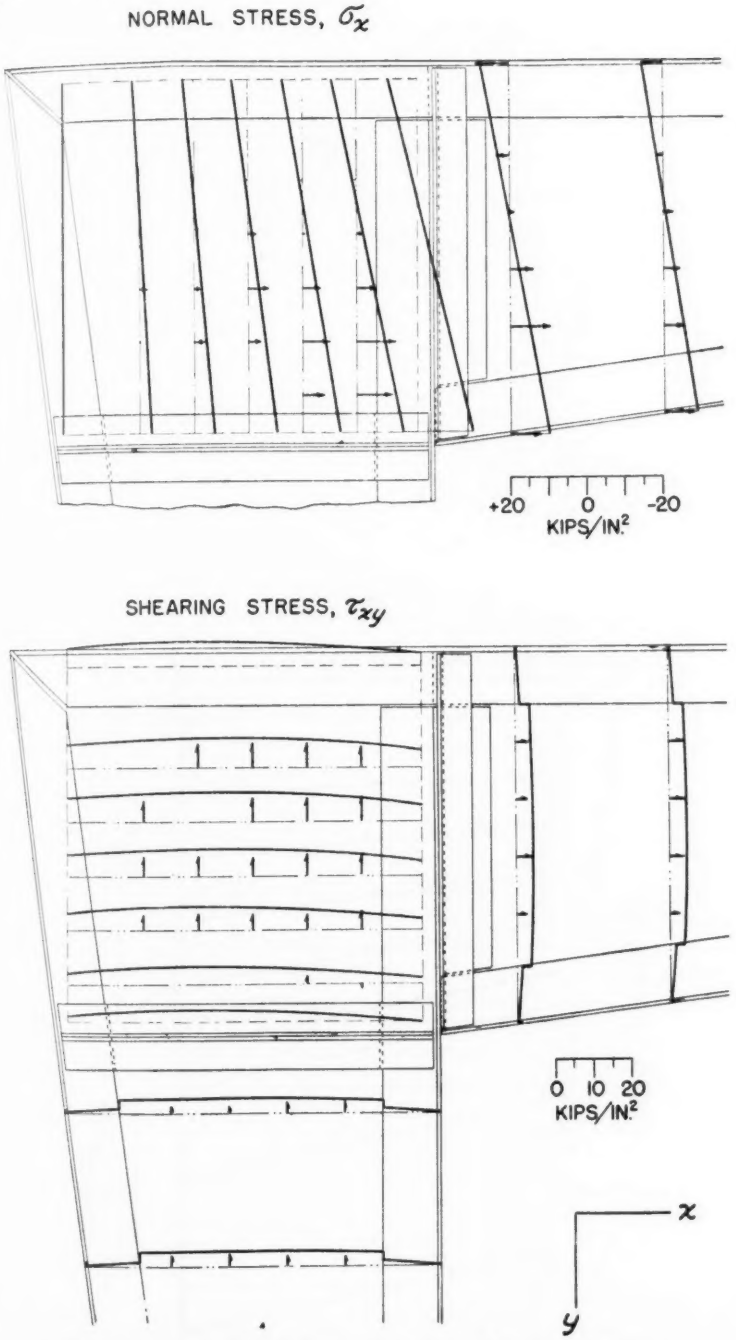

FIGURE 31.—*Test 4. Theoretical stresses and measured stresses.*
The curves represent theoretical, and the arrows measured, stresses.

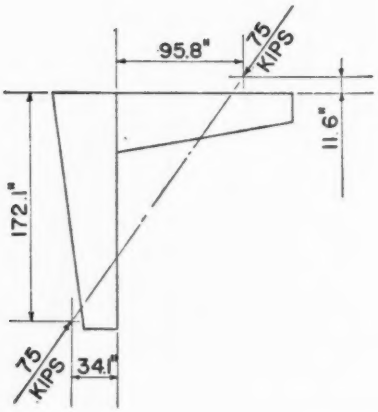
95.8"
75
KIPS
11.6"
172.1"
75
KIPS
34.1"

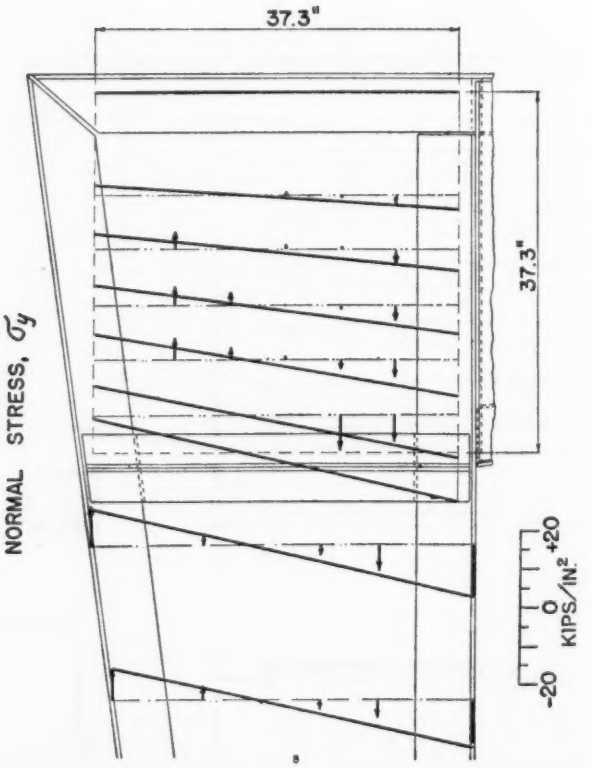
37.3"
37.3"
NORMAL STRESS, σ_y
-20
0
+20
KIPS/IN.²

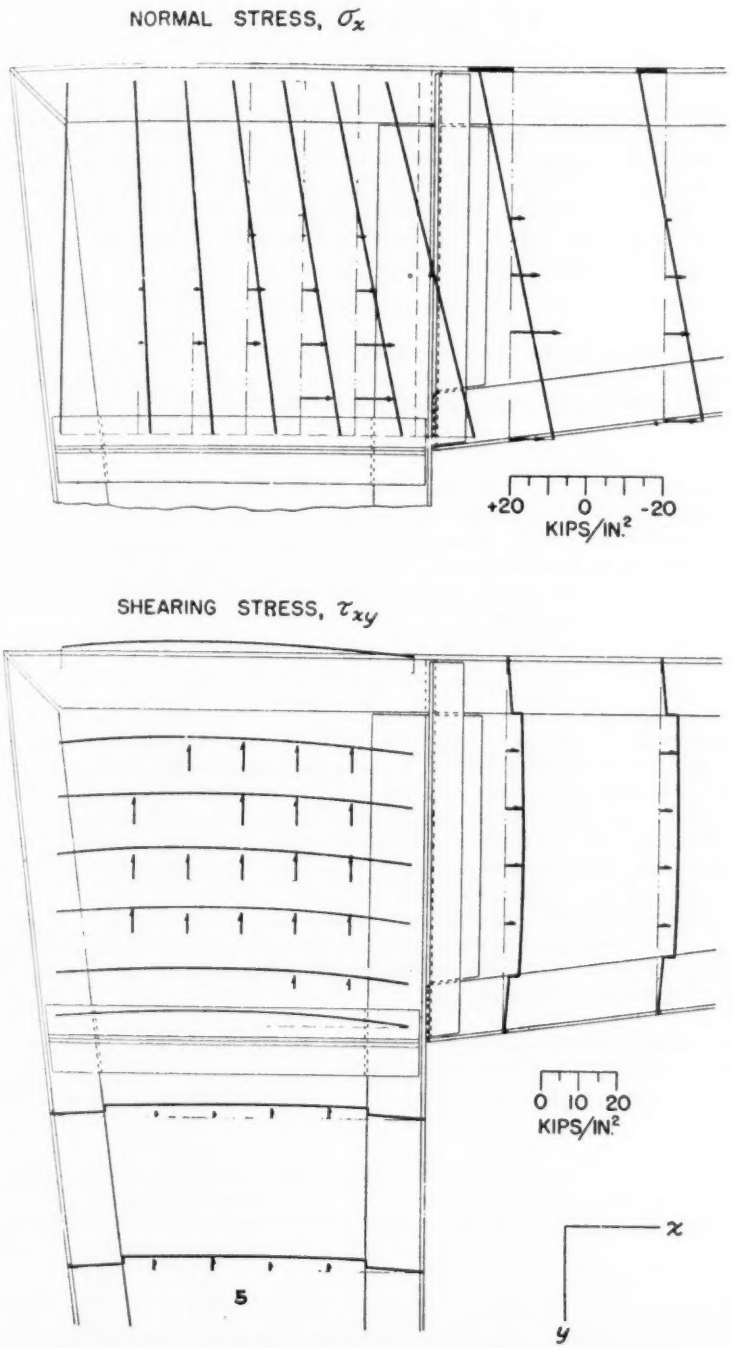

FIGURE 32.—*Test 5. Theoretical stresses and measured stresses.*
The curves represent theoretical, and the arrows measured, stresses.

VII. GREATEST STRESSES

1. THE LEGS

From figures 29 to 32, inclusive, it is evident that the ordinary theory for a beam subjected to combined axial and flexural loading predicts the stresses in the legs accurately. The agreement between the stresses computed from this theory and the measured stresses is close for the lower leg, and would probably have been equally close for the upper leg if there had been full bearing of the inner flanges of the legs at the inner corner of the knee.

2. THE KNEE WEB

The stresses in the knee web may exceed those in the legs. Expressions for the greatest stresses in the knee web are obtained below. By "greatest stress" will be understood the numerically largest stress.

(a) GREATEST NORMAL STRESS

The experimental results given in section IV indicate that the greatest normal stress in the knee web of frames of the type considered here occurs, as would be expected, at the inner corner, $x=a$, $y=b$. The greatest normal stress at this point may be obtained by evaluating eq 6, 7, and 8 for σ_x, σ_y, and τ_{xy} at $x=a$, $y=b$ and substituting the results in the expression

$$\left.\begin{matrix}\sigma_u\\ \sigma_v\end{matrix}\right\}=\frac{\sigma_x+\sigma_y}{2}\pm\sqrt{\left(\frac{\sigma_x-\sigma_y}{2}\right)^2+\tau^2_{xy}}. \tag{16}$$

If the applied load, as in figure 28, tends to decrease the angle between the positive axes of x and y, σ_v will be numerically greater than σ_u and a compressive stress. If the load is reversed (signs of H and V changed), σ_u will be numerically greater than σ_v and a tensile stress. In this case the discontinuous inner flange would transmit no stress to the knee, and the solution, approximate but on the safe side, would be obtained by taking $\lambda=\nu=0$.

Table 2 gives the greatest normal stresses in the rigid-frame specimen. The measured stresses are the stresses at a rosette. The computed stresses in the knee web were obtained from eq 16 (for σ_v) and those in the legs from eq 14.

TABLE 2.—*Greatest normal stresses in the rigid-frame specimen*

Test	Greatest normal stresses (compressive)		
	Knee web		Legs—Computed
	Measured	Computed	
	kips/in.^{2}	*kips/in.*^{2}	*kips/in.*^{2}
2	13.4	20.2	15.8
3	14.5	17.5	13.4
4	12.4	14.5	11.6
5	13.1	15.2	13.9

The computed greatest normal stresses in the knee web are somewhat higher than those in the legs.

(b) GREATEST SHEARING STRESS

The maximum shearing stress at any point in the knee web in terms of the normal stresses σ_x and σ_y and the shearing stress τ_{xy} is given by

$$\tau_{\max}=\sqrt{\left(\frac{\sigma_x-\sigma_y}{2}\right)^2+\tau^2_{xy}}. \tag{17}$$

To locate the point where $\tau_{\max}$ is a maximum, differentiate $\tau^2_{\max}$ partially with respect to x and y and set these derivatives equal to zero. One obtains

$$\left.\begin{aligned}\frac{\partial}{\partial x}\tau^2_{\max}&=\frac{1}{2}(\sigma_x-\sigma_y)\frac{\partial}{\partial x}(\sigma_x-\sigma_y)+2\tau_{xy}\frac{\partial}{\partial x}\tau_{xy}=0,\\ \frac{\partial}{\partial y}\tau^2_{\max}&=\frac{1}{2}(\sigma_x-\sigma_y)\frac{\partial}{\partial y}(\sigma_x-\sigma_y)+2\tau_{xy}\frac{\partial}{\partial y}\tau_{xy}=0.\end{aligned}\right\} \tag{18}$$

Substitution of the values of σ_x, σ_y, and τ_{xy} from eq 2, 3, and 4 into eq 18 gives, after some reduction,

$$\left.\begin{aligned}&[(c_3+d_4y)(a+x)-(b_3+b_4x)(b+y)][(c_3+d_4y)-b_4(b+y)]\\ &\quad+4\left(b_2+b_3x+c_3y+\frac{1}{2}b_4x^2+\frac{1}{2}d_4y^2\right)(b_3+b_4x)=0,\\ &[(c_3+d_4y)(a+x)-(b_3+b_4x)(b+y)][d_4(a+x)-(b_3+b_4x)]\\ &\quad+4\left(b_2+b_3x+c_3y+\frac{1}{2}b_4x^2+\frac{1}{2}d_4y^2\right)(c_3+d_4y)=0.\end{aligned}\right\} \tag{19}$$

A solution of eq 19 is seen by inspection to be

$$x=-\frac{b_3}{b_4},\qquad y=-\frac{c_3}{d_4}, \tag{20}$$

and this is a possible location for the greatest maximum shearing stress, $(\tau_{\max})_{\max}$. Evaluation of x and y by means of the relations 5 and 10 for the various cases of loading considered in this investigation and comparison with the measured stresses indicate that this is a significant and the only significant solution for the coordinates of the point where $\tau_{\max}$ is a maximum. The values of x and y given by eq 20 make $\sigma_x=\sigma_y=0$ (eq 2 and 3) and therefore (eq 17)

$$(\tau_{\max})_{\max}=(\tau_{xy})_{\max}.$$

The maximum shearing stress may then be obtained simply from eq 4 by inserting the values just found for x and y.

Table 3 gives the greatest shearing stresses in the rigid-frame specimen. The measured stresses are the stresses at a rosette. The computed stresses in the knee web were obtained as just explained, and those in the leg webs from eq 15. The shearing stresses in the knee web are much larger than those in the leg webs.

TABLE 3.—*Greatest shearing stresses in the rigid-frame specimen*

Test	Greatest shearing stresses		
	Knee web		Leg webs—Computed
	Measured	Computed	
	kips/in.²	*kips/in.²*	*kips/in.²*
2	10.2	11.8	4.8
3	8.8	9.6	4.6
4	6.7	7.8	4.8
5	8.7	8.8	5.2

VIII. MAXIMUM LOAD

The rigid-frame specimen is shown in figure 33 in the testing machine for determining the maximum load. The load line was the same as for test 2, and the gussets had been removed from the outer corner. The steel structure shown in figure 33 prevented lateral deflection of the outer corner of the specimen. Before loading, the specimen was coated with a cement wash to make Lüders' lines clearly visible where the material was stressed to the yield point during the test.

The maximum load sustained by the specimen was 168,000 lb. Failure occurred by lateral deflection of the inner corner with attendant buckling of the outstanding legs of the inner flange angles on one side, as shown in figure 34. No rivets failed, so far as could be noticed visually. For test 2, the ratio of the load to the greatest measured stress was 4.35 kips per kip/in^2. The ratio of the maximum load to the tensile yield point of the angles (see table 1) was 4.31 kips per kip/in^2. If one assumes a linear variation of stress with load up to the yield point and the compressive and tensile yield points to be equal, it is evident that practically the full compressive strength of the material was utilized.

The knee web after failure is shown in figure 35. The Lüders' lines, which run horizontally and vertically, are clearly visible. The diagonal streak of granulated appearance parallel to the load line is due to a buckle in the web.

IX. CONCLUSIONS

The distribution of stress in a riveted steel rigid-frame specimen having straight flanges was determined experimentally and theoretically, and the maximum load was measured. The following conclusions were drawn:

1. The stresses at the outer corner of the knee of the specimen were small, and reinforcing the outer corner had a negligible effect on the distribution of stress in the specimen.

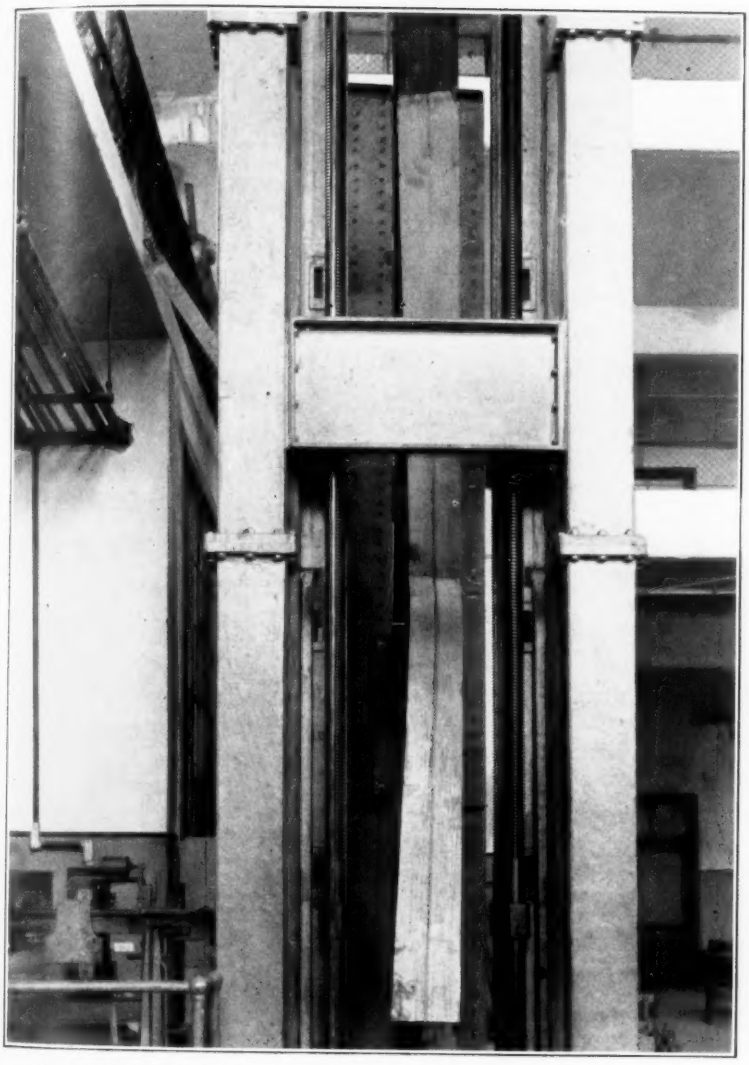

FIGURE 33.—*Rigid-frame specimen at the maximum load of 168,000 lb.*

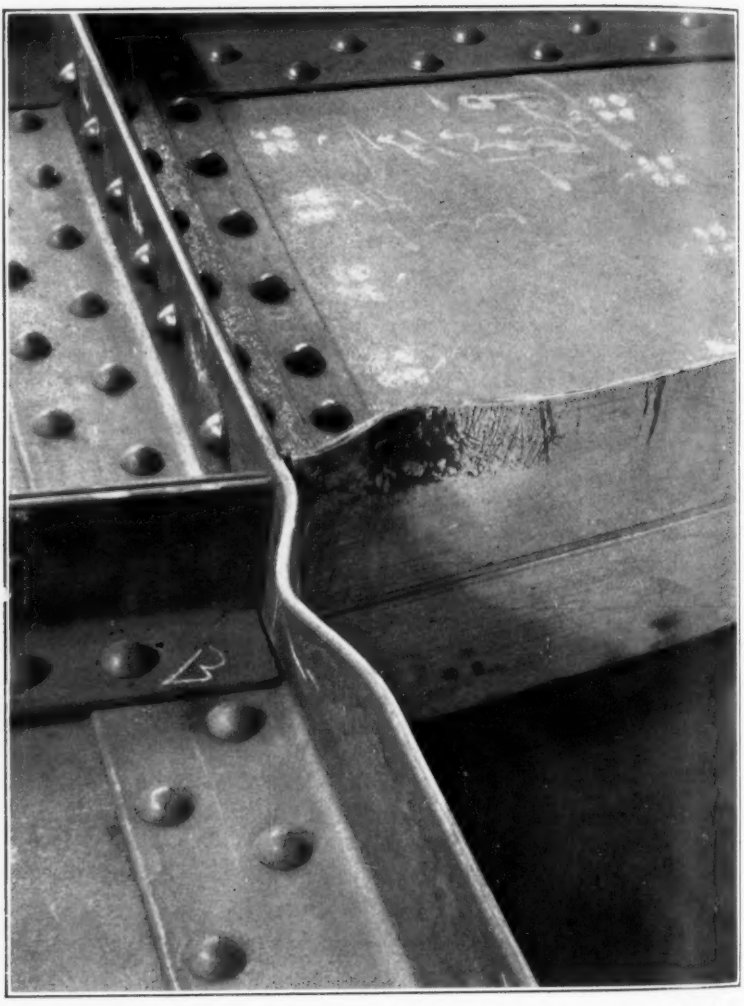

FIGURE 34.—*Inner corner of the knee of the rigid-frame specimen after failure.*

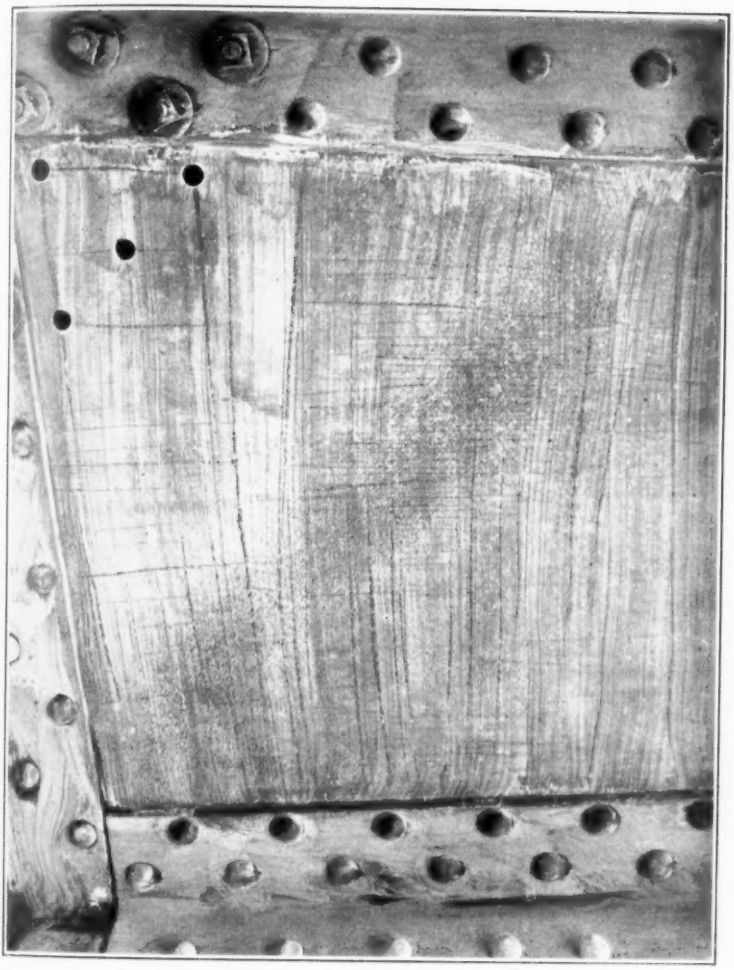

FIGURE 35.—*Knee web of the rigid-frame specimen after failure.*

UNIV. OF MICH.

2. The ordinary beam theory gives stresses in the legs in satisfactory agreement with those obtained experimentally.
3. The formulas developed for the computation of the stresses in the knee give stresses in satisfactory agreement with those obtained experimentally.
4. The material of the frame was so disposed as to develop its full yield strength in compression.
5. Bearing of the discontinuous inner flange against the continuous one, and of the latter against the stiffeners, is essential to prevent possibility of overstressing the webs.

X. APPENDIX—STRESSES FROM STRAIN DATA

In the case of plane stress three quantities are required to determine completely the state of stress at a point. These may be taken as two normal stresses and a shearing stress with respect to a given set of axes, or as the two principal stresses and the direction of one of them with respect to a given set of axes. In order to determine the state of stress from measurements of strain, in addition to the elastic constants of the material,[5] the strains at a point in at least three directions must be known. If the strains are known in more than three directions, the data are redundant, and the solution for the stresses may be obtained by the method of least squares or in some other way.

A graphical solution for the stresses from strains on three intersecting gage lines has been given by Osgood and Sturm [12]. The analytical solutions are summarized below.

Let ϵ denote strain and the subscript to ϵ the gage line along which the strain is measured. Gage lines 1 and 3 in figure 36 are at right angles to each other. Gage lines 2 and 4 are at right angles to each other and at 45° to gage lines 1 and 3. Gage lines a, b, and c in figure 37 are mutually at 120°. Then, if E is Young's modulus of elasticity, the following formulas give the maximum principal stress, σ_u; the minimum principal stress, σ_v; and the angle θ, measured

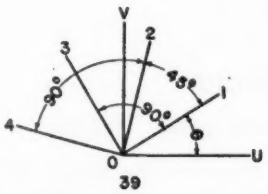

FIGURE 36.—*Four gage lines (1, 2, 3, 4) intersecting at 0. Directions (u, v) of principal stresses.*

As shown above, the angle θ is positive.

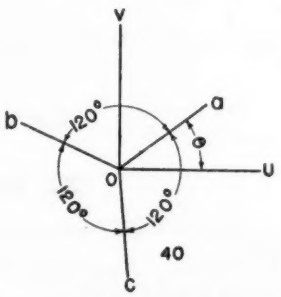

FIGURE 37.—*Three gage lines (a, b, c) intersecting at 0. Directions (u, v) of principal stresses.*

As shown above, the angle θ is positive.

[5] Young's modulus of elasticity and Poisson's ratio. A homogeneous isotropic material is assumed.

positive in the 123 or *abc* direction from the direction of σ_u to gage line 1, or gage line *a*.

Case 1.—Strains measured on gage lines 1, 2, 3, 4 [13, 14]. Poisson's ratio taken as 1/3.

$$\sigma_u=\frac{3}{8}E\left[\epsilon_1+\epsilon_2+\epsilon_3+\epsilon_4+\sqrt{(\epsilon_1-\epsilon_3)^2+(\epsilon_2-\epsilon_4)^2}\right],$$

$$\sigma_v=\frac{3}{8}E\left[\epsilon_1+\epsilon_2+\epsilon_3+\epsilon_4-\sqrt{(\epsilon_1-\epsilon_3)^2+(\epsilon_2-\epsilon_4)^2}\right],$$

$$\tan 2\theta=-\frac{\epsilon_2-\epsilon_4}{\epsilon_1-\epsilon_3}.$$

When the solution of these equations is required a large number of times, the work may be facilitated by the use of nomographic charts [15].

Case 2.—Strains measured on gage lines 1, 2, 3 ($\epsilon_4=\epsilon_1+\epsilon_3-\epsilon_2$ *in case 1*). *Poisson's ratio taken as 1/3.*

$$\sigma_u=\frac{3}{8}E\left[2(\epsilon_1+\epsilon_3)+\sqrt{(\epsilon_1-\epsilon_3)^2+(\epsilon_1-2\epsilon_2+\epsilon_3)^2}\right],$$

$$\sigma_v=\frac{3}{8}E\left[2(\epsilon_1+\epsilon_3)-\sqrt{(\epsilon_1-\epsilon_3)^2+(\epsilon_1-2\epsilon_2+\epsilon_3)^2}\right],$$

$$\tan 2\theta=\frac{\epsilon_1-2\epsilon_2+\epsilon_3}{\epsilon_1-\epsilon_3}.$$

Case 3.—Strains measured on gage lines a, b, c [16]. m=*Poisson's ratio.*

$$\sigma_u=E\left[\frac{1}{3(1-m)}(\epsilon_a+\epsilon_b+\epsilon_c)+\frac{\sqrt{2}}{3(1+m)}\sqrt{(\epsilon_a-\epsilon_b)^2+(\epsilon_b-\epsilon_c)^2+(\epsilon_c-\epsilon_a)^2}\right],$$

$$\sigma_v=E\left[\frac{1}{3(1-m)}(\epsilon_a+\epsilon_b+\epsilon_c)-\frac{\sqrt{2}}{3(1+m)}\sqrt{(\epsilon_a-\epsilon_b)^2+(\epsilon_b-\epsilon_c)^2+(\epsilon_c-\epsilon_a)^2}\right],$$

$$\tan 2\theta=\frac{\sqrt{3}(\epsilon_b-\epsilon_c)}{2\epsilon_a-\epsilon_b-\epsilon_c}.$$

XI. REFERENCES

[1] H. D. Hussey, *Rigid frames for bridges and buildings.* Am. Inst. Steel Const. (1937).

[2] C. D. Williams, *Rigid frame design by elementary mechanics.* Eng. News-Record **116,** 18 (1936).

[3] J. M. Frankland, *The analysis of multiple-span rigid frame bridges by Castigliano's Theorem.* Am. Inst. Steel Const. (1934).

[4] H. C. von Widdern, *Polarisationsoptische Spannungsmessungen an Stabecken.* Mitteilungen aus dem Mechanisch-Technischen Laboratorium der Technischen Hochschule München, No. 34, Theodor Ackermann, Munich.

[5] H. Kurzhals, *Polarisationsoptische Untersuchungen an rechtwinkeligen auf Biegung beanspruchten Stabecken.* Theodor Ackermann, Munich.

[6] F. E. Richart and T. A. Olson, *Rapid and long time tests on reinforced concrete knee frames.* J. Am. Concrete Inst. **8,** 474 (1937).

[7] *Standard specifications for steel for bridges.* Fig. 1, ASTM Standards pt. I, 4 (1936).
[8] L. B. Tuckerman, *Discussion on proportional limit.* Proc. Am. Soc. Testing Materials **29,** pt. II, 538 (1929).
[9] G. Grüning, *Spannungsverteilung in stählernen Rahmenecken.* Der Bauingenieur **18,** 158 (1937).
[10] S. Timoshenko, *Theory of elasticity,* Chap. 2. (McGraw-Hill Book Co., Inc., New York, N. Y., 1934.)
[11] *Specification for the design, fabrication, and erection of structural steel for buildings.* Steel Construction (Am. Inst. Steel Const. 259, New York, N. Y. 1937).
[12] Wm. R. Osgood and Rolland G. Sturm, *The determination of stresses from strains on three intersecting gage lines and its application to actual tests.* J. Research NBS **10,** 685 (1933) RP559.
[13] Wm. R. Osgood, *Determination of principal stresses from strains on four intersecting gage lines 45° apart.* J. Research NBS **15,** 579 (1935) RP851.
[14] Georg Schnadel, *Die Spannungsverteilung in den Flanschen dünnwandiger Kastenträger.* Jahrb. Schiffbautechnischen Ges. **27,** 246 (1926).
[15] Ambrose H. Stang and Martin Greenspan, *Graphical computation of stresses from strain data.* J. Research NBS **19,** 437 (1937) RP1034.
[16] O. S. Heck, *Untersuchung ebener Spannungszustände mit Hilfe von Dehnungsmessern.* Ing.-Arch. **8,** 30 (1937).

Washington, June 7, 1938.

U. S. Department of Commerce National Bureau of Standards

RESEARCH PAPER RP1131

Part of Journal of Research of the National Bureau of Standards, Volume 21, September 1938

PHASE EQUILIBRIA STUDIES ON MIXTURES OF THE COMPOUNDS $4CaO.Al_2O_3.Fe_2O_3$–$2CaO.Fe_2O_3$–$K_2O.Al_2O_3$

By William C. Taylor [1]

ABSTRACT

A portion of the system CaO–Al_2O_3–Fe_2O_3–K_2O has been investigated. The quenching method of study of phase equilibria was employed. No ternary compounds containing K_2O were observed. The compounds $K_2O.Al_2O_3$ and $4CaO.Al_2O_3.Fe_2O_3$ were found to form a binary system with one eutectic. Since it was observed that, for a given ratio of $4CaO.Al_2O_3.Fe_2O_3$ to $2CaO.Fe_2O_3$, the solid solution of these two compounds and $K_2O.Al_2O_3$ resembled a binary system with a single eutectic, these compounds are considered as forming a pseudobinary system. Pertinent optical and thermal data have been presented. Temperature-concentration diagrams for sections of the quaternary system are constructed.

CONTENTS

	Page
I. Introduction	315
II. Experimental method	316
III. Phase equilibria	317
1. The system $4CaO.Al_2O_3.Fe_2O_3$-$K_2O.Al_2O_3$	317
2. Relations of $4CaO.Al_2O_3.Fe_2O_3$-$2CaO.Fe_2O_3$	319
3. Relations of 90 percent of $4CaO.Al_2O_3.Fe_2O_3$, 10 percent of $2CaO.Fe_2O_3$-$K_2O.Al_2O_3$	320
4. Relations of 70 percent of $4CaO.Al_2O_3.Fe_2O_3$, 30 percent of $2CaO.Fe_2O_3$-$K_2O.Al_2O_3$	321
5. Relations of 50 percent of $4CaO.Al_2O_3.Fe_2O_3$, 50 percent of $2CaO.Fe_2O_3$-$K_2O.Al_2O_3$	322
6. General relations of $4CaO.Al_2O_3.Fe_2O_3$-$2CaO.Fe_2O_3$-$K_2O.Al_2O_3$	322
IV. Significance of the study in regard to the constitution of portland cement	323
V. Summary	324
VI. References	325

I. INTRODUCTION

Fundamental thermal studies on various systems of the components of portland cement have, for several years, occupied a prominent part in the program of the Portland Cement Association Fellowship at the National Bureau of Standards. Likewise, other workers have made important contributions in this field. Brownmiller and Bogue [1][2] present a comprehensive bibliography in this connection with their paper "The X-ray Method Applied to A Study of the Constitution of Portland Cement." These studies referred to, together with subsequent data obtained by Lea and Parker [2], Dahl [3], and

[1] Research Associate at the National Bureau of Standards, representing the Portland Cement Association Fellowship.

[2] Figures in brackets indicate the literature references at the end of this paper.

McMurdie and Insley [4], among others, form the basis of the present conception of the constitution of portland cement with reference to the principal oxides, namely, CaO, SiO_2, Al_2O_3, Fe_2O_3, and MgO.

Of the minor constituents, the alkalies, because of their prevalence, are probably the most important. It was found by the analyses of 23 commercial clinkers used in connection with a current study by the fellowship staff that Na_2O and K_2O each was present in all clinkers. The amount of the former varied from 0.1 to 0.7 percent, and the amount of the latter from 0.1 to 1.6 percent. The average percentage of each was 0.3 and 0.6, respectively. While these percentages in themselves are of small magnitude, combination of the alkalies with the other constituents may be such as to have a significant effect on the ratio of lime to the remaining acidic constituents available.

Accordingly, studies of systems involving the alkalies are being made as a continuation of the series undertaken for the purpose of establishing the constitution of portland cement clinker. The system CaO–Na_2O–Al_2O_3 has been examined by Brownmiller and Bogue [5] and the system CaO–K_2O–Al_2O_3 by Brownmiller [6].

It was found that $K_2O.Al_2O_3$ is the only compound of K_2O which is stable at the liquidus in the portion of the CaO–K_2O–Al_2O_3 system studied. This means that $K_2O.Al_2O_3$ will crystallize from the melt in all portions of the diagram which were studied. But this does not necessarily mean that $K_2O.Al_2O_3$ exists in portland cement clinker. Before the manner in which K_2O is combined in clinker can be predicted, thermal studies of systems involving $K_2O.Al_2O_3$ and the silica and the iron compounds of cement are necessary. The present investigation on a portion of the system CaO–Al_2O_3–Fe_2O_3–K_2O is one of such studies.

II. EXPERIMENTAL METHOD

Four series of base compositions were made. In each series the ratio of $4CaO.Al_2O_3.Fe_2O_3$ to $2CaO.Fe_2O_3$ (by weight) was constant but the $K_2O.Al_2O_3$ content varied. The ratios of $4CaO.Al_2O_3.Fe_2O_3$ to $2CaO.Fe_2O_3$ employed were 100:0, 90:10, 70:30, and 50:50. The percentage of $K_2O.Al_2O_3$ in the 100:0 series varied from 0 to 60, but in the other series from 0 to 25.

In preparing the base compositions, $4CaO.Al_2O_3.Fe_2O_3$ and $2CaO.Fe_2O_3$ were first made independently. These compounds were mixed in the desired proportions and then the Al_2O_3 and K_2O were added separately. Potassium oxalate was used as the source of K_2O since it is not hygroscopic and weighing difficulties are eliminated by its use. After the addition of Al_2O_3 and K_2O, the samples were burned at about 1,250° C for ½ hour. The amount of K_2O in the sample was checked by determining the weight difference before and after burning. Corrections were made when necessary. Potash does not appear to be volatilized rapidly after it has once combined and for that reason combination was first effected by the preliminary burning at temperatures not exceeding 1,250° C.

The small quenching charges were taken from the base samples which had been thoroughly ground after each step in the preparation. These charges were tightly enclosed in platinum foil, the edges of the foil being folded over at least three times. Heating was for as short a time as possible (15 to 20 minutes was found to be ample to bring about equilibrium) in order to avoid loss of potash. The consistency

with which various melting temperatures could be checked was accepted as evidence that the loss of K_2O resulting from this procedure was slight.

Very small samples were used because the utmost rapidity is required in quenching. Even so, in samples containing the high percentages of the iron compounds, quench growths were found to occur and interpretations had to be made accordingly. In most studies of systems containing Fe_2O_3, heretofore, the quenching method has been limited in use because of the rapid crystallization of the iron compounds. Thermal studies were made with heating curves. However, in the presence of alkalies, thermocouples are readily attacked and for this reason the quenching method is necessary.

The charges were suspended by a very fine platinum wire in the hot zone of a vertical platinum-rhodium resistance furnace. Temperatures were measured by means of a platinum, platinum-rhodium thermocouple connected with a Leeds and Northup potentiometer. Temperature control was effected by the use of a Robert's regulator [7]. Because of the susceptibility to attack by the potash, the thermocouple in use was calibrated frequently by comparison with a standard couple held in reserve, or by checking the melting points of eutectics in the CaO–Al_2O_3 system.

The common procedure of thermal study by the quenching method was followed, whereby the appearance of the sample under the petrographic microscope is used as a means for determining the condition of the charge at the temperature of the furnace just prior to the quenching.

The samples containing K_2O were found to be very hygroscopic and extreme precautions were necessary to avoid hydration of the quenches. The agate mortar and pestle with which they were ground had to be heated previously, and the portions to be examined transferred directly and quickly to the microscope slide.

III. PHASE EQUILIBRIA

1. THE SYSTEM $4CaO.Al_2O_3.Fe_2O_3$-$K_2O.Al_2O_3$

Only compositions within the range from 100 percent of $4CaO.Al_2O_3.Fe_2O_3$ to 60 percent of $4CaO.Al_2O_3.Fe_2O_3$—40 percent of $K_2O.Al_2O_3$ were investigated. In regions high in $K_2O.Al_2O_3$, complete melting of the charges occurs only at very high temperatures. At such temperatures a certain amount of uncertainty is felt as to the accuracy of the data obtained because of the likelihood of loss of K_2O by volatilization. Although varying amounts of K_2O are lost upon prolonged heat treatment, no dissociation of $K_2O.Al_2O_3$ was observed in the sense that there exists some definite dissociation temperature. Moreover, all of the information which may be pertinent to portland-cement composition can be obtained from that part of the system in which the percentages of K_2O are low, because cements are low in K_2O generally.

No evidence of any compounds other than $4CaO.Al_2O_3.Fe_2O_3$ and $K_2O.Al_2O_3$ was obtained. The results indicate that the system is a binary system with one eutectic having the composition 81 percent of $4CaO.Al_2O_3.Fe_2O_3$—19 percent of $K_2O.Al_2O_3$. The eutectic melts at 1,343° ±5° C. On the $K_2O.Al_2O_3$ side of this composition, the melting points rise very rapidly; the melting point of the composition

containing 25 percent of $K_2O.Al_2O_3$ being 1,520° ±5° C. The melting relations in this binary system are shown in table 1. In addition to the data given in the table, the eutectic melting temperature and composition were checked by observing the temperature at which liquid disappeared when compositions on each side of the eutectic composition were cooled from higher temperatures. A partial temperature-concentration diagram of this system is given in figure 1(A).

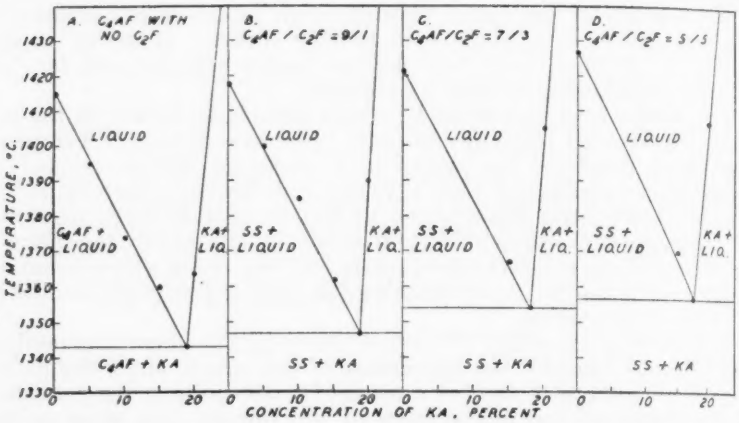

FIGURE 1.—*Temperature-concentration diagram showing the melting relations of* C_4AF *with* KA *and of solid solutions of* C_4AF+C_2F *(designated SS) with* KA.

TABLE 1.—*Thermal data relative to the system* C_4AF–KA

Composition		Temperature of quench	Examination
C_4AF	KA		
Percent	*Percent*	°C	
100	0	1,418	Glass; few quench growths.
		1,410	All crystalline.
95	5	1,400	Glass.
		1,391	Very small amount C_4AF; glass.
		1,340	All crystalline.
90	10	1,378	Glass.
		1,370	C_4AF; glass.
		1,348	Do.
		1,340	C_4AF; KA.
85	15	1,364	Glass; very few quench growths.
		1,356	C_4AF; glass.
		1,348	Do.
80	20	1,365	Glass.
		1,360	KA; glass.
		1,343	Very small amount of glass; KA; C_4AF.
75	25	1,520	Glass; only trace of KA.
		1,500	KA; glass.
70	30	1,560	Do.
		1,345	KA; glass; quench growths.
		1,340	KA; C_4AF.
60	40	1,340	KA; C_4AF; trace of glass.
40	60	1,580	KA; glass.

The compound $4CaO.Al_2O_3.Fe_2O_3$ apparently takes up some $K_2O.Al_2O_3$ in solid solution, inasmuch as there exists a difference in pleochroism of the $4CaO.Al_2O_3.Fe_2O_3$ grains in the absence and presence of $K_2O.Al_2O_3$. The amount of solid solution must be very limited, however, because only a slight change in the indices of refraction of the $4CaO.Al_2O_3.Fe_2O_3$ was observed. The compound $K_2O.Al_2O_3$, likewise, takes up some $4CaO.Al_2O_3.Fe_2O_3$ in solid solution. The grains of $K_2O.Al_2O_3$ containing $4CaO.Al_2O_3.Fe_2O_3$ show no birefraction, but the index of refraction has a value of 1.625 as compared with the index of 1.603, the value ascribed to the pure compound by Brownmiller [6]. It is doubtful that the amount of $4CaO.Al_2O_3.Fe_2O_3$ which goes into solution in the $K_2O.Al_2O_3$ is appreciable, because the $K_2O.Al_2O_3$ grains do not lose their isotropism. $K_2O.Al_2O_3$ was found to crystallize as colorless, rounded grains, which sometimes had the appearance of octahedrons. Possible further evidence of solid solution of $4CaO.Al_2O_3.Fe_2O_3$ was found in the optical properties of the $K_2O.Al_2O_3$ crystals contained in a charge of the composition 70 percent of $4CaO.Al_2O_3.Fe_2O_3$—30 percent of $K_2O.Al_2O_3$, which had been cooled slowly from 1,372° to 1,320° C. The index of the grains, in general, was about 1.625, but in some of the grains there were portions which appeared to have an index of about 1.61 or a trifle lower. No grains which had a index intermediate to the values 1.625 and 1.61 were observed. This would indicate that the slightest amount of solid solution is sufficient to raise the index to the maximum value of 1.625. Because the amounts of solid solution are indeterminate, the solid solutions are not indicated in figure 1(A), and the solidus is represented by a straight line.

2. RELATIONS OF $4CaO.Al_2O_3.Fe_2O_3$-$2CaO.Fe_2O_3$

Hansen, Brownmiller, and Bogue [8] found that $4CaO.Al_2O_3.Fe_2O_3$ and $2CaO.Fe_2O_3$ form a complete series of solid solutions. The temperature-concentration diagram as constructed by them is reproduced in figure 2. Ordinarily the figure demonstrating a complete

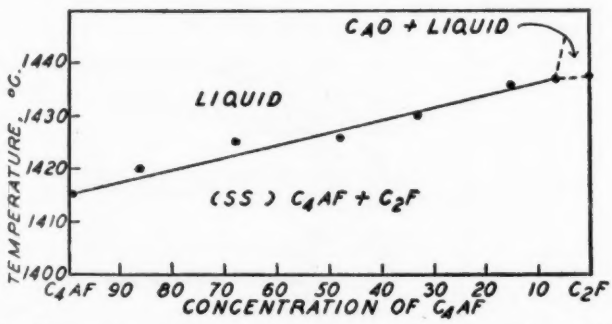

FIGURE 2.—*Temperature-concentration diagram showing the melting relations in the solid solution of* C_4AF *and* C_2F.

series of solid solutions consists of two curves, representing the liquidus and the solidus, respectively. In this particular case, these workers found that the melting range of the solid solutions could not be determined. The heating curve method of study was employed and

only one distinct break was obtained on each of the heating curves. The conclusion drawn was that the melting range of these solid solutions is very narrow, and, consequently the temperature-concentration diagram was constructed with a single curve.

3. RELATIONS OF 90 PERCENT OF $4CaO.Al_2O_3.Fe_2O_3$, 10 PERCENT OF $2CaO.Fe_2O_3$-$K_2O.Al_2O_3$

The series of compositions having the amounts of $4CaO.Al_2O_3.Fe_2O_3$ and $2CaO.Fe_2O_3$ in the definite ratio of 9:1, respectively, and in which the percentage of $K_2O.Al_2O_3$ varies, cannot be considered as a true binary system, although $4CaO.Al_2O_3.Fe_2O_3$ and $2CaO.Fe_2O_3$ do go into solid solution and separate as one phase. Strictly speaking, as the solid solution melts, there exists a difference in the compositions of the liquid and the remaining solid. But, as has been mentioned above, the melting range is very narrow and the difference in composition between the liquid and solid phases necessarily must be slight. Since, except for the most exacting interpretations, the relationships which obtain are similar to those of a binary system this may be referred to as forming a pseudobinary system. (For the same reason, compositions in which $4CaO.Al_2O_3.Fe_2O_3$ and $2CaO.Fe_2O_3$ are in some other definite ratio are treated as belonging to a pseudobinary system in conjunction with $K_2O.Al_2O_3$.)

The composition represented by the lowest point on the liquidus curve is 81.5 percent of $4CaO.Al_2O_3.Fe_2O_3+2CaO.Fe_2O_3$ (73.35 percent of $4CaO.Al_2O_3.Fe_2O_3$, 8.15 percent of $2CaO.Fe_2O_3$) and 18.5 percent of $K_2O.Al_2O_3$. The melting point of this mixture is 1,347° ±5°C.

TABLE 2.—*Thermal data relative to mixtures of* C_4AF+C_2F (*9 to 1*)-KA

Composition			Temperature of quench	Examination
C_4AF	C_2F	KA		
Percent	*Percent*	*Percent*	*°C*	
90	10	0	1,420	Quench growths; glass.
			1,415	All crystalline.
85.5	9.5	5.0	1,410	Only trace of biref. iron material, believed to be quench growths; glass.
			1,395	Solid solution C_4AF+C_2F; glass.
			1,351	Solid solution C_4AF+C_2F; glass.
			1,345	All crystalline.
81.0	9.0	10.0	1,390	Glass.
			1,385	Trace of solid solution C_4AF+CA_2F; glass.
			1 346	Trace of glass; solid solution C_4AF+C_2F; KA.
			1,343	All crystalline.
76.5	8.5	15.0	1,380	Glass.
			1,370	Do.
			1,365	Do.
			1,360	Solid solution C_4AF+C_2F; glass.
			1,355	Do.
			1,343	All crystalline.
72.0	8.0	20.0	1,390	Trace of KA; glass.
			1,380	KA; glass.
			1,370	Do.
			1,360	Do.
			1,350	Do.
67.5	7.5	25.0	1,530	Glass.
			1,520	KA; glass.
			1,354	Do.
			1,346	Trace of glass; KA; solid solution C_4AF+C_2F.

The melting relations are given in table 2 and the temperature-concentration diagram is shown in figure 1(B). It will be observed that the same type of temperature-concentration relationships obtain as those which hold for the $4CaO.Al_2O_3.Fe_2O_3$–$K_2O.Al_2O_3$ system without the $2CaO.Fe_2O_3$.

The index of $K_2O.Al_2O_3$ was found to be 1.625. The birefracting iron-bearing phase had the indices; α_{Li} 1.98 and γ_{Li} about 2.05. These indices agree closely with those determined by Hansen, Brownmiller, and Bogue [8] for this particular solid solution.

4. RELATIONS OF 70 PERCENT OF $4CaO.Al_2O_3.Fe_2O_3$, 30 PERCENT OF $2CaO.Fe_2O_3$–$K_2O.Al_2O_3$

The melting points of compositions in this series are slightly higher than those of comparable compositions of the preceding series. The composition 82 percent of $4CaO.Al_2O_3.Fe_2O_3$+$2CaO.Fe_2O_3$ (57.4 percent of $4CaO.Al_2O_3.Fe_2O_3$, 24.6 percent of $2CaO.Fe_2O_3$) and 18 percent of $K_2O.Al_2O_3$, which melts at 1,354° ± 5°C, is the lowest-melting composition. No additional compounds were observed. $K_2O.Al_2O_3$ grains retain their index of 1.625. The minimum index for lithium light of the crystalline solid solution of $4CaO.Al_2O_3.Fe_2O_3$ and $2CaO.Fe_2O_3$ was found to be about 2.05. This value is very close to that which was read from the diagram constructed by Hansen, Brownmiller, and Bogue [8] in which the indices of refraction of the solid solutions are plotted against composition. The thermal relations of compositions in this pseudobinary system are given in table 3 and the graphic interpretation is shown in figure 1(C).

TABLE 3.—*Thermal data relative to mixtures of* C_4AF+C_2F *(7 to 8)*–KA

Composition			Temperature of quench	Examination
C_4AF	C_2F	KA		
Percent	*Percent*	*Percent*	°C	
70.0	30.0	0.0	1,425	Glass; quench growths.
			1,420	Mostly crystalline; trace of glass.
66.5	28.5	5.0	1,430	Glass; quench growths.
			1,420	Do.
			1,410	Do.
			1,362	Solid solution C_4AF+C_2F; glass.
			1,357	Solid solution C_4AF+C_2F; small amount of glass.
			1,353	Solid solution C_4AF+C_2F; KA; only trace of glass.
			1,340	All crystalline.
63.0	27.0	10.0	1,420	Glass; quench growths.
			1,410	Do.
			1,357	Solid solution C_4AF+C_2F; glass.
			1,350	All crystalline.
59.5	25.5	15.0	1,380	Glass.
			1,370	Do.
			1,365	Solid solution C_4AF+C_2F; glass.
			1,357	Solid solution C_4AF+C_2F; KA; small amount of glass.
			1,350	All crystalline.
56.0	24.0	20.0	1,410	Glass.
			1,400	KA; glass.
			1,390	Do.
52.5	22.5	25.0	1,520	Trace of KA; glass.
			1,510	KA; glass.
			1,357	Poorly defined crystals; some glass.
			1,350	All crystalline.

5. RELATIONS OF 50 PERCENT OF $4CaO.Al_2O_3.Fe_2O_3$, 50 PERCENT OF $2CaO.Fe_2O_3$-$K_2O.Al_2O_3$

The same relationships hold for this pseudobinary system as for the preceding systems in which one component is composed of $4CaO.Al_2O_3.Fe_2O_3$ and $2CaO.Fe_2O_3$ in a definite proportion. The melting points are, in general, increased as a result of the increased amount of $2CaO.Fe_2O_3$ in the solid solution. The composition of the lowest-melting compostion is 82.5 percent of $4CaO.Al_2O_3.Fe_2O_3+2CaO.Fe_2O_3$ (41.25 percent of $4CaO.Al_2O_3.Fe_2O_3$, 41.25 percent of $2CaO.Fe_2O_3$) and 17.5 percent of $K_2O.Al_2O_3$. It melts at 1,357° ± 5°C. The data pertaining to the quenches in this system are shown in table 4, and the temperature-concentration diagram in figure 1(D). The index of $K_2O.Al_2O_3$, as in the preceding systems, was 1.625. The minimum index for lithium light of the crystalline iron-bearing material was slightly less than 2.10, probably 2.08. This value, likewise, is in close agreement with that reported by Hansen, Brownmiller, and Bogue.

TABLE 4.—*Thermal data relative to mixtures of* C_4AF+C_2F *(5 to 5)*–KA

Composition			Temperature of quench	Examination
C_4AF	C_2F	KA		
Percent	*Percent*	*Percent*	*°C*	
50	50	0		Melting temperature 1,427° C, according to Hansen, Brownmiller, and Bogue.
47.5	47.5	5.0	1,357	Few quench growths; mostly crystalline.[1]
45.0	45.0	10.0	1,357	Do.[1]
42.5	42.5	15.0	1,380	Glass.
			1,370	Trace solid solution C_4AF+C_2F; glass.
40.0	40.0	20.0	1,410	Glass.
			1,405	KA; glass.
			1,357	KA; some solid solution C_4AF+C_2F; trace of glass.
37.5	37.5	25.0	1,530	Glass.
			1,520	Trace KA; glass.
			1,515	Much KA; glass.

[1] Quenches of samples containing less than 15 percent of KA were very unsatisfactory.

6. GENERAL RELATIONS OF $4CaO.Al_2O_3.Fe_2O_3$-$2CaO.Fe_2O_3$-$K_2O.Al_2O_3$

No compounds of potash other than $K_2O.Al_2O_3$ were found to exist at equilibrium in the region studied. The compound $4CaO.Al_2O_3.Fe_2O_3$ is stable in the presence of $K_2O.Al_2O_3$ and forms a series of solid solutions with $2CaO.Fe_2O_3$ as it does in the absence of $K_2O.Al_2O_3$. Figure 3 is the diagram showing the fields of primary crystallization and the 1,400° and 1,500° C isotherms. The boundary curve separating the field of $K_2O.Al_2O_3$ from the field of the solid solutions of $4CaO.Al_2O_3.Fe_2O_3$ and $2CaO.Fe_2O_3$ may be considered as defining the lowest-melting compositions which will exist in any mixture of $K_2O.Al_2O_3$, $4CaO.Al_2O_3.Fe_2O_3$, and $2CaO.Fe_2O_3$ in which the ratio of $4CaO.Al_2O_3.Fe_2O_3$ to $2CaO.Fe_2O_3$ does not exceed 1.0 (the limit of the region studied). It will be seen that the percentage of $K_2O.Al_2O_3$ present in the lowest-melting compositions decreases slightly as the ratio of $4CaO.Al_2O_3.Fe_2O_3$ to $2CaO.Fe_2O_3$ decreases. There is a small rise in the melting temperatures of these compositions as the ratio of $4CaO.Al_2O_3.Fe_2O_3$ to $2CaO.Fe_2O_3$ decreases, as shown in

figure 1. The temperatures required for complete melting of the compositions in the field in which $K_2O.Al_2O_3$ is the primary phase, increase very sharply as the percentage of $K_2O.Al_2O_3$ increases.

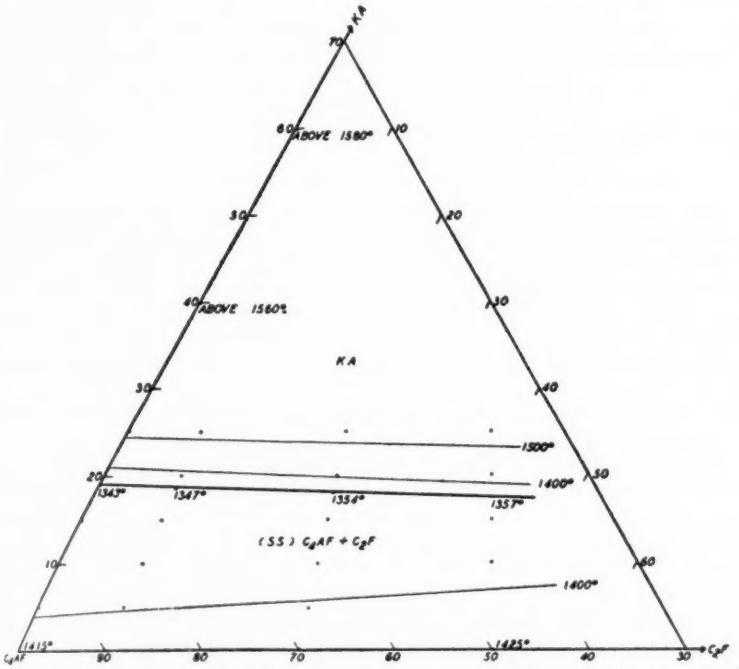

FIGURE 3.—*Diagram showing fields of primary crystallization and isotherms with mixtures of* C_4AF, C_2F, KA.

IV. SIGNIFICANCE OF THE STUDY IN REGARD TO THE CONSTITUTION OF PORTLAND CEMENT

Although the alkalies generally are referred to as being among the minor constituents of portland cement clinker, it is recognized that K_2O and Na_2O may combine with other oxides present in such a manner as to be of great effect in determining the ultimate composition. It was found in a study of the influence of K_2O on the burnability of cement compositions in this laboratory [9] that, although the first small increments of K_2O favored combination, higher free-lime values obtained in clinkers burned at a definite temperature as K_2O was substituted for like percentages of CaO beyond an optimum value. This optimum amount was found to vary with the composition of the base mixture, but, generally was less than 1 percent. A typical example is given in table 5.

TABLE 5.—*The effect of varying amounts of* K_2O *on the combination of* CaO *at a definite temperature*

Percentage composition of mixture					Burning temperature	Free CaO
CaO	K_2O	Al_2O_3	Fe_2O_3	SiO_2		
					°C	*Percent*
67.0	0.0	7.5	2.5	23.0	1,450	1.1
66.5	.5	7.5	2.5	23.0	1,450	.5
66.0	1.0	7.5	2.5	23.0	1,450	1.8
65.0	2.0	7.5	2.5	23.0	1,450	4.3
64.0	3.0	7.5	2.5	23.0	1,450	7.3

The manner in which K_2O is combined in portland cement clinker is to be established, step by step, by a series of phase-equilibria studies involving K_2O and the other constituents. The results of Brownmiller's investigation of the system $CaO–K_2O–Al_2O_3$ show that $K_2O.Al_2O_3$ is the only compound of K_2O in that system which exists in compositions related to portland-cement compositions. This study shows that $K_2O.Al_2O_3$ likewise is stable in the presence of $4CaO.Al_2O_3.Fe_2O_3$. Furthermore, the compound $K_2O.Al_2O_3$ can exist in the presence of $2CaO.Fe_2O_3$, which may be present in rare instances in cements having an Al_2O_3: Fe_2O_3 ratio less than 0.64.

Phase equilibria studies on mixtures of $K_2O.Al_2O_3$ and the other constituents of cement clinker necessarily must follow. In the event that such studies indicate that $K_2O.Al_2O_3$ is stable in the presence of $3CaO.SiO_2$ and $2CaO.SiO_2$, then it may be that $K_2O.Al_2O_3$ exists in clinker. On the other hand, if $K_2O.Al_2O_3$ reacts with any of these compounds to form a new combination, such as $xCaO.yK_2O.zSiO_2$ or $xK_2O.ySiO_2$, then it will be necessary to study the relations of that combination with the various cement constituents $3CaO.Al_2O_3$, $4CaO.Al_2O_3.Fe_2O_3$, etc.

In view of recent discoveries by Insley and McMurdie (10), the latter condition appears to be likely. With the development of the technique for examining polished sections of clinkers in reflected light, these workers have observed a dark prismatic interstitial material in many commercial cement clinkers. It was found that this material did not occur in alkali-free laboratory preparations, but did exist if either or both Na_2O and K_2O were present. The mean refractive index of this weakly birefracting phase was found to be near 1.72. No crystals possessing optical properties similar to those of $K_2O.Al_2O_3$ were observed.

Although the treatment in this paper has been concerned exclusively with equilibrium crystallization of the phases studied, it should not be lost sight of that clinker contains varying amounts of glass and that this glass may contain a part or all of the alkali components. The degree of crystallization of the alkali phases at any temperature can only be determined through further study of the course of crystallization now in progress.

V. SUMMARY

A portion of the quaternary system $CaO–Al_2O_3–Fe_2O_3–K_2O$ has been investigated. The quenching method of study was employed for the determination of temperature relations. The results of thermal and optical studies are presented.

No additional compounds were observed in the regions studied. The maximum index of refraction of $K_2O.Al_2O_3$ in the presence of the iron compounds is 1.625.

The compounds $4CaO.Al_2O_3.Fe_2O_3$ and $K_2O.Al_2O_3$ form a binary system with one eutectic.

For a given ratio of $4CaO.Al_2O_3.Fe_2O_3$ to $2CaO.Fe_2O_3$, the solid solution of these two compounds and $K_2O.Al_2O_3$ form a pseudobinary system with a definite lowest-melting composition.

Detailed thermal data are given.

Temperature-concentration diagrams for the various series were constructed.

The author gratefully acknowledges the assistance given by L. T. Brownmiller, formerly of this staff, who began this study and advised in outlining the procedure for its continuance.

VI. REFERENCES

[1] L. T. Brownmiller and R. H. Bogue, BS J. Research **5,** 813 (1930) RP233; Am. J. Sci. **20,** 241 (1930).
[2] F. M. Lea and T. W. Parker, Bldg. Research Tech. Pap. 16 (1935).
[3] L. A. Dahl, Rock Products **35,** No. 12, 31 (1932).
[4] H. F. McMurdie and H. Insley, J. Research NBS **16,** 467 (1936) RP884.
[5] L. T. Brownmiller and R. H. Bogue, BS J. Research **8,** 289 (1932) RP414; Am. J. Sci. **23,** 501 (1932).
[6] L. T. Brownmiller, Am. J. Sci. **29,** 260 (1935).
[7] Adams, J. Opt. Soc. Am. **9,** 599 (1924).
[8] W. C. Hansen, L. T. Brownmiller, and R. H. Bogue, J. Am. Chem. Soc. **50,** 396 (1928).
[9] W. C. Taylor, Unpublished data.
[10] H. Insley and H. F. McMurdie, J. Research NBS **20,** 173 (1938) RP1074.

WASHINGTON, March 18, 1938.

U. S. DEPARTMENT OF COMMERCE NATIONAL BUREAU OF STANDARDS

RESEARCH PAPER RP1132

Part of Journal of Research of the National Bureau of Standards, Volume 21, September 1938

QUANTITATIVE FORMATION OF FURFURAL FROM XYLOSE

By Elizabeth E. Hughes and S. F. Acree

ABSTRACT

A study has been made of various methods of distillation of solutions of furfural and of xylose with the object of increasing the 88-percent yield of furfural obtained from xylose by the present standard method of distillation. Sources of error that have been considered are: Decomposition of furfural, volatilization of furfural, effect of rubber stoppers used in the distillation procedure, incompleteness of distillation, furfural formed from hexuronic acid, and substances other than furfural or methylfurfural in the distillate.

A procedure has been developed which prevents superheating of the solution but which gives rapid formation and removal of the furfural. The apparatus has only glass in contact with the hot vapors and acid, and is closed with a trap to prevent evaporation from the distillate. The procedure employs 12-percent hydrochloric acid saturated with sodium chloride to accelerate the formation of furfural, which is then removed by steam distillation. This prevents decomposition of the furfural and gives a practically theoretical yield of furfural from xylose.

CONTENTS

	Page
I. Introduction	327
II. Sources of error in pentosan determinations	328
1. Loss of furfural by volatilization	328
2. Decomposition of furfural	329
3. Use of rubber stoppers	330
4. Tests to determine furfural in the distillate	331
5. Oxycellulose (hexuronic acid) in the fibers	331
6. Presence of substances other than furfural or methylfurfural in the distillate	331
III. Yields of furfural from furfural solutions and from xylose by varying the method of distillation	332
IV. Procedure used for obtaining 100-percent yields of furfural from xylose	334
V. References	336

I. INTRODUCTION

The present methods for the determination of pentosans in natural products depend upon their change to pentoses and methylpentoses, and in turn to furfural and methylfurfural, by boiling them with 12-percent hydrochloric acid and removing the aldehydes for analysis from the reaction vessel by simple distillation. If hexose compounds are present some hydroxymethylfurfural may also appear in the distillate.

Before attempting to analyze the distillates obtained from the boiling of fibrous materials, it seemed advisable to replace the phloro-

glucinol precipitation method of determining the aldehydes prescribed in the standard procedure [1][1] with a more rapid and sensitive method for determining and differentiating the furfural, methylfurfural, and hydroxymethylfurfural. For this purpose the bromate method of analysis was developed to apply to solutions of pure furfural, methylfurfural, and mixtures of these. The results have been published [2]. It seemed desirable to apply the same analytical method to the distillates of pure pentoses, for example, xylose, arabinose, and rhamnose, and to determine the corresponding yields of aldehydes from these sugars.

It is known that by employing the standard method of direct distillation with 12-percent hydrochloric acid, xylose and arabinose give different yields of furfural. Most workers report about 88 percent of the theoretical yield of furfural from xylose and about 75 percent from arabinose. The low yields have been ascribed to the destruction of furfural by the action of the hot hydrochloric acid, although Kullgren and Tyden [3] in their comprehensive studies believed that the equation for the conversion of pentose to furfural does not adequately represent the changes taking place. The theoretical yields of furfural from xylose reported by Jolles [4] and by Pervier and Gortner [5] have been questioned by many workers in this field who have tried without success to reproduce their results. The titrimetric methods used for their analyses have since been found subject to error because of varying temperatures. For this reason it is believed that their analytical methods may have given high results and thus compensated for actually lower yields. Although Pervier and Gortner developed their electrometric bromate titration method to give concordant results with pure furfural solutions, they reported a yield of 95 percent of furfural from xylose by the standard method of distillation, which is not in agreement with the 88 percent found by other workers and ourselves. If the 95 percent found by them is actually the 88 percent obtained by this distillation procedure, then their high results may be attributable to over-oxidation in the electrometric bromate titration at room temperatures, as found by Magistad [6] and ourselves [2]. For this reason, their reported theoretical yields of furfural obtained by steam distillation from xylose and arabinose may be correspondingly high. Their work has been very helpful, however, in indicating that some changes in the method of distillation might bring about higher yields. The method of Kullgren and Tyden, modifying the distillation procedure by saturating the hydrochloric acid with sodium chloride, thereby accelerating the reaction, also pointed the way to improvements in the distillation procedure. In line with these suggestions, the present authors tried several other methods of distillation on solutions of pure furfural and pure xylose.

II. SOURCES OF ERROR IN PENTOSAN DETERMINATIONS

1. LOSS OF FURFURAL BY VOLATILIZATION

The standard method of distillation, as previously used, allows the distillate to drop from the end of the condenser into the receiver without special precaution against loss by volatilization. That appreciable losses may occur, however, was observed by Kline and Acree [7].

[1] Figures in brackets indicate the literature references at the end of this paper.

This error can be prevented by the use of equipment designed for the purpose, such as that illustrated in figure 1.

The effectiveness of the small scrubber trap, 4, figure 1, in collecting furfural vapors was tested. Air was slowly bubbled through 200 ml of solution containing 25 mg of furfural in a titration flask, and then passed through the trap. An analysis showed that the solution in the flask contained about 2 percent less furfural than before the passage of the air. This amount was found in the trap. Larger traps may be used for more rapid distillations.

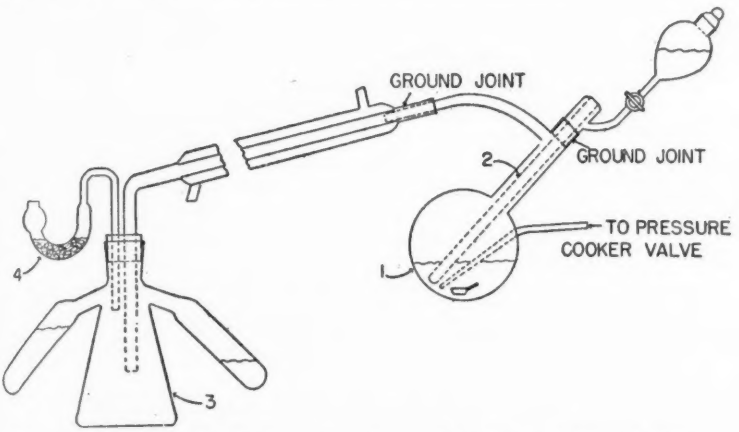

FIGURE 1.—*Steam distillation apparatus used for furfural determinations.*

1, distillation flask; 2, thermometer well; 3, titration flask; and 4, scrubber trap containing water and Raschig Pyrex rings.

2. DECOMPOSITION OF FURFURAL

To prevent decomposition or polymerization of the furfural by prolonged contact with the hot acid in the distillation flask, a modification of the standard procedure was tried. A stream of air was passed through the distillation flask during the distilling process at a rate of approximately 80 ml a minute. This modification of the standard method did not increase the yield of furfural and the presence of 1 percent of the furfural in the trap showed that the use of air was undesirable. A decided improvement was observed when steam was substituted for the air.

Direct distillation with a flame may cause local superheating and may be responsible for decomposition of some of the furfural. Some workers have recognized this source of possible error and have used calcium chloride, metal, and oil baths for heating, but the authors prefer an easily controlled electric cone heater [2] in which the distillation flask may be placed.

That superheating in hot acid may be responsible in part for the low yields obtained from the pentoses by ordinary distillation methods was indicated by a series of experiments including the use of different temperatures for the distillation of pure furfural solutions. The fur-

[2] A general purpose 350-w electric heater, Aminco No. 1521-01, and laboratory rheostat, Aminco No. 1522-02, were used in these experiments.

fural was purified by the method previously described [2]. The results are given in table 1.

TABLE 1.—*Effect of distillation method on recovery of furfural*

Solution in flask	Furfural found in control [2]	Furfural found in distillate	Recovery distillate control
	METHOD *A* [1]		
	g	*g*	*Percent*
Water	0.07178	0.07120	99.2
12-percent HCl (103° to 108° C)	.07186	.06950	96.7
	METHOD *B* [1]		
Water (115° C)	0.1037	0.1033	99.6
	.07449	.07344	98.6
	.1039	.1018	98.0
	.1039	.1022	98.4
12-percent HCl (115° C)	.07341(a)	.06812	92.8
	.2931 (b)	.2714	92.6
	.2827 (c)	.2681	94.8

[1] *A*, standard distillation method using 100 ml of solution in 350-ml flask; flame heat. Furfural added to solution slowly through separatory funnel, adding more water or 12-percent hydrochloric acid, respectively, as needed, until 400 ml of distillate was obtained; *B*, special distillation flask suspended within steam chamber (18-quart household pressure cooker). Furfural added in one lot to 250 ml of solution in flask; cooker closed and heated to a gage pressure of 10 pounds per square inch (115° C). 600 ml of distillate collected for (a), 1,000 ml for (b), and 1,200 ml for (c). Trap contained 0.00161, 0.00139, and 0.00192 gm of furfural, respectively, for (a), (b), and (c).

[2] Control contained the same amount of furfural placed in the titration flask which was allowed to stand on bench during the distillation so that the distillate and control were subjected to similar conditions except the distillation procedure.

In method *A*, involving the standard distillation procedure, excess local heating was indicated by darkening of the solutions even though heat was applied at a continuous rate. Losses of about 3 percent of furfural were observed when it was distilled from 12-percent hydrochloric acid, and of about 0.8 percent when distilled from water. In method *B* the heat was applied to the distillation flask by suspending it in a chamber of steam at a 10-pound gage pressure per square inch (115° C). The average losses were greater at this higher temperature.

3. USE OF RUBBER STOPPERS

Early in the studies of xylose at this Bureau, Mary T. Kanagy found that, when rubber stoppers are used in contact with the hot vapors of hydrochloric acid, a volatile substance could be detected which reacted with bromine. This was further confirmed by the authors, who found that when 2 g of ground rubber was distilled with 12-percent hydrochloric acid, 0.32 ml of 0.1 *N* potassium bromate-bromide solution was required by 200 ml of distillate, if the bromine titration was made as for furfural determinations.

By actual experiment it was found that when ordinary rubber stoppers were used for closing the distillation flask, an error of magnitude corresponding to 0.04 to 0.06 ml of 0.1 *N* standard potassium bromate-bromide solution for every 200 ml of distillate was produced. For accurate work, ground-glass joints are preferred for connections which may come in contact with the hot vapors. However, a two-hole rubber stopper was used at the end of the condenser to hold the trap and close the receiving flask. (See fig. 1.)

4. TESTS TO DETERMINE FURFURAL IN THE DISTILLATE

In determining the end point of the formation of furfural during the distillation, the procedure generally recommended is to test a few drops of the distillate with a solution of aniline acetate or of aniline in alcohol, or with aniline hydrochloride paper. The distillation is continued until the test no longer shows a pink color.

Considerable work has been done by Cunningham and Dorée [8] on the color reactions of furfural, methylfurfural, and hydroxymethylfurfural produced from the pentoses, hexoses, and from cellulose. The importance of adjusting the pH of the solution in developing the color for the test apparently has been overlooked.

The hydrochloric acid in the furfural distillate is excessive for the test and causes decided suppression or even prevention of the characteristic selective light absorption even though a considerable amount of furfural be present. The test should therefore be performed by neutralizing 0.5 to 1 ml of the distillate with standard alkali and phenolphthalein and adding it to a 1-ml portion of a mixture of 1 ml of freshly distilled aniline, 9 ml of glacial acetic acid, and 10 ml of water. The pH of this solution is about 3, which is the optimum for the test. Lack of appearance of a pink color in 5 to 15 minutes indicates absence of appreciable quantity of furfural.

5. OXYCELLULOSE (HEXURONIC ACID) IN THE FIBERS

In the distillation of fibers any hexuronic acid naturally present or formed in bleaching operations gives rise to some furfural and an equivalent of carbon dioxide. By collecting the carbon dioxide in special equipment [9] and determining its amount, or by direct titration of the hexuronic acid in the fibers, it may be differentiated from pentosans.

6. PRESENCE OF SUBSTANCES OTHER THAN FURFURAL OR METHYLFURFURAL IN THE DISTILLATE

In the determination of the aldehydes from pure pentoses, one is concerned only with furfural from xylose or arabinose, or methylfurfural from rhamnose. When fibers, pulps, or hexoses are distilled, however, as is the case for pentosan determinations, it has been shown by many workers [3, 8, 10, 11] that hydroxymethylfurfural may be present in the distillate. This is a source of error in all existing procedures, and its magnitude is subject to question. Kullgren and Tyden, who also used a modification of the bromate method for their analyses, redistilled the distillate to decompose the hydroxymethylfurfural. They claim that this also destroys about 33 percent of the methylfurfural, and about 3 percent of the furfural, for which they make a correction.

It has been claimed that barbituric acid does not precipitate hydroxymethylfurfural in dilute acid solutions [12], but Schmidt-Neilson and Hammer [13] obtained a precipitate with pure hydroxymethylfurfural. The authors have made some preliminary studies on hydroxymethylfurfural produced by the distillation of glucose and

find that, taking the bromate titer for the 5-minute reaction period at 0° C as 100 percent, as used for furfural, there is an increased bromine consumption of about 14 percent in 30 minutes and of about 27 percent in 60 minutes. Since these values are between those for furfural (2 and 3 percent, respectively) and those for methylfurfural (57 and 70 percent, respectively), and the three curves for time versus moles of consumed bromine have different shapes, it is believed that the bromate method can be applied to mixtures of the three aldehydes in the manner previously described [2] for furfural and methylfurfural. Considerable work on pure hydroxymethylfurfural is necessary, however, for devising exact methods of analyzing mixtures of the three aldehydes. Work on the distillates from arabinose and rhamnose is in progress.

III. YIELDS OF FURFURAL FROM FURFURAL SOLUTIONS AND FROM XYLOSE BY VARYING THE METHOD OF DISTILLATION

Several forms of equipment for the production of furfural from xylose and for the recovery of furfural from solutions were tried, including the standard distillation equipment previously used, a simple steam-distillation flask, an especially designed percolator type of steam-distillation flask, and a distillation flask designed to receive the steam while enclosed in a steam chamber. In each experiment the distillation flask was fitted by means of a ground-glass joint with a glass condenser having a straight condenser tube approximately 50 cm long and of 1.2 cm internal diameter. The distillate was received in a sealed titration flask fitted as shown at 3, figure 1.

To test the efficiency of the different distillation procedures in the recovery of furfural from solutions, a standard solution of furfural was prepared by accurately weighing, with special precautions [2], a definite amount of furfural and dissolving it in a measured volume of water. One aliquot portion of the standard solution was added to the distillation flask containing water for some experiments, and 6- or 12-percent hydrochloric acid for others, with and without the addition of sodium chloride.

The results given in table 2 show that almost complete recovery of furfural was obtained with all forms of steam distillation applied. The effects of slow steam distillation, standard distillation, and slow steam distillation with the addition of sodium chloride on the conversion of xylose to furfural and its recovery are shown in table 3.

TABLE 2.—*Recovery of furfural by steam distillations*

Solution in flask	Furfural used	Furfural recovered
	g	*Percent*
METHOD *C*[1]		
Water	0.05076	100.3
	.05267	100.2
	.05460	100.1
	.05460	99.9
3-percent HCl	.05277	100.2
	.05277	100.2
6-percent HCl	.05149	100.1
	.05149	99.5
	.05149	100.2
12-percent HCl	.05149	100.5
	.05149	99.5
	.05499	98.6
	.05499	99.3
	.09992	99.3
	.09992	99.5
12-percent HCl with NaCl added	.05499	99.8
	.1100	98.6
METHOD *D*[1]		
12-percent HCl	0.02864	100.4
	.03580	99.4
	.03914	100.5
	.05440	100.2
16-percent HCl	.07160	99.4
	.08072	99.4

[1] *C*, all distillations made using 500-ml steam-distillation flask with ground joints; very slow steam distillation; flask heated by electric cone heater. Furfural added in one lot to 250 ml of solution; 200-ml portions of distillate collected in titration flask previously prepared with potassium bromate-bromide and potassium iodide solutions; and *D*, a special percolator type of steam-distillation apparatus; very slow steam distillation; special electric spiral heater. Furfural added in one lot to 75 ml of solution; 200-ml portions of distillate collected as in *C*.

TABLE 3.—*Furfural yields from xylose by various methods of distillation*

Solution in flask	Amount of xylose present	Number of fractions	Total distillate	Furfural yield
	g		*ml*	*Percent*
METHOD *A*[1]				
12-percent HCl	0.2314	7	350	87.4
	.2002	2	330	89.8
	.2046	5	1,050	89.8
METHOD *C*[1]				
12-percent HCl	0.2056	4	860	92.6
	.2006	6	1,200	92.3
	.2020	7	1,400	92.3
	.5003	1	1,800	92.0
	.2214	15	3,000	94.0
12-percent HCl with NaCl	.2035	4	875	94.6
	.2046	5	1,000	94.1
	.2050	4	1,000	95.1
	.1940	7	2,000	95.3

[1] See footnote at end of table.

TABLE 3.—*Furfural yields from xylose by various methods of distillation*—Continued

Solution in flask	Amount of xylose present	Number of fractions	Total distillate	Furfural yield
	METHOD *D*[1]			
	g		*ml*	*Percent*
12-percent HCl	.1274	4	800	93.9
	.0545	7	1,400	93.2
	.1566	3	3,000	94.1
6-percent HCl with NaCl	.2525	2	2,000	92.7
	.2610	2	1,400	95.5
12-percent HCl with NaCl	.1512	8	1,650	95.6
	.2715	2	2,000	96.5
	.1495	9	2,040	96.3
	.1502	10	2,120	96.5

[1] *A*, standard distillation method using 350-ml and 500-ml flasks with 100 and 250 ml of solution, respectively; flame heat; more acid added to distillation flask as needed; *C*, slow steam distillation using 500-ml distillation flask with 250 ml of solution at start and more acid added as needed; heated by electric cone heater; and *D*, slow steam distillation in percolator apparatus with 100 ml of solution at start and more acid added as needed; heated by spiral electric heater.

IV. PROCEDURE USED FOR OBTAINING 100-PERCENT YIELDS OF FURFURAL FROM XYLOSE

The procedure for completely converting xylose into furfural is essentially the same as that designated *C* in table 3, but with rapid distillation. By the use of the equipment illustrated in figure 1 with 12-percent hydrochloric acid saturated with sodium chloride for the distillation of xylose it was found that practically 100-percent yields of furfural were obtained. Typical results are given in table 4.

TABLE 4.—*Conversion of xylose to furfural by 12-percent hydrochloric acid saturated with sodium chloride, and recovery of furfural by rapid steam distillation*

Amount of xylose present	Number of fractions	Total distillate	Yield
		ml	*Percent*
0.0629	10	2,000	99.5
.1004	7	1,300	100.6
.1600	11	2,200	100.8
.2013	13	2,723	100.3
.2427	12	2,400	99.0
.3418	14	2,800	99.7

The xylose was weighed in the Pyrex micro-pan which was placed in the distillation flask, 1, and approximately 20 g of sodium chloride was added. The distillation flask was closed by an especially constructed head with a ground joint carrying a separatory funnel and a thermometer well, 2, which extended almost to the bottom of the flask. The flask was placed on the cone heater, and the steam inlet tube was attached to rubber tubing which connected with a needle valve attached to the top of a pressure cooker. The outlet tube of the distillation flask extended well into the condenser and was made tight by means of a ground-glass joint. The outlet of the condenser was bent at an angle to reach into the receiving flask, 3, through a two-

hole rubber stopper. In these experiments the receiving flask was the side-arm titration flask, described earlier [14], which had been previously prepared with standard potassium bromate-bromide and potassium iodide solutions, and marked for 200 ml of distillate. A scrubber trap, 4, containing Pyrex Raschig rings and water, was also attached through the rubber stopper to prevent the escape of furfural vapors from the flask. After the system was closed, 100 ml of 12-percent hydrochloric acid was added through the separatory funnel and heat was applied by the electric-cone heater. The water in the pressure cooker was previously brought, with air bleeding, to a 10-pound gage pressure per square inch (115° C), which was then maintained. As soon as the solution in the distillation flask reached a temperature of about 103° to 105° C, steam was introduced through the needle valve. Wrapping the flask with a towel helped to give a uniform rate of distillation. The level of the distilling solution was about even with the top of the heater, and fresh 12-percent hydrochloric acid was added as needed. The temperature of the solution did not vary more than 2° C and the distillation took place at about 110° C. The distillate was collected at the rate of 200 ml every 30 minutes, and as soon as one receiving flask was removed it was replaced by another one similarly prepared. The acidity of each fraction was determined by removing 1 ml of distillate, titrating it with 0.1 *N* sodium hydroxide, using phenolphthalein as indicator, replacing the portion removed and adjusting the distillate to about 1 *N* acidity. The acidity of the fractions in a distillation differed from about 1 *N* for the first to about 0.7 *N* for the last. The distillation was continued until the final fraction contained no furfural. The receiving flasks containing the distillates were closed and placed in an icebox or ice bath to attain a temperature of 0° C. In these experiments an icebox regulated for a temperature of −2° C was used, and the series of distillates collected in 1 day were allowed to stand overnight. The titrations with thiosulfate were made in the usual manner after the bromine was allowed to react with the furfural for 5 minutes.

It is convenient to make a titration of each 200-ml fraction and thereby obtain the rate of production of the furfural from xylose as well as the total amount of furfural recovered. For many routine analyses it may be desirable to collect the distillate in one fraction, and larger Erlenmeyer flasks may be used so that the distillate may be analyzed directly or by the use of aliquot portions.

As raw materials may contain pentosans and methylpentosans, aliquot portions of the distillates should be analyzed at two or three different periods of time, as suggested previously [2], to prevent an error in the furfural value when methylfurfural or hydroxymethylfurfural is present.

87595—38——6

V. REFERENCES

[1] Official and Tentative Methods of Analysis of the Association of Official Agricultural Chemists, p. 344 (1935).
[2] E. E. Hughes and S. F. Acree, Ind. Eng. Chem., Anal. Ed. **6,** 123 (1934); **9,** 318 (1937).
[3] C. Kullgren and H. Tyden, Ing. Vetenskaps Akad. Handl. **94,** 3 (1929).
[4] A. Jolles, Sitzber. Akad. Wiss. Wien, **114,** 1191 (1905).
[5] N. C. Pervier and R. A. Gortner, Ind. Eng. Chem. **15,** 1167 and 1255 (1923).
[6] O. Magistad, Ind. Eng. Chem., Anal. Ed., **5,** 253 (1933).
[7] G. M. Kline and S. F. Acree, BS J. Research **8,** 35 (1932). RP398.
[8] M. Cunningham and C. Dorée, Biochem. J. **8,** 438 (1914).
[9] W. H. Dore, J. Am. Chem. Soc. **48,** 232 (1926).
[10] W. Gierisch, Cellulosechemie **6,** 61 and 81 (1925).
[11] E. Heuser, and coworkers, Cellulosechemie **3,** 61 (1922); **4,** 15 and 85 (1923); **5,** 45 (1924).
[12] E. Unger and R. Jäger, Ber. deut. chem. Ges. **36,** 1222 (1903).
[13] S. Schmidt-Neilson and L. Hammer, Selskab, Forhandlicher, **5,** 84 (1932).
[14] E. E. Hughes and S. F. Acree, Ind. Eng. Chem., Anal. Ed., **6,** 292 (1934).

WASHINGTON, JULY 8, 1938.

U. S. DEPARTMENT OF COMMERCE NATIONAL BUREAU OF STANDARDS

RESEARCH PAPER RP1133

Part of Journal of Research of the National Bureau of Standards, Volume 21, September 1938

SURFACE TENSION OF VITREOUS ENAMEL FRITS AT AND NEAR FIRING TEMPERATURES

By William N. Harrison and Dwight G. Moore

ABSTRACT

A method is described for measuring at high temperatures the surface tension of liquids with viscosities as high as 10,000 poises. It consists in weighing the portion of the liquid supported by the meniscus adhering to a platinum cylinder, the bottom edge of which is at the level of the undisturbed surface of the liquid. The method insures a zero angle of contact and eliminates the necessity of determining the specific gravity of the sample at the temperature of test. Results were in good agreement with those obtained by the bubble-pressure method on molten sodium chloride and also on a molten "soft" ground-coat frit at a viscosity of 400 poises. The results obtained on eight typical commercial vitreous enamel frits at 850° C showed, with one exception, maximum differences of less than 10 percent. The mean value for seven of the frits was approximately 250 dynes/cm, while that for a high lead composition was about 200 dynes/cm. The surface tension in all cases increased with decreasing temperature between 925° and 775° C, the maximum increase being less than 10 percent. Mill additions had very little effect on the surface tension.

CONTENTS

	Page
I. Introduction	338
II. Method of test	338
III. Calibration of apparatus	339
1. Calibration with weights	339
2. Calibration with known liquids	339
3. Corrections applied	340
(a) Change in level of liquid	340
(b) Diameter of dish	340
(c) Oxidation of suspension chain	341
(d) Contact angle	341
IV. Tests with enamel frits	343
1. Description of frits	343
2. Measured surface tensions	343
(a) Test procedure	343
(b) Reproducibility	343
(c) Results on frits	344
3. Comparison with bubble-pressure method	344
4. Effect of mill additions	344
V. Conclusion	345
VI. References	346

I. INTRODUCTION

As the second part of an extensive investigation of the properties of vitreous enamels, a method has been developed for measuring the surface tension of highly viscous liquids against air at elevated temperatures. Measurements have been made of the surface tension at firing temperatures of eight vitreous-enamel frits chosen as representative of the field of enamels in commercial use. The consistencies of these enamels have been reported in an earlier paper [1].[1]

The results of the present work are of interest because differences in the degree to which various enamels are subject to surface irregularities have, from time to time, been attributed wholly or partly to differences in their surface tension.

II. METHOD OF TEST

Several investigations have been reported on the surface tension of molten glasses at elevated temperatures, but none on vitreous enamels. In the present investigation, the pull on a hollow vertical cylinder, touching the liquid at its lower end, was measured with a torsion balance. Following Hall [2], the lower end of the cylinder was kept at the level of the undisturbed surface of the test liquid and buoyancy effects were thereby eliminated. The surface tension is given by the relation:

$$T=\frac{Kg\alpha}{2L\cos\theta}$$

in which

T=surface tension in dynes per centimeter.
K=calibration constant for torsion balance in grams per degree of twist.
g=gravitational acceleration, 980.1 cm/sec/sec.
α=twist of torsion wire, in degrees, required to balance pull of the meniscus.
L=average of outside and inside circumference of cylinder, in centimeters, at the temperature of test.
θ=angle between cylinder wall and tangent to the meniscus curve at the point of contact with the cylinder.

The angle of contact, θ, was made equal to zero as described later, and therefore:

$$T=\frac{Kg\alpha}{2L}$$

The apparatus is shown in figure 1. The platinum–5-percent-iridium cylinder, C, which is 2.5 cm in diameter and whose walls are 0.01 cm thick, is suspended from a pulley on the torsion wire by a chain of 22-gage Alumel wire, the tare, B, nearly balancing the assembly. The tare permits the use of a sensitive torsion wire and the pulley provides a constant lever arm for different levels of the cylinder. The telescope and curved scale at the right in figure 1, in conjunction with a small mirror attached to the pulley on the torsion wire, serve to determine displacements of the bottom of the cylinder from the plane of the undisturbed liquid surface. The test liquid is contained in the

[1] Figures in brackets indicate the literature references at the end of this paper.

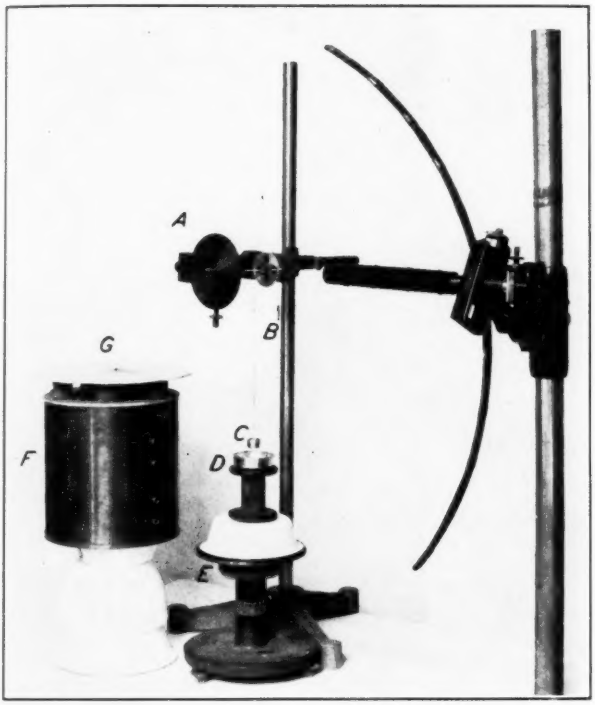

FIGURE 1.—*Surface tension apparatus with furnace displaced to left to show essential parts.*

A, torsion-wire balance; *B*, counterweight; *C*, platinum–5 percent of iridium hollow cylinder; *D*, platinum–5 percent of iridium dish; *E*, adjustable supporting stand for furnace; *F*, Nichrome-wound furnace; and *G*, asbestos radiation shield.

UNIV OF MICH

platinum–5-percent iridium dish, *D* (7.5 cm diameter by 2 cm deep) and can be raised by the adjustable stand, *E*, until contact is established with the bottom edge of the cylinder.

The furnace, *F*, displaced to the left in figure 1 from its normal position on the stand, *E*, is 8 cm inside diameter and 25 cm tall, and has a main winding and bottom heater, both of Nichrome. A thermocouple of platinum to platinum-rhodium is inserted through the furnace top and is placed, during test, just above the surface of the specimen. The asbestos shield, *G*, at the top of the furnace is supported on insulating blocks and prevents excessive rise of the temperature of the torsion balance. In practice, this temperature did not exceed 30° C.

III. CALIBRATION OF APPARATUS

1. CALIBRATION WITH WEIGHTS

The balance was calibrated by replacing the cylinder with a weight pan and establishing the conversion factor between known applied weights and the number of degrees of twist in the torsion wire required to maintain the original level of the pan. With an 0.014-inch-diameter spring-steel wire at 30° C, the calibration constant was 0.0617 g per degree of twist, and the angle of twist could be read with certainty to 0.1 degree, equivalent to a surface-tension increment of 0.38 dyne/cm.

2. CALIBRATION WITH KNOWN LIQUIDS

Table 1 shows the values of surface tension obtained with this apparatus for water, benzene, and a viscous oil (viscosity, 780 poises at 25° C), as compared with values obtained by the capillary rise method. Table 2 gives the values obtained on molten sodium chloride as compared with those of other investigators. In these tables the method used in this study is referred to as the "pull-on-cylinder" method.

TABLE 1.—*Determinations of surface tension by method used in this study, compared with determinations by capillary rise method*

Liquid	Temperature	Surface tension	
		Pull-on-cylinder method [1]	Capillary rise method [2]
	° C	*Dynes/cm*	*Dynes/cm*
Water	20	72.8	72.75
Do	21	72.5	72.59
Do	23	72.5	72.28
Do	25	71.8	71.97
Do	26	71.4	71.82
Benzene	22	29.1	28.60
Do	24	29.1	28.35
Do	26	28.6	28.09
Viscous oil	24	31.9	31.2

[1] Determinations made with 0.012-inch-diameter wire in balance, having a sensitivity of 0.2 dyne/cm. A larger wire was found necessary in the test on molten enamel frits because of the greater stresses encountered.

[2] Values for water and benzene from International Critical Tables; value for the viscous oil determined for this comparison.

TABLE 2.—*Surface tension of sodium chloride*

Investigators	Method	Surface tension	
		857° C	945° C
		Dynes/cm	*Dynes/cm*
Washburn and Libman	Dipping cylinder	115.2	107.4
Jaeger	Bubble pressure	109.9	103.6
National Bureau of Standards [1]	Pull on cylinder	109.6	103.7

[1] Values obtained from determined surface tension-temperature curve with 0.014-inch-diameter wire in balance.

3. CORRECTIONS APPLIED

(a) CHANGE IN LEVEL OF LIQUID

Small changes in the level of the surface of the specimen with respect to the cylinder after the initial contact are potential sources of error. The magnitude of such errors will be small since the cylinder walls were thin and the volume of liquid displaced or lifted through such changes in relative level is, therefore, small. The sources of such changes were evaluated as follows:

1. Lowering of the liquid level through the loss of material into the volume of liquid supported by the meniscus on the cylinder, and through thermal contraction of the molten frit when cooled for test at a lower temperature, was calculated to the required accuracy from available data on surface tension, density, and thermal expansion.

2. The sag in the torsion wire caused by pull of the meniscus was evaluated by observing, with a cathetometer, the sag caused by a series of weights.

3. The effect of dimensional changes in the apparatus during the series of tests at different temperatures was evaluated by means of the calibrated screw and an electric circuit with which the making and breaking of contact could be detected. No permanent "creep" or elongation of the Alumel wire suspending the cylinder was apparent.

The maximum change in level from all three sources was 0.5 mm (equivalent to 0.5 dyne/cm). During test, changes in level were compensated by adjustment of the calibrated screw supporting the stand.

(b) DIAMETER OF DISH

In the type of test used, appreciable error may be introduced unless the dish is large enough in diameter to provide an area of flat surface on the test liquid beyond the outside of the meniscus around the cylinder [3]. To determine experimentally whether the 7.5-cm-diameter dish was sufficiently large, a platinum strip 30 cm long by 1 cm wide was shaped into a cylinder of adjustable diameter and placed in the platinum-iridium dish so as to decrease the effective diameter of the latter. The results, as given in table 3, indicate that the 7.5-cm dish is sufficiently large to prevent significant error from this source.

TABLE 3.—*Surface tension of enamel frit 1 at 925° C, tested in dish of varying effective diameter*

Effective diameter of dish	Surface tension
Cm	*Dynes/cm*
7.5	245.0
7.5	245.7
6.0	245.7
5.0	246.1
5.0	245.7

(c) OXIDATION OF SUSPENSION CHAIN

To determine whether oxidation of the Alumel suspension chain during test would increase its weight enough to introduce significant error, the cylinder was suspended free in the furnace for 2 hours at 900° C and for an additional 1½ hours between 700° and 900° C. At the end of this period the reading of the torsion balance had not changed, indicating that any increase in weight due to oxidation was less than the sensitivity of the balance.

(d) CONTACT ANGLE

It was recognized that the determination of the surface tension of materials as viscous as enamel frits at firing temperatures requires a technique somewhat different from that required for even the most viscous of the liquids used in calibration. In the first tests with molten enamel frit, the bottom of the cylinder was not allowed to sink appreciably below the surface of the specimens at any time, but was held at the surface level by continuously increasing the torque to balance the weight of the material which slowly climbed onto the cylinder walls. Though gradual at all times, the rate of increase in weight of the meniscus was relatively rapid at first, after which it was progressively slower. Several hours were necessary with this procedure before an apparently steady condition was reached, and even after an apparent equilibrium had been attained there was no assurance of a zero angle of contact. A more rapid procedure was desirable to minimize any possible change in composition of the specimen during test, through selective volatilization. One method of hastening the establishment of equilibrium is to adjust the procedure so that the force of gravity accelerates the attainment of equilibrium instead of retarding it as with the procedure in which the cylinder was held at the surface.

This can be done by allowing the cylinder to sink and become wetted to a height equal to or exceeding the equilibrium height of the meniscus, then withdrawing it to its initial level and allowing the meniscus to drain to its equilibrium position.

Figure 2 shows graphically the results of a study of the effect of initial depth of immersion on the apparent surface tension of frit 1 at 900° C. The two lower curves show the apparent surface tension gradually increasing with time, indicating that the cylinder had not been dipped a distance as great as the normal height of the meniscus, so that at the end of the tests the molten frit was still climbing on the cylinder toward the equilibrium position. In the two upper curves the cylinder had been dipped a greater distance than the equilibrium

height of the meniscus and the decrease in apparent surface tension with time was caused by the continued draining of the liquid from the cylinder walls. The center curve indicates that a condition of equilibrium at 246.6 dynes/cm was reached within 7 minutes after the cylinder had been returned to the surface level.

In all five tests the cylinder was carefully examined after its removal from the furnace. In the tests represented by the two upper curves a film of enamel about 0.04 mm thick remained on the cylinder walls above the meniscus proper. Under these conditions there exists in effect a dipping cylinder made of the same material as the specimen, its rigidity resulting from the platinum core. This is an ideal way of securing perfect wetting, which insures a zero angle of contact. To obtain correct results, however, the weight of the film above the equilibrium height of the meniscus must be considered. It was found difficult to make corrections for this film as it was impossible

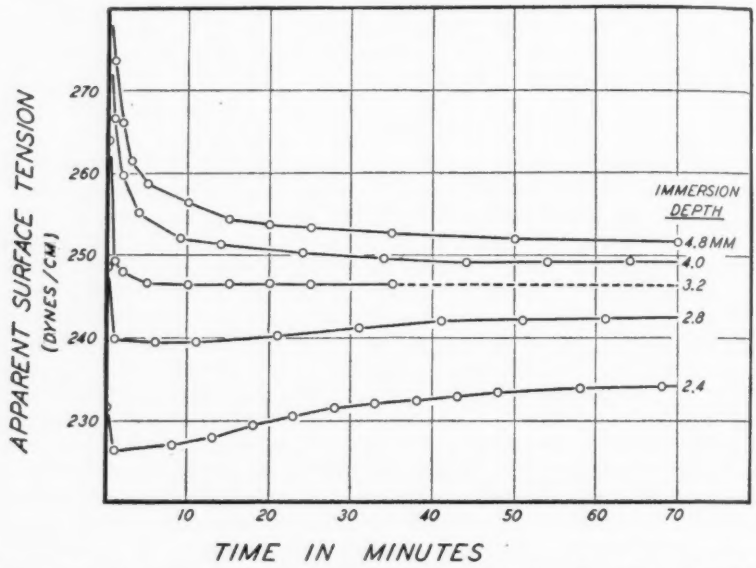

FIGURE 2.—*Apparent surface tension plotted against time for frit 1 at 900° C, showing effect of initial immersion depth of the cylinder.*

to determine accurately the point at which the meniscus merged into the vertical-walled film adhering to the cylinder above the meniscus. A condition was, therefore, sought in which the depth of immersion would be such a small amount greater than the equilibrium height of the meniscus that the weight of the vertical-walled film would be negligible, although its presence would insure the full benefits of the method. It is thought that the center curve in figure 2, representing an immersion to a depth of 3.2 mm, closely represents this condition.

In view of these tests with the soft ground-coat frit 1, it was decided to allow the cylinder to dip to a depth of 3.2 mm in each of the tests with the other frits, and to plot the results as in figure 2. If the resulting curve was of the same general shape as the center curve in figure 2, indicating that equilibrium had been reached quickly, it was concluded that the cylinder had been dipped to the desired depth.

IV. TESTS WITH ENAMEL FRITS

1. DESCRIPTION OF FRITS

The compositions and methods of selection of the eight representative commercial enamel frits used in this study have been reported in a previous paper [1]. The types represented are as follows:

Frit 1, a "soft" sheet-iron ground-coat frit, to be mixed with a harder frit before use.

Frit 11, a "hard" sheet-iron ground-coat frit, used with admixture of a softer frit.

Frit 6, an acid-resisting type of white cover-coat frit for sheet iron.

Frit 25, an "ordinary" white cover-coat frit for sheet iron.

Frit 35, a very opaque white cover-coat frit for sheet iron.

Frit 65, a leadless dry-process frit for cast iron.

Frit 72, a high-lead (40 percent of PbO) wet-process frit for cast iron.

Frit 85, a lead-bearing (10 percent of PbO) dry-process frit for a cast iron.

It is thought that this variety of types is sufficiently representative of the field of commercial enamels that the conclusions drawn from them should be generally applicable.

2. MEASURED SURFACE TENSIONS

(a) TEST PROCEDURE

In each test the furnace was heated to 925° C in 2 hours and the temperature held constant for 30 minutes before making initial contact.

Since the resistance to flow of the molten frits increases greatly with decrease in temperature, it was thought desirable to make the initial determination for each frit at the highest temperature of test (925° C), and then lower the temperature without disturbing the specimen for determinations at lower temperatures. As a check on values obtained at the lower temperatures by this method, independent determinations at 850° and 775° C were made on frit 1. The results obtained at 850° C by the two procedures were the same (247 dynes/cm), while the result after making contact at 775° C was 1.1 percent (2.7 dynes/cm) lower than when contact was made at 925° C. This was considered a satisfactory agreement.

(b) REPRODUCIBILITY

To determine the reproducibility of determinations by the described method, six determinations were made on frit 1 at 925° C. These results, given in table 4, all fell between 245.0 and 246.1 dynes/cm, the extreme variation being 0.28 percent from the average.

TABLE 4.—*Results of six determinations of the surface tension of frit 1 at 925° C*

Test	Surface Tension
	Dynes/cm
1	245.7
2	245.0
3	245.7
4	245.7
5	246.1
6	245.7
Average	245.7

(c) RESULTS ON FRITS

The determined values for surface tension of the eight frits are given in table 5. It will be noted that values for frits 11 and 6 at 775° C remain undetermined. Their viscosities at that temperature, about 36,000 and 160,000 poises, respectively, are too high to permit satisfactory surface-tension measurements by this method. Some satisfactory determinations were, however, made on specimens having viscosities (or apparent viscosities) as high as about 10,000 poises. The table shows that seven of the eight frits gave values within a narrow range around 250 dynes/cm, and the other one approximately 200 dynes/cm. The exception was the wet-process cast-iron frit 72 containing about 40 percent of lead oxide.

TABLE 5.—*Surface tensions of eight frits at three temperatures*

Enamel type	Enamel frit number	Time for equilibrium at 925° C	Surface tension at—		
			925° C	850° C	775° C
		Minutes	*Dynes/cm*	*Dynes/cm*	*Dynes/cm*
Soft ground coat [1]	1	7	246	247	249
Hard ground coat [1]	11	9	243	245	
Ordinary white [2]	25		233	240	248
Very opaque white	35	10	242	250	259
Acid-resisting white [2]	6	14	249	256	
Cast iron–leadless	65	6	248	258	270
Cast iron–high lead [4]	72	23	187	196	206
Cast iron–low lead	85	5	244	251	260

[1] The value reported for frit 1 at 925° C is the average for 6 closely agreeing determinations (see table 4), and that for frit 1 at 850° C was obtained in 2 independent determinations (see text). The values for each of the other frits comprise a single determination at each temperature.

[2] Too viscous for measurement at 775° C.

[3] Readings on frit 25 at 925° C, unlike those on other frits, increased noticeably after remaining nearly constant for 25 minutes. Values at 850° and 775° C were obtained by making initial contact at 850° C. The 925° C value was a minimum reading obtained before the apparent surface tension began increasing.

[4] First determination indicated a large increase in surface tension from 850° to 775° C. Later tests allowing 16 hours for equilibrium gave the 775° C value as listed. The stiff consistency of the enamel at low-rates of flow was responsible for the original error.

From the values given in table 5, it is apparent that at any one temperature, the surface tensions of the frits, with the exception of frit 72, vary less than 10 percent. The change in surface tension of any given enamel throughout the temperature range of 150° C is likewise less than 10 percent.

3. COMPARISON WITH BUBBLE-PRESSURE METHOD

A sample of frit 1 was kindly tested by Badger, Parmelee, and Williams [4] at 925° C by the bubble-pressure method. They reported a surface tension of 244 dynes/cm, which was only 0.7 percent lower than that obtained in this study. Frit 1 at 925° C had a viscosity of 400 poises.[1]

4. EFFECT OF MILL ADDITIONS

To determine the extent to which mill additions affect the surface tension of enamels, experiments were made on frit 1 at 925° C with additions of borax, clay, and tin oxide. The results are given in table 6, and indicate that mill additions up to 12 percent have little effect on the surface tension.

TABLE 6.—*Effect of mill additions on surface tension of frit 1*

Additions per 100 parts frit	Surface tension
Parts	*Dynes/cm*
None	246
Clay 6.0, borax 0.1	247
Tin oxide, 6.0	247
Tin oxide, 12.0	250

V. CONCLUSION

The method of determining surface tension which was used in this study is believed to be satisfactory for measurements at high temperatures on materials of viscosities up to the order of 10,000 poises. A zero angle being assured, the necessity for measuring the contact angle is eliminated. Further, because there is no buoyancy effect resulting from immersion of the cylinder in the liquid specimen, the difficulty of determining the specific gravity of the specimen at the temperature of test is avoided. Surface tension can be computed from an observed angular deflection, merely by using a conversion factor.

The enamel frits studied cover a wide range of commercial types. With one exception they differed only slightly in surface tension from a central value approximating 250 dynes/cm.

Temperature variations in the vicinity of firing temperatures affected the surface tension of the different frits to various degrees, but the maximum change was only about 10 percent for a 150° C change in temperature.

Mill additions of clay, and tin oxide up to 6 percent had almost no effect on the surface tension of a frit. Twelve percent of tin oxide caused a slight increase in surface tension.

The exceptional frit was a cover-coat used in wet-process enameling on cast iron, which contains about 40 percent of lead oxide and had a surface tension of approximately 200 dynes/cm. The ease with which this type of enamel flows out to form a smooth surface in firing is well known. A knowledge of the physical properties of this type of frit has diminished importance, however, because of the fact that such high-lead enamels are becoming obsolete. A dry-process frit containing about 10 percent of lead oxide was found to have a surface tension nearly equal to the average for frits containing no lead.

In estimating the possible importance of the observed differences in surface tension of the enamel frits, it is necessary to consider the forces of gravity and surface tension, which usually tend to produce flow in the enamel during firing, and viscosity or internal friction resisting flow.

The effect of gravity must ordinarily be negligible, since a successful enamel may be fired in any position and the resulting coating is apparently the same. Hence, the only force consistently operating against internal friction to smooth the irregular surfaces of continuous enamel coatings during the firing must be surface tension. But since variations in the surface tension of enamels with composition are small, while variations in viscosity are often very large [1], the latter factor would seem a more important source of any differences in the ease with which the several enamels flow out to form a smooth surface when fired.

It is true that a decrease in the surface tension of a cover coat, other things being equal, would increase its tendency to spread on the ground coat and hence facilitate the healing of any discontinuities which might occur during the firing process, such as from "curling" of the dried coating prior to fusion. In this respect, the low surface tension of the high-lead enamel must contribute to its recognized tendency to form a smooth surface when fired. But since ordinarily an enamel coating is well spread before fusion, whether applied by the wet or the dry process, variations in its tendency to spread on the underlying material are of restricted importance. That the effect of surface tension on spreading tendency is not the controlling factor in obtaining satisfactory coatings of enamel is indicated by the fact that frit 35, having a higher surface tension than ground-coat frits 1 and 11, and frit 25, having a lower surface tension, are both suitable for application over a ground coat made up of frits 1 and 11.

In summary, it would appear that the high surface tension of enamels under firing conditions is an important factor in overcoming their high viscosity, or internal friction, to flatten wavy surfaces, but that variations in surface tension with composition are far less effective in this respect than the accompanying changes in consistency.

VI. REFERENCES

[1] Harrison, Stephens, and Shelton, *Consistency of eight types of vitreous enamel frits at and near firing temperatures.* J. Research NBS **20,** 39 (1938) RP1063.
[2] T. P. Hall, Phil. Mag. [5] **36,** 385 (1893).
[3] N. E. Dorsey, *Measurement of surface tension.* BS Sci. Pap. **21,** 572 (1926) S540.
[4] Surface tension of various molten glasses. J. Am. Ceram. Soc. **20,** 328 (1937).

WASHINGTON, June 21, 1938.

U. S. Department of Commerce National Bureau of Standards

RESEARCH PAPER RP1134

Part of Journal of Research of the National Bureau of Standards, Volume 21, September 1938

STABILITY OF THE VISCOSE TYPE OF OZAPHANE PHOTOGRAPHIC FILM

By Arnold M. Sookne [1] and Charles G. Weber

ABSTRACT

Viscose Ozaphane, a new type of film with a base of regenerated cellulose sheeting, and having certain advantages for record use, was tested to determine its comparative stability. Its stability was compared with that of cellulose nitrate, and also with that of cellulose acetate, which is widely used for film-slides, and which has been found to be a very stable material for preserving records in libraries. The viscose type of film apparently is not suitable for permanent records, but does appear to have properties to recommend its use for reading-room copies that can be replaced when they become unserviceable. The stability was determined by measuring changes in its chemical and physical properties under accelerated aging. The changes observed were increase in acidity and copper number, and decrease in viscosity, weight, and flexibility.

CONTENTS

	Page
I. Introduction	347
II. Determination of stability by accelerated aging	348
III. Effects of accelerated aging	348
1. Loss of folding endurance	348
2. Loss of weight	349
3. Increase in acidity	350
4. Increase in copper number	350
5. Decrease in viscosity	351
IV. Summary and conclusions	352

I. INTRODUCTION

Viscose Ozaphane, a relatively new type of motion-picture film, was investigated with reference to its suitability for use as a record material. In this new type of film, a light-sensitive dye incorporated within the base performs the function of the emulsion coating on the conventional type of film now in use. The film tested had a base of transparent viscose sheeting about 0.002 inch in thickness, plasticized with glycerin to obtain greater flexibility. The new type of film is of particular interest for record purposes for several reasons. It is grainless, gives high contrast, is slow-burning, the image is not readily damaged by scratching, and the film is only one-third as thick as the films of the emulsion type. The cellulose-acetate film now used for

[1] Research Associate at the National Bureau of Standards, representing the National Research Council.

record purposes has been found in previous studies to be [2] a very stable material when properly made [3] and properly processed photographically. The purpose of this study was to determine the relative stability of this type of Ozaphane film.

II. DETERMINATION OF STABILITY BY ACCELERATED AGING

The stability of the new type of film was determined by measuring changes in its chemical and physical properties under accelerated aging. The accelerated-aging treatment used was the same as that previously employed in evaluating acetate and nitrate films, namely, that of heating in dry air at 100° C. This test had formerly been found suitable for paper.[4,5] Loss of flexibility of papers and films, measured by a folding-endurance test, is the most significant property, because the flexibility is most sensitive to changes produced by deterioration. Measurements of the loss in weight on heating were also made. Other tests consisted in determinations of the decrease in viscosity of solutions of the film, and increase in the copper number and in acidity measured as pH. To assist in interpretation of the results, data previously [6] obtained for acetate and nitrate films under comparable aging treatments are included in the graphs for purposes of comparison.

III. EFFECTS OF ACCELERATED AGING

1. LOSS OF FOLDING ENDURANCE

The Schopper folding-endurance tester, which is an instrument widely used for determining the folding endurance of paper, was used to measure the effects of aging on the flexibility of the film. Results of tests with the MIT folder indicated that it was unsatisfactory because of excessive stretch of the specimens under test; and the film was found to be too thin to be successfully tested in the Pfund tester which had been used for acetate and nitrate films. All folding tests on the Ozaphane film were made under constant atmospheric conditions of 50-percent relative humidity and 75° F, the conditioning time being 24 hours for all specimens. The standard humidity of 65 percent was not selected, because stretch of the specimens under test was troublesome at that humidity. Control and aged specimens were conditioned and tested under identical conditions, and all specimens were humidified by adsorption to avoid variations attributable to hysteresis in moisture sorption.

The effects of oven aging on the folding endurance of Ozaphane as compared to acetate- and nitrate-base films are shown graphically in figure 1. The results show a more rapid loss of flexibility under the heat test for Ozaphane than for the acetate-base film. It was, however, much more resistant than the nitrate-base film. After 30 days of oven aging, the acetate film retained approximately 67 percent of the original strength, while Ozaphane retained only 13 percent. None of the nitrate film retained any measurable folding endurance after 15 days of heating.

[2] J. Research NBS 17, 871 (1936) RP950.
[3] Misc. Pub. BS M158 (1937).
[4] BS J. Research 3, 476 (1929) RP107.
[5] Paper Trade J. 95, 28 (July 1932).
[6] J. Research NBS 17, 871 (1936) RP950.

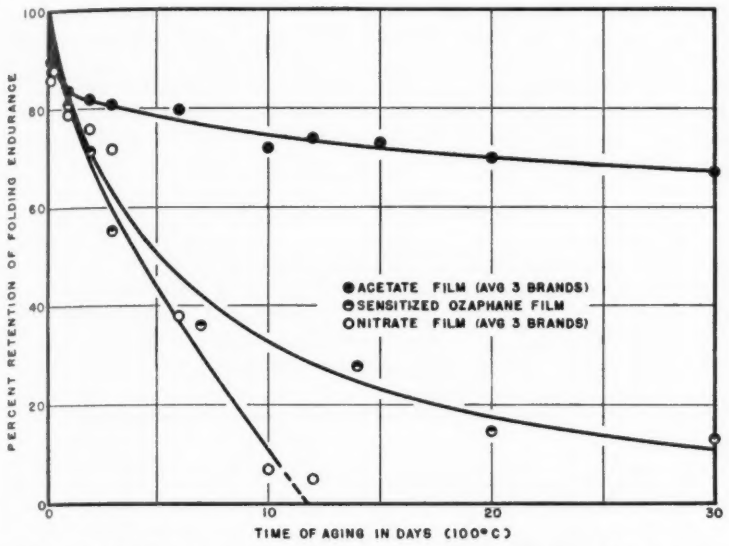

FIGURE 1.—*Effect of oven aging on flexibility of viscose Ozaphane film as compared to effects of similar treatment on acetate and nitrate film.*

2. LOSS OF WEIGHT

Oven aging caused losses in weight for all types of films. However, the Ozaphane type showed only slight losses even for extended periods of heating. Figure 2 shows loss in weight for Ozaphane, acetate, and

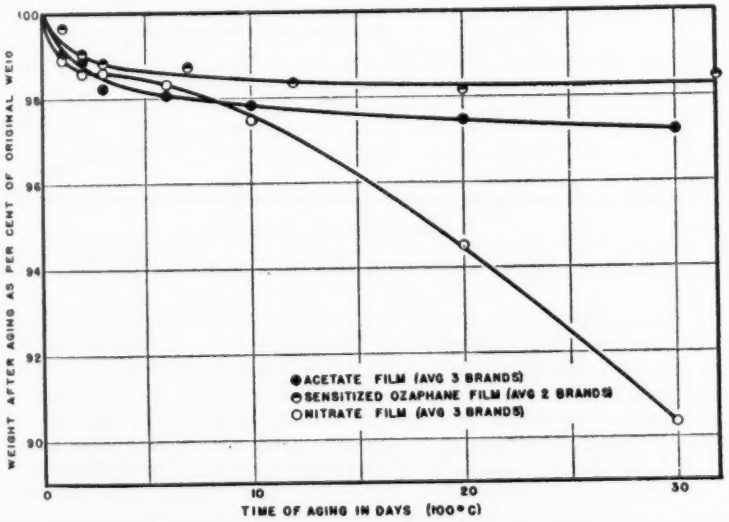

FIGURE 2.—*Loss in weight during oven-aging of viscose Ozaphane, acetate, and nitrate films.*

nitrate films. The relatively rapid initial decrease for acetate and nitrate films was probably caused by loss of residual solvents and plasticizers. On further heating, the nitrate continued to lose appreciably through escape of gaseous products of decomposition. The slight loss for Ozaphane was apparently plasticizer with possibly a little dye. All weighings were made after conditioning at 65-percent relative humidity and 70° F.

3. INCREASE IN ACIDITY

Chemical degradation of cellulosic materials is often accompanied by increased acidity. The changes in acidity of Ozaphane with aging were followed by means of pH determinations. The method used consisted in heating 1 g of the ground material in 100 ml of distilled water of pH 6.0 to 7.0 for 1 hour in a steam bath, then measuring the

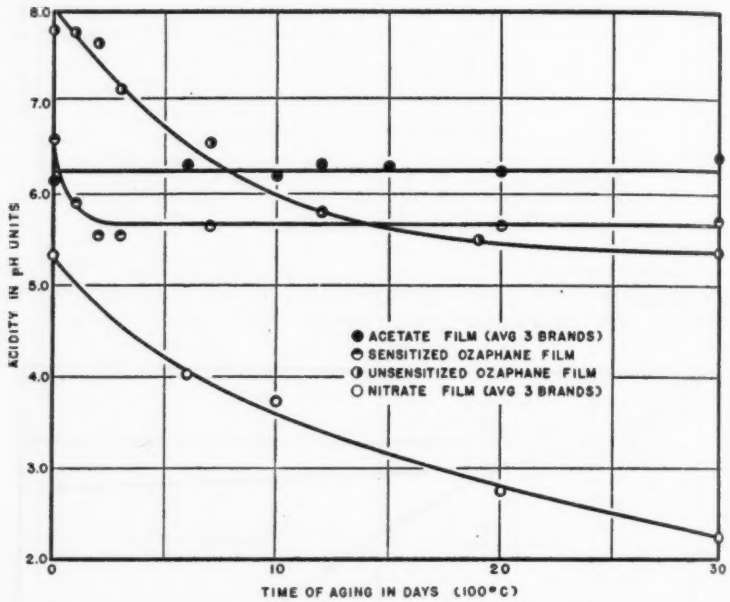

FIGURE 3.—*Effect of oven aging on acidity of record films.*

pH of the extract with a glass electrode. The results obtained on both sensitized and unsensitized Ozaphane are shown in figure 3, which also includes data on aqueous acetone solutions of acetate- and nitrate-base film for purposes of comparison. The unsensitized Ozaphane showed a gradual increase in acidity with aging; however, the pH value was 5.4, which is moderate, after 30 days. The unsensitized film was intermediate in this respect between the acetate, which showed no measurable increase in acidity, and the nitrate, the acidity of which increased markedly on aging. Sensitized Ozaphane showed little change of pH after 1 day of heating, possibly because of buffering action of the dye in the film, some of which went into solution during extraction.

4. INCREASE IN COPPER NUMBER

The copper number of cellulose is defined as the number of grams of copper reduced from the cupric to the cuprous state by 100 g of the material under defined conditions. An increase of copper number is accepted as indicative of degradation of a cellulosic material; hence, the rate of increase during accelerated aging is considered a measure of stability. Figure 4 shows the effects of accelerated aging on the copper number of unsensitized Ozaphane film and acetate-base film. The tests were made in accordance with the official method of the Technical Association of the Pulp and Paper Industry.[7] Unsensitized Ozaphane was used for the copper-number determinations to avoid errors introduced by the reducing effect of the dye in the sensitized film. Although the copper number for unaged acetate-base film is relatively high, it changes very slowly on aging, the increase

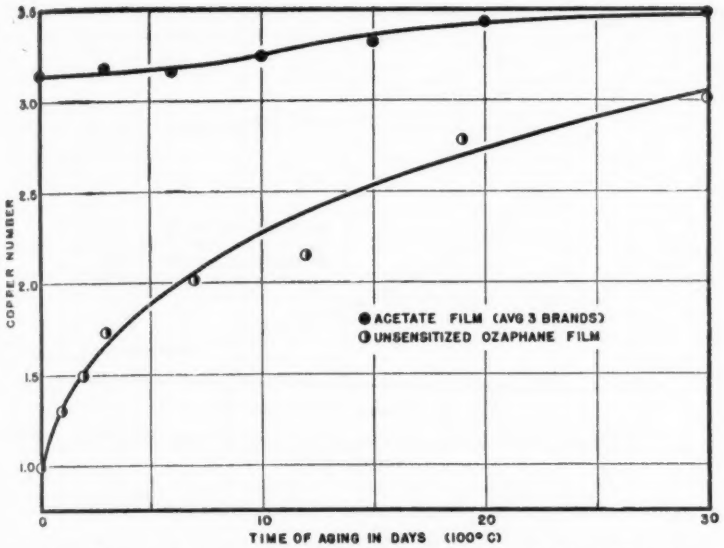

FIGURE 4.—*Change of copper number during oven aging of viscose Ozaphane, and acetate films.*

being 10 percent for 30 days' aging. The increase for Ozaphane was 200 percent for the same treatment, which indicates definitely poorer stability under oven aging.

5. DECREASE IN VISCOSITY

Data on the viscosity of solutions of cellulosic films provide the most reliable measure of their chemical degradation. According to Staudinger,[8] the specific viscosity of long-chain molecules is directly proportional to the molecular weight, for dilute solutions of equal concentration. Molecular break-down should therefore be accompanied by a proportional decrease in specific viscosity. Clibbens and Ridge [9] have shown that decreases in strength of cotton fibers

[7] TAPPI Standard T430m, Tech. Assn. of the Pulp and Paper Ind.
[8] H. Staudinger, Die Hochmolecularen Organischen Verbindungen (Berlin, 1932).
[9] J. Text. Inst. 19, 390T (1928).

produced by a variety of reagents are accompanied by corresponding decreases in the viscosities of their solutions.

The effects of accelerated aging on the viscosity of Ozaphane were determined by measuring the viscosities of solutions made before and after various aging periods. The procedure used was that recommended by the British Fabrics Research Committee [10] and described by Clibbens and Little,[11] except that the concentration of ammonia in the standard cuprammonium solvent was 240 g per liter, as recommended by Clibbens and Geake.[12] The measurements were made at $21 \pm 0.05°$ C, using solutions containing 2 g of dry Ozaphane per 100 ml of solution. Hill and Weber [13] determined the viscosities of acetate and nitrate films by using acetone solutions containing 1 g of film per

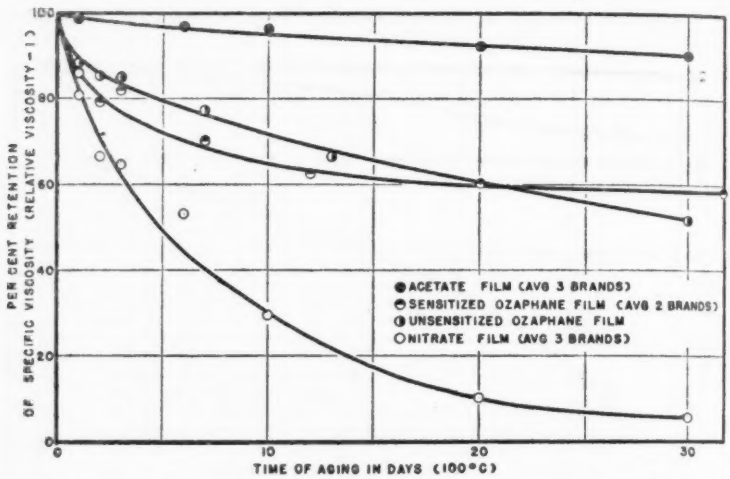

FIGURE 5.—*Effect of oven-aging on the viscosity of viscose Ozaphane, acetate, and nitrate films.*

100 ml of solution. Acetone could not be used for Ozaphane because it is not a solvent for Cellophane.

Figure 5 is a graphic comparison of the retention of viscosities of acetate, Ozaphane, and nitrate films. The acetate retained over 90 percent of its original specific viscosity after 30 days of aging, while the Ozaphane films retained less than 60 percent and the nitrate 6 percent. Here again, the Ozaphane is intermediate in chemical stability between the stable acetate-base and unstable nitrate-base films.

IV. SUMMARY AND CONCLUSIONS

The data indicate that the Ozaphane type of film having a viscose base is definitely inferior to good acetate film as regards stability under accelerated aging. It is not suitable for permanent records, but apparently it has sufficient stability for positives for reading-room use. Its stability is comparable to that of ordinary sulfite wood-fiber

[10] The Viscosity of Cellulose Solutions. Fabrics Research Comm., Dept. Sci. and Ind. Research, London (1932).
[11] J. Text. Inst. **27**, 285T (1936).
[12] J. Text. Inst. **19**, 77T (1928).
[13] J. Research NBS **17**, 871 (1936) RP950.

papers, which are known to last 25 years or longer under ordinary conditions if they are well made. Since the reading-room copies that are in use will doubtless become largely unserviceable from mechanical wear in less than 25 years, greater stability for that purpose does not appear essential. The Ozaphane type of film has certain advantages for use as positives: It is grainless, gives high contrast, is only one-third as thick as acetate, and has no emulsion to become scratched during projection and handling.

Although the viscose-base film apparently is not sufficiently stable for permanent records, it is not designed for use where the highest permanence is required. Negative films are in reality the master records, and the dyes employed at present in Ozaphane are too slow to permit its use for original photographs.

It is quite possible that the stability of the Ozaphane type of film can be improved by using for a base a sheeting having higher initial purity. It is understood that a film of this kind has recently been developed and investigation of it is planned as a further part of the work.

WASHINGTON, July 26, 1938.

U. S. DEPARTMENT OF COMMERCE NATIONAL BUREAU OF STANDARDS

RESEARCH PAPER RP1135

Part of Journal of Research of the National Bureau of Standards, Volume 21, September 1938

RELATION OF COMPOSITIONS AND HEATS OF SOLUTION OF PORTLAND CEMENT CLINKER

By Herbert Insley, Einar P. Flint, Edwin S. Newman, and J. Arthur Swenson

ABSTRACT

The results of chemical and microscopic analyses and heat-of-solution measurements on samples of commercial portland cement clinker are reported. Differences between quantitative microscopic analysis and compound composition calculated from chemical analysis have systematic relationships with chemical composition of the clinker. The heats of solution calculated from compound composition by microscopic and by chemical analysis show fair correspondence with the observed heats of solution. Assumptions on which both methods of calculation are based are shown to be somewhat faulty.

CONTENTS

	Page
I. Introduction	355
II. Materials	356
III. Methods and apparatus	356
1. Preparation of samples	356
2. Chemical analysis	357
3. Microscopic examination	357
4. Heat of solution	358
IV. Results	358
1. Quantitative determinations	358
2. Qualitative microscopic examination	359
(a) $3CaO.SiO_2$	359
(b) $2CaO.SiO_2$	360
(c) "Light interstitial" material	360
(d) "Dark interstitial" material	361
(e) Free MgO	361
(f) Free CaO	362
V. Discussion	362
VI. Summary	364
VII. References	365

I. INTRODUCTION

It has long been recognized [1] [1] that many of the properties of concrete are dependent in part on the relative proportions of the compounds which are present. Determinations of the contributions of individual compounds to the properties of cements and concretes [2, 3] have been based on the assumptions of previous investigators that the cement clinker is completely crystalline and that no more than six phases—$3CaO.SiO_2$, $2CaO.SiO_2$, $3CaO.Al_2O_3$, $4CaO.Al_2O_3.Fe_2O_3$, free CaO, and free MgO (periclase)—are present.

[1] Figures in brackets indicate the literature references at the end of this paper.

The accuracy of such methods depended in large part on the validity of these two assumptions. The recent development of a method for the microscopic examination of polished and etched specimens of portland cement clinker using reflected light [4, 5] permits ready distinction of the constituents and precise determination of the boundaries of individual crystals. The combination of this method with one for measuring the relative amounts of the different constituents makes possible a quantitative and qualitative comparison of the phases actually present in the clinker with those calculated from the chemical analyses.

It is the purpose of the present paper to make such comparisons for a series of commercial cement-clinker samples [2] and to compare the heats of solution obtained by calculation from both microscopic measurement and chemical analysis with the experimentally determined heats of solution.

II. MATERIALS

Twenty-six different samples of clinker were available for this study from five different sources. These included ten samples of "modified low-heat" (type B) clinkers representative of nine brands of cement used in dam construction by the Tennessee Valley Authority (designated by index letter T), three samples of clinker representative of "modified low-heat" cements used in the construction of the Tygart River Dam, West Virginia (designated with index letter W), and two samples of clinker representative of "low-heat" cements used in the construction of Boulder Dam (index letter B). A fourth source was a group of 50 samples of clinker obtained through the generous cooperation of Dalton G. Miller, senior drainage engineer, U. S. Department of Agriculture (index letter M). Ten samples showing wide variations in composition were chosen from this group after a study of the analyses of the corresponding cements. A single sample obtained from the manufacturer (index letter P) is listed because its Al_2O_3 and Fe_2O_3 content is low and its CaO content high.

The pure compounds used for the determination of heat of solution were obtained from several sources. Tricalcium aluminate and $4CaO.Al_2O_3.Fe_2O_3$, which were procured from William Lerch, were examined microscopically and found to be essentially homogeneous. Samples of CaO and MgO were obtained by heating the chemically pure carbonates at about 1,400° C and $\beta 2CaO.SiO_2$ was made by heating $CaCO_3$ and SiO_2 in the proper proportions together with an amount of H_3BO_3 sufficient to give 0.2 percent of B_2O_3 in the final product.

III. METHODS AND APPARATUS

1. PREPARATION OF SAMPLES

The samples of commercial clinker weighed from 1 to 2 kg. About one-third of each sample was so crushed as to avoid the production of a large amount of fine material and then sieved. The material passing a No. 4 and retained on a No. 14 sieve was used for the experiments, one portion being reserved for chemical analysis, another for microscopic examination and a third for heat-of-solution measurements.

[2] Some preliminary quantitative results on a small number of clinker samples were given in a paper by Swenson and Flint [6].

2. CHEMICAL ANALYSIS

The usual methods of quantitative analysis were used for all determinations except those of the alkalies, in which case the J. Lawrence Smith method of decomposition was followed by the determination of Na_2O by precipitation as sodium zinc uranyl acetate and of K_2O as potassium chloroplatinate. Free CaO was determined by the ammonium-acetate method [7].

3. MICROSCOPIC EXAMINATION

For examination in polished etched preparations by reflected light the crushed clinker sample was placed in a shell vial of about 1.5 cm inside diameter and immersed in Bakelite BR 0014 liquid resinoid. The preparation was evacuated in a vacuum desiccator by means of a faucet aspirator for 2 or 3 hours and then heated in an oven at about 80° C for about 15 hours. The temperature was then raised to 100° C and the heating continued about 7 hours or until the Bakelite was thoroughly hardened. After breaking the vial away, the lower surface of the preparation was ground down with No. 150 silicon carbide and water on a rotating lap until the clinker grains were exposed. Final grinding was done by hand with emery and alcohol on a slab of plate glass. The specimen was carefully washed with alcohol and polished with rouge and alcohol on a canvas-covered disk rotating at about 1,200 rpm. The polished sections were examined with a vertical illuminator [5].

A Wentworth recording micrometer [8] was used for quantitative microscopic analysis. This instrument has five micrometer screws, each one of which moves the specimen independently across the field beneath the reference cross hair in the eyepiece. The micrometer screw assigned to a particular constituent (phase) in the clinker is used for traversing grains of that constituent. The readings on the micrometer heads at the end of a complete traverse record the total linear intercepts for the different constituents. A series of traverses were made on each specimen, consecutive traverses being spaced at constant intervals. The specimens were of such a size that 11 traverses, 1 mm apart, could be made. Assuming uniform distribution of constituents of sufficiently small grain size, the ratios of the linear intercepts of the constituents are equal to the volumetric ratios of the constituents in the specimen. The average of the micrometer readings on five different preparations was taken for the analysis of each sample brand. The average deviations from the mean were less than ±2 percent for most samples. In recalculating volume percentages to weight percentages, the density values were as follows: $\beta 2CaO.SiO_2$, 3.28 [9]; $3CaO.SiO_2$, 3.13 [10]; $4CaO.Al_2O_3.Fe_2O_3$, 3.77 [10]. Because the composition of the glass phase is variable and indeterminable, a value of 3.00 for the density of $3CaO.Al_2O_3$, found by averaging two previously determined values [10, 11] was used for the total "dark interstitial" material.

The preparations were first etched with water for 2 seconds, immediately rinsed with alcohol and dried. This etching served to distinguish free MgO, free CaO, and crystalline "dark interstitial" material [12] from the rest of the clinker constituents. After quantitative microscopic analysis for these three constituents, the preparation was etched for 3 seconds in a 1-percent alcoholic solution of HNO_3 to

differentiate $2CaO.SiO_2$, $3CaO.SiO_2$, $4CaO.Al_2O_3.Fe_2O_3$, and total "dark interstitial" material.

As a part of the qualitative examination, all samples were examined petrographically mounted as powders in liquids of known refractive index. Thin sections and polished thin sections [12] were also made of a few samples.

4. HEAT OF SOLUTION

The heats of solution of the clinker samples and of the pure compounds were determined at 25° C with an isothermal calorimeter previously described [13, 14], in a solvent consisting of a mixture of 648.5 g of 2. 500 ± 0.002 *N* HNO_3 and 11.5 g of reagent quality HF (48 percent). All experimental heats of solution were calculated on an ignition-loss-free basis. The values of the heats of solution of the pure compounds which were used in the computation of the heats of solution of the clinkers as derived from chemical and microscopic analysis are given in table 1. Differences between these values and those given by Lerch and Brownmiller [15] for the same compounds may be attributed to differences in calorimeters and to volumes and concentrations of the solvents used. In calculating the heat of solution of glass, a value of 700 cal/g was used. This value represents an approximate mean of the values reported by Lerch and Brownmiller [15] for glasses with the same range in Al_2O_3/Fe_2O_3 ratios as the clinker samples in the present paper.

TABLE 1.—*Heats of solution of pure compounds*

Compound	Heat of solution	Ignition loss
	cal/g	*Percent*
$3CaO.SiO_2$	639	0.51
$\beta 2CaO.SiO_2$	572	.71
$4CaO.Al_2O_3.Fe_2O_3$	592	.14
$3CaO.Al_2O_3$	799	.17
MgO	876	(a)
CaO	848	(a)

a MgO and CaO were freshly ignited.

IV. RESULTS

1. QUANTITATIVE DETERMINATIONS

The results of chemical analysis, quantitative microscopic analysis and heat-of-solution determinations are given in table 2. In order to facilitate comparison of results, the values for corresponding constituents as found by calculation of the compound composition according to the Bogue method [16, 17] and by microscopic analysis are given in adjacent columns. The designations C_3S ($3CaO.SiO_2$) and C_2S ($2CaO.SiO_2$) are used for both calculated compound composition and microscopic analysis. The constituent designated "light interstitial" by microscopic analysis is considered equivalent to C_4AF ($4CaO.Al_2O_3.Fe_2O_3$) by calculation, and the constituent designated "total dark interstitial" by microscopic analysis is considered the nearest equivalent to C_3A ($3CaO.Al_2O_3$) by calculation. The values given in the column headed "crystalline dark interstitial" are for

TABLE 2.—*Compositions and heats of solution of commercial clinker samples*

[All quantities excepting oxide composition are calculated on an ignition-loss-free basis]

Clinker	Source [a]	Oxide composition									Free MgO (microscopic)	Free CaO		C_3S			C_2S			Light interstitial			Total dark interstitial		
		Loss on ignition	SiO_2	Fe_2O_3	Al_2O_3	CaO	SO_3	Na_2O	K_2O	MgO		Chemical	Microscopic	Calculated [b]	Microscopic	Difference	Calculated [b]	Microscopic	Difference	Calculated C_4AF [b]	Microscopic	Difference	Calculated C_3A [b]	Microscopic	Difference
		%	%	%	%	%	%	%	%	%	%	%	%	%	%		%	%		%	%		%	%	
1	*T*	0.25	22.02	4.90	4.20	63.86	0.23	0.07	0.27	4.31	2½	0.8	½	52.8	48	−5	26.3	29	3	14.9	18	3	3.0	2	−1
2	*T*	.22	21.98	5.99	5.35	64.40	.15	.04	.19	1.61	<¼	.1	<¼	49.8	46	−4	25.6	27	1	18.2	25	7	4.1	2	−2
3	*B*	.97	23.62	5.90	5.38	61.74	.07	.83	.48	0.70	<¼	0	<¼	27.3	30	3	48.1	43	−5	18.2	20	2	4.3	7	3
4	*W*	.50	20.66	6.84	6.22	62.46	.69	.29	.64	1.55	<¼	.5	<¼	41.0	38	−3	29.0	27	−2	21.0	30	9	5.1	5	0
5	*B*	.97	22.16	5.81	5.38	60.02	.07	.92	.26	4.52	3	.05	<¼	39.0	37	−2	32.9	33	0	18.0	23	5	4.3	4	0
6	*T*	.83	22.16	5.21	4.77	63.18	.25	.17	.31	3.08	1½	.4	<¼	46.7	54	7	28.9	23	−6	15.9	19	3	4.1	2½	−2
7	*T*	.36	21.03	5.01	5.08	63.14	.47	.12	.48	4.39	2½	1.0	1	48.3	52	4	24.7	22	−3	15.2	20	5	5.1	2½	−3
8	*T*	3.11	22.20	3.80	4.08	62.52	.12	.07	.42	3.73	1½	1.6	<¼	46.7	50	3	30.4	27	−3	11.9	18	6	4.7	3	−2
9	*T*	0.41	20.31	5.13	5.77	62.59	.78	.18	1.16	3.73	2½	0.5	<¼	45.2	51	6	25.7	21	−5	15.5	22	6	6.7	3½	−3
10	*T*	.12	21.40	4.90	5.50	62.30	.58	.15	0.31	4.78	2½	.1	<¼	43.9	46	2	28.4	28	0	14.9	21	6	6.5	2½	−4
11	*T*	.36	21.10	4.90	5.50	65.26	.07	.13	.46	2.27	½	.9	½	57.0	60	3	17.7	11	−7	14.9	23	8	6.5	5	−2
12	*T*	.35	23.52	4.31	4.81	63.94	.10	.17	.23	2.52	1½	.5	<¼	40.5	42	1	37.1	33	−4	13.1	20	7	5.7	3	−3
13	*T*	1.99	22.50	4.40	5.38	64.10	.06	.07	.23	1.22	<¼	.8	<¼	44.3	50	6	32.3	29	−3	13.6	18	4	7.2	3	−4
14	*W*	0.66	21.76	5.12	6.30	64.34	.32	.08	.44	0.96	<¼	.8	½	42.2	47	5	31.1	24	−7	15.6	24	8	8.3	4	−4
15	*W*	.47	22.26	5.05	6.33	63.24	.73	.11	.66	1.24	<¼	.6	1	33.5	35	1	39.0	34	−5	15.4	25	10	8.5	5	−4
16	*M*	.89	22.48	4.01	5.37	64.48	.32	.15	.56	1.75	<¼	0	<¼	48.6	51	2	28.4	23	−5	12.3	23	11	7.7	3	−5
17	*P*	.38	24.18	2.22	3.84	66.84	.03	.25	.28	2.15	<¼	.1	<¼	58.6	65	6	25.4	18	−7	6.8	12	5	6.4	5	−1
18	*M*	.14	21.28	3.90	6.94	65.12	.32	.18	.50	1.60	½	.2	<¼	47.3	51	4	25.3	17	−8	11.8	22	10	12.4	9	−3
19	*M*	.87	19.62	3.50	7.24	66.62	.59	.20	.60	0.84	<¼	.5	½	64.3	69	5	8.2	3	−5	10.7	10	−1	13.6	17	3
20	*M*	.29	21.50	3.22	6.80	66.78	.12	.10	.21	1.00	<¼	.5	<¼	55.1	57	2	20.3	17	−3	9.8	11	1	12.8	15	2
21	*M*	.15	19.74	3.11	7.89	66.48	.25	.08	.58	1.60	<¼	.8	1½	58.5	63	5	12.7	7	−6	9.5	7	−3	15.9	21	5
22	*M*	.52	22.10	1.98	5.22	65.68	.19	.30	.43	3.86	2	.9	1	56.7	67	10	20.8	11	−10	6.0	6	0	10.7	13	2
23	*M*	.11	20.48	2.93	7.85	66.48	.39	.14	.62	1.22	1	.8	1	53.0	54	1	18.7	14	−5	8.9	10	1	16.0	20	4
24	*M*	.71	22.50	1.99	5.55	62.63	.45	.34	1.08	4.72	5	.5	<¼	37.9	47	9	36.1	26	−10	6.1	7	1	12.4	15	3
25	*M*	.48	21.08	2.21	6.39	66.92	.04	.13	0.14	2.61	1	1.6	2	58.5	71	12	16.7	3	−14	6.8	5	−2	15.4	18	3
26	*M*	.27	23.10	1.97	7.35	65.44	.08	.19	.39	1.29	<¼	0.6	<¼	35.2	41	6	39.8	35	−5	6.0	6	0	16.4	18	2

[a] Index letters indicate source as follows: *T*=Tennessee Valley Authority type *B* clinker; *W*=Tygart River Valley modified "low heat" clinker; *M*=Miller's Series; *B*=Boulder Dam "low heat"; *P*=from producer.

[b] Compound composition calculated by the Bogue method from the chemical analysis.

[c] Heat of solution of glass—700 cal/g.

[d] Not determined.

[e] Heats of solution used in calculations:

Compound	
C_3A	
C_3S	
C_2S	
C_4AF	
MgO	
CaO	

[f] Microscopically determined.

lution of commercial clinker samples

calculated on an ignition-loss-free basis]

Differ-ence	C_2S			Light interstitial			Total dark interstitial			Dark interstitial		Glass (Lerch method)	Heat of solution [a]			$\frac{Al_2O_3}{Fe_2O_3}$ ratio
	Calculated [b]	Microscopic	Difference	Calculated C_4AF [b]	Microscopic	Difference	Calculated C_3A [b]	Microscopic	Difference	Crystalline [c]	Glass [c]		Observed	Calculated from microscopic analysis [a]	Calculated from compound composition [b]	
	%	%		%	%		%	%		%	%	%	cal/g	cal/g	cal/g	
−5	26.3	29	3	14.9	18	3	3.0	2	−1	½	1½	3	632	621	629	0.86
−4	25.6	27	1	18.2	25	7	4.1	2	−2	¼	2	5	625	610	620	.89
3	48.1	43	−5	18.2	20	2	4.3	7	3	4	3	(d)	603	610	598	.91
−3	29.0	27	−2	21.0	30	9	5.1	5	0	½	4½	(d)	616	625	613	.91
−2	32.9	33	0	18.0	23	5	4.3	4	0	1½	2½	5	615	618	618	.92
7	28.9	23	−6	15.9	19	3	4.1	2½	−2	½	2	7	630	619	621	.92
4	24.7	22	−3	15.2	20	5	5.1	2½	−3	¼	2½	(d)	634	624	634	1.01
3	30.4	27	−3	11.9	18	6	4.7	3	−2	½	2½	(d)	635	619	629	1.07
6	25.7	21	−5	15.5	22	6	6.7	3½	−3	1	2½	6	627	623	619	1.12
2	28.4	28	0	14.9	21	6	6.5	2½	−4	½	2	3	628	618	626	1.12
3	17.7	11	−7	14.9	23	8	6.5	5	−2	½	4½	12	643	627	634	1.12
1	37.1	33	−4	13.1	20	7	5.7	3	−3	¼	3	10	624	613	615	1.12
6	32.3	29	−3	13.6	18	4	7.2	3	−4	1½	1½	(d)	619	616	617	1.22
5	31.1	24	−7	15.6	24	8	8.3	4	−4	½	3½	(d)	626	616	622	1.23
1	39.0	34	−5	15.4	25	10	8.5	5	−4	1	4	5	613	610	613	1.25
2	28.4	23	−5	12.3	23	11	7.7	3	−5	½	2½	11	629	620	623	1.34
6	25.4	18	−7	6.8	12	5	6.4	5	−1	3	2	8	638	628	633	1.73
4	25.3	17	−8	11.8	22	10	12.4	9	−3	5	4	5	632	629	632	1.78
5	8.2	3	−5	10.7	10	−1	13.6	17	3	8	9	13	647	651	629	2.07
2	20.3	17	−3	9.8	11	1	12.8	15	2	12	3	(d)	638	643	642	2.11
5	12.7	7	−6	9.5	7	−3	15.9	21	5	11	10	(d)	646	658	651	2.53
10	20.8	11	−10	6.0	6	0	10.7	13	2	6	7	(d)	652	649	644	2.64
1	18.7	14	−5	8.9	10	1	16.0	20	4	14	6	(d)	639	656	644	2.68
9	36.1	26	−10	6.1	7	1	12.4	15	3	6	9	(d)	641	646	630	2.78
12	16.7	3	−14	6.8	5	−2	13.4	18	5	8	10	13	660	661	654	2.89
6	39.8	35	−5	6.0	6	0	16.4	18	2	14	4	(d)	631	637	619	3.73

[a] Heats of solution used in calculations:

Compound	cal/g
C_3A	799
C_3S	639
C_2S	572
C_4AF	592
MgO	876
CaO	848

[c] Microscopically determined.

material rapidly etched by H_2O and determined microscopically. The difference between that value and the value found under the heading, "total dark interstitial", is recorded in the column under "dark interstitial—glass." Determinations of glass by the heat-of-solution method [15] were made on several samples by William Lerch. These are recorded in the column designated "Glass—Lerch Method."

2. QUALITATIVE MICROSCOPIC EXAMINATION

No attempt will be made in the following record of the qualitative microscopic examinations to give detailed results on each brand of clinker, because the structural and optical variations of most of the constituents in individual samples do not at present have a recognizable relation to the chemical composition or to the heats of solution.

(a) $3CaO.SiO_2$

The samples examined show a wide range in size and perfection of outer form of the tricalcium silicate crystals. The crystals of this compound are on the average larger than those of any other compound, but the variation in size is large, not only from one lot of clinker to another, but from one piece of clinker to another. The crystals in some samples show considerable perfection of form, the individuals in polished section having straight edges and sharp angles. In other samples there is marked corrosion with rounding of angles and deep embayment of edges. A tabulation of the observations made on the whole set of samples indicates that the tricalcium silicate crystals in samples with low Al_2O_3/Fe_2O_3 ratios have greater perfection of form, whereas the crystals in samples with high Al_2O_3/Fe_2O_3 ratios are deeply corroded and embayed. The corroded crystals are generally, although not always, surrounded by a fringe of minute crystals of $2CaO.SiO_2$ (see p. 360).

The existence of zoning in $3CaO.SiO_2$, and its relation to solid solution, have been noted in a previous publication [5]. Some degree of zoning is present in all the samples studied in the present investigation, although in several cases it can be observed only under the most favorable etching conditions.[3] The most pronounced zoning was observed in tricalcium silicate crystals in samples 10, 23, and 26, whereas samples 6, 8, 11, 12, and 16 exhibited very little zoning. The zone boundaries generally parallel the crystal edges, although infrequently the boundaries appear to be curved or irregular. Rhythmic zoning is not unusual, weakly etched alternating with strongly etched zones. The degree of etching and the development of the zoning are affected considerably by the orientation of the crystals. Surfaces parallel to basal faces etch weakly and show no zoning, whereas surfaces normal to basal faces etch most strongly and show the greatest development of zoning. No close relation between the zoning of $3CaO.SiO_2$ and the composition of the clinker has yet been found.

Solid solution in $3CaO.SiO_2$ crystals is shown by other optical evidence as well as zoning. Samples which contain crystals that show strong zonal etching are also found to contain crystals with marked zonal extinction when examined petrographically. A change

[3] The most satisfactory etching conditions to produce evidence of zoning were 3 seconds at 25° C in a solution of 1 percent of HNO_3 in alcohol.

in index of refraction from interior to exterior of such crystals or from a strongly zoned to an unzoned crystal is, however, not detectable.

(b) $2CaO.SiO_2$

All dicalcium silicate in industrial clinker is believed to be of the beta form. Three types of $\beta 2CaO.SiO_2$ differing somewhat in twinning and in habit have been distinguished. These were named types I, II, and III in a previous paper [5]. Another variant has been observed in many clinker specimens in the present investigation. It is called type Ia and is distinguished from type I by the presence of discrete particles along what are apparently traces of twinning planes (figs. 1 and 2). This structure is believed to be caused, according to Tavasci's theory [4], by unmixing during cooling of a material in solid solution in $2CaO.SiO_2$.

Examples of all four types have been found in the clinker specimens studied. Type II, containing a single set of parallel twinning lamellae, occurs only in samples 4 and 15. Type III, often containing irregular cracks or veinlets but without distinctive twinning lamellae, occurs sometimes as overgrowths on crystals of types I and Ia and sometimes as individual crystals. Types I and Ia are sometimes found in the same clinker piece. Crystals of type I are more abundant than those of any other type in the majority of the samples. All of the dicalcium silicate crystals studied exhibit rounded or serrated edges with no evidence of regular external form.

In many of the specimens, crystals of $3CaO.SiO_2$ are surrounded by a fringe of minute rounded particles (figs. 3 and 4). Although these particles are generally too small to show the characteristic internal structure with the microscope, their etching behavior indicates that they are $2CaO.SiO_2$. This fringing material generally surrounds $3CaO.SiO_2$ crystals exhibiting considerable corrosion and embayment and, therefore, it has been found in this investigation in samples with the higher Al_2O_3/Fe_2O_3 ratios. The other types of $2CaO.SiO_2$ apparently bear no relation to the chemical composition of the clinker samples.

Crystals of dicalcium silicate show a wide range in size, but are in general smaller than those of the tricalcium silicate.

(c) "LIGHT INTERSTITIAL" MATERIAL

In the investigation of cement clinker by means of the reflecting microscope, two types of interstitial material have been differentiated which have been called, because of their relative reflectivity and reaction to etchants, the "light interstitial" material and the "dark interstitial" material [12]. The evidence previously gathered and supported by the results of the present investigation indicates that the light interstitial material is crystalline with optical properties like those of $4CaO.Al_2O_3.Fe_2O_3$. The light interstitial material is intimately associated with the dark interstitial in most of the clinker specimens. Not only the size of the aggregates but the size of the individual crystals appears to bear some relation to the chemical composition, those clinker samples with the lower Al_2O_3/Fe_2O_3 ratios generally containing the larger crystals of $4CaO.Al_2O_3.Fe_2O_3$. The form of the crystals is also somewhat dependent on chemical composition. When the Al_2O_3/Fe_2O_3 is low, the crystals of $4CaO.Al_2O_3.Fe_2O_3$

FIGURE 1.—$2CaO.SiO_2$ *of types* Ia *and* III *in clinker sample 17.*

Etched with 1-percent alcoholic solution of HNO_3. Reflected light. Magnification, ×1000.

FIGURE 2.—$2CaO.SiO_2$ *of types* Ia *and* III *in clinker sample 26.*

Etched with 1-percent alcoholic solution of HNO_3. Reflected light. Magnification, ×500.

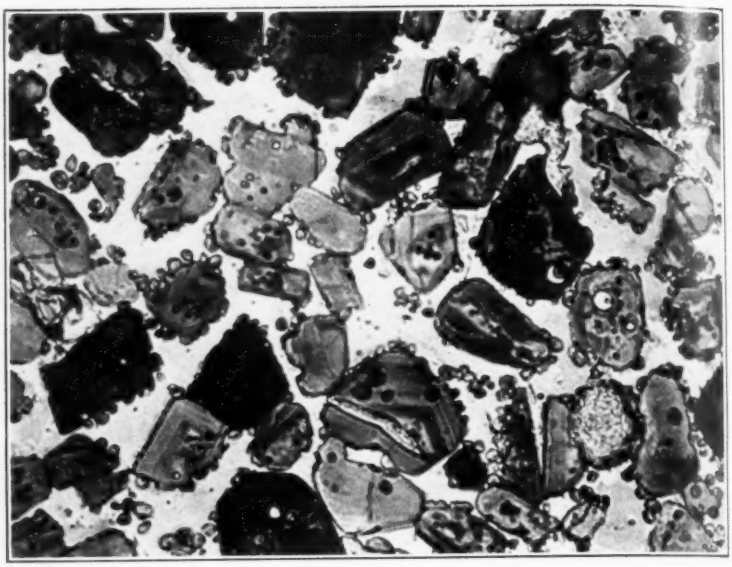

FIGURE 3.—*Corroded crystals of* $3CaO.SiO_2$ *fringed with unusually large, rounded grains of* $2CaO.SiO_2$

From clinker sample 21. Etched with 1-percent alcoholic solution of HNO_3. Reflected light. Magnification, ×500.

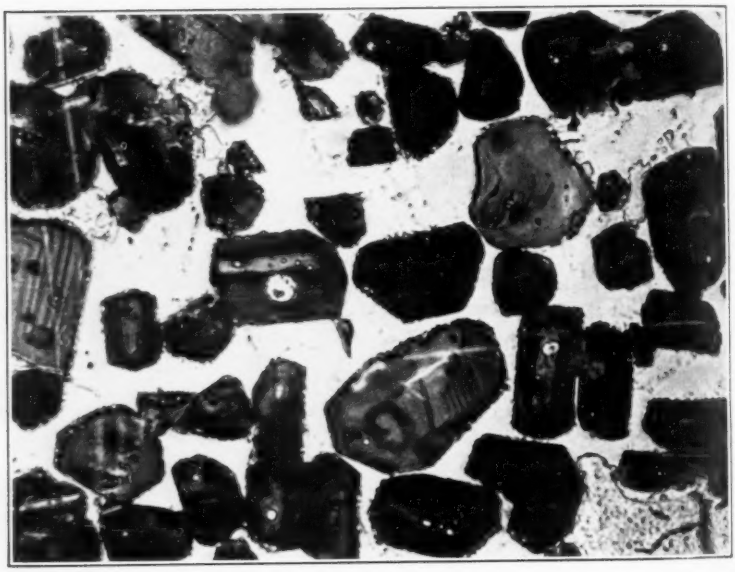

FIGURE 4.—*Corroded crystals of* $3CaO.SiO_2$ *fringed with rounded grains of* $2CaO.SiO_2$ *of normal size.*

From clinker sample 21. Etched with 1-percent alcoholic solution of HNO_3. Reflected light. Magnification, ×500.

have good prismatic development with straight edges, but when the Al_2O_3/Fe_2O_3 ratio is high the faces are poorly developed, probably because they form at a later stage of the crystallization of the clinker.

Most of the $4CaO.Al_2O_3.Fe_2O_3$ crystals found in commercial cement clinker are pleochroic, but the pleochroism varies widely from one clinker sample to another and even from one crystal to another in the same sample. This variation appears to have no relation to the chemical composition of the sample. In one sample examined (No. 4) the larger crystals were light amber in color with no perceptible pleochroism, whereas the smaller crystals in the same clinker piece were much darker and exhibited strong pleochroism.

(d) "DARK INTERSTITIAL" MATERIAL

The dark interstitial material has been classified into crystalline and glassy types. One method of distinction is the rate of reaction with water when used as an etching reagent, the former type being rapidly etched and the latter slowly etched.[4] The crystalline dark interstitial material can be subdivided into a rectangular isotropic form and a prismatic anisotropic form, whereas the glassy type has a variable index of refraction and is apparently isotropic when observed in thin section or powdered form.[5]

In the samples investigated the rectangular crystalline form, which has the optical properties of $3CaO.Al_2O_3$, is found in only two samples (20 and 21) and there in only very small amounts. The anisotropic prismatic form, which appears to be produced only in the presence of alkali [12], is a much more abundant constituent. It occurs to some extent in all the samples examined; in samples with low Al_2O_3/Fe_2O_3 ratios it is present in small amounts and in localized clusters of crystals as if it were the result of nonuniformity of the mix, whereas in other samples the prismatic crystals are distributed more uniformly.

The dark interstitial material which reacts slowly with water has been found to some extent in all the samples in this series. Although it is impossible to measure the indices of refraction of this phase accurately, those samples having low Al_2O_3/Fe_2O_3 ratios contain glass which is microscopically colorless with an index of refraction less than 1.72, whereas those with high Al_2O_3/Fe_2O_3 ratios contain glass with an index higher than 1.72 and with a green color. In all the samples the glassy phase is intimately mixed with the prismatic crystals of $4CaO.Al_2O_3.Fe_2O_3$.

(e) FREE MgO

Free MgO occurs as angular grains with the optical properties of periclase. These have been identified in polished sections of commercial clinker [12]. In the present investigation free MgO has been seen in the majority of the samples. Although the magnesia grains are small, it is observed that, in general, the greater the amount of MgO the larger the grain size of the periclase. The free MgO is associated with the interstitial material in all the samples. In most of the samples the periclase grains are more or less uniformly dis-

[4] After immersion in water for 1 to 2 seconds, the first type is etched noticeably while the second type shows no perceptible effect.

[5] Continuous homogeneous grains of this glassy form appear perfectly isotropic, although they are so small that they may actually be slightly birefringent. Therefore, it is impossible to decide whether or not the glassy phase is equivalent to the "metastable phase" of Brownmiller [18].

tributed throughout the specimens examined, but in some (notably No. 5) the grains occur in clusters. This may be the result of improper mixing of raw materials.

(f) FREE CaO

Free CaO occurs as rounded grains which are detected by etching reactions previously described [12]. In most of the samples the free CaO grains are present as clusters associated with concentrations of $3CaO.SiO_2$ crystals and, therefore, are probably the result of some lack of uniformity in the batch.

V. DISCUSSION

A comparison of direct and indirect methods of quantitative determination of the phases present in portland cement clinker shows certain systematic relations (table 2). These are most apparent when the columns headed "difference" are examined. These columns show the differences between the values for equivalent constituents as determined microscopically and chemically. It will be observed that the percentages of $2CaO.SiO_2$ determined microscopically exceed those determined chemically only for two samples with the lowest Al_2O_3/Fe_2O_3 ratios, whereas the percentages of $3CaO.SiO_2$ obtained microscopically are less than those obtained chemically only for samples with low Al_2O_3/Fe_2O_3 ratios. The microscopic values for "light interstitial" material tend to be greater than those for calculated $4CaO.Al_2O_3.Fe_2O_3$ for samples with low Al_2O_3/Fe_2O_3 ratios, but the differences are close to zero for samples with Al_2O_3/Fe_2O_3 ratios of 2.00 or greater. The reverse is true when microscopically determined total "dark interstitial" material is compared with calculated $3CaO.Al_2O_3$. The microscopic values are less than or equal to the calculated (with one exception) for low Al_2O_3/Fe_2O_3 ratios and greater than the calculated for ratios more than 2.00.

Several reasons may be given for the differences between the compositions determined microscopically and those obtained by calculation. The fact that tricalcium silicate contains other material in solid solution would tend to make the observed amount greater than that obtained by calculation by the Bogue method [16] as pure $3CaO.SiO_2$. Moreover, Lea and Parker [19] have shown from a consideration of the system $CaO\text{-}Al_2O_3\text{-}Fe_2O_3\text{-}SiO_2$ that cement clinkers with high Al_2O_3/Fe_2O_3 ratios contain greater amounts of $3CaO.SiO_2$ and lesser amounts of $2CaO.SiO_2$ when crystallization is arrested during cooling than when complete equilibrium is attained.

Because there is partial solid solution between $4CaO.Al_2O_3.Fe_2O_3$ and $3CaO.Al_2O_3$ in the system $CaO\text{-}Al_2O_3\text{-}Fe_2O_3$ [20], it seems probable that the excess of observed light interstitial material over calculated $4CaO.Al_2O_3.Fe_2O_3$ in clinker with low Al_2O_3/Fe_2O_3 ratios may be explained by the earlier crystallization of $4CaO.Al_2O_3.Fe_2O_3$ with solid solution of material approximating $3CaO.Al_2O_3$ in composition. In clinkers with high Al_2O_3/Fe_2O_3 ratios, dark interstitial material may be expected to crystallize first and to take some $4CaO.Al_2O_3.Fe_2O_3$ into solid solution. The prismatic doubly refracting constituents [12] presumably produced by alkalies are not accounted for in the Bogue method of calculation. Their presence would tend to increase the amount of dark interstitial material, but what the quantitative effect

would be on the discrepancies between calculated and microscopically determined compositions is not known.

To account for the rather large differences between the light interstitial constituent and calculated $4CaO.Al_2O_3.Fe_2O_3$ in some samples, it has been suggested that the light interstitial constituent may consist of another phase besides $4CaO.Al_2O_3.Fe_2O_3$, for instance, a highly refractive iron-bearing glass which is not distinguished from $4CaO.Al_2O_3.Fe_2O_3$ by the etching reagents used. Attempts to differentiate the light interstitial material into two phases by the use of other etching reagents and illuminating methods have thus far been unsuccessful.

In the Bogue method all the MgO is calculated as free MgO (periclase). In all but one of the samples examined the free MgO as determined by microscopic analysis is less than the total MgO by chemical analysis. Evidently a part of the MgO is dissolved in the glass or in one or more of the crystalline constituents.

The agreement between the microscopic method and the ammonium acetate method in the determination of free CaO is, in general, good. The somewhat lower results by the microscopic method for most samples are to be expected because the chemical method includes both free $Ca(OH)_2$ and free CaO, whereas the microscopic method distinguishes only crystalline CaO. The large difference for sample 8 is probably to be attributed to a partial hydrolysis of the clinker constituents, as indicated by the high ignition loss.

Although the presence of glass is evidence that commercial clinkers are not the product of crystallization under equilibrium conditions, the simultaneous occurrence of fine-grained crystalline light and dark interstitial material with glass in the same specimen indicates also that the clinkers have not been completely quenched. The commercial product may, therefore, be considered as an intermediate stage between a material quenched from a definite temperature and one crystallized at continuous equilibrium conditions.

In comparing calculated and observed heats of solution (table 2) it is evident that, in general, the heats of solution as computed from calculated compound composition agree somewhat better with the observed than do those calculated from microscopic analysis, the average difference between observed and microscopic analysis being 8.3 cal/g and between observed and calculated compound composition being 5.6 cal/g. In making the heat of solution calculations based upon the Bogue method of determining compound composition, it was assumed that:

1. The compounds calculated to be present had the compositions and the heats of solution of the pure compounds unaffected by solid solution.
2. The oxides present in minor amounts, such as alkalies, did not enter into compounds or affect the heats of solutions.
3. Perfect equilibrium crystallization took place during cooling without the formation of glass.

In making the calculation of heats of solution from microscopic analyses it was not only necessary to use the heats of solution of the pure compounds but also to use the heat of solution of $3CaO.Al_2O_3$ for all the crystalline dark interstitial material, whether rectangular or prismatic. A constant value of 700 cal/g was used for all the glass, although the composition and consequently the heat of solution of

the glass vary with the composition and rate of cooling of the clinker specimen.

All the assumptions made with respect to both types of calculation are known to be inexact, but they are felt to be the closest approximations that can be made at the present state of knowledge. Considering the errors in the basic assumptions, the degree of correspondence of either of the methods of calculations with the observed heats of solution has little significance.

The glass content by the Lerch method (table 2) is greater than the glass content by the microscopic method for all samples on which determinations were made. Because the Lerch method is essentially a heat-of-solution method it is open to some of the same errors (already pointed out by Lerch and Brownmiller [15]) that affect the calculation of heat of solution from compound compositions, namely, the assumption that the compounds present are free from solid solution and the assumption that the alkalies and other minor oxides have no effect on the heat of solution. The accuracy of the method will be increased as more knowledge is obtained on the actual composition and properties of these compounds in cement clinker.

VI. SUMMARY

The results of chemical and microscopic analysis and heat-of-solution measurements on 26 samples of commercial portland cement clinker are reported.

A comparison of compound composition by microscopic analysis and by calculation from chemical analysis shows that:

1. The content of $3CaO.SiO_2$ by microscopic analysis is greater than by calculation, except for very low Al_2O_3/Fe_2O_3 ratios.
2. The content of $2CaO.SiO_2$ is less by microscopic analysis, except for very low Al_2O_3/Fe_2O_3 ratios.
3. Microscopically determined "dark interstitial" material is less than calculated $3CaO.Al_2O_3$ for low Al_2O_3/Fe_2O_3 ratios and greater for high Al_2O_3/Fe_2O_3 ratios.
4. Microscopically determined "light interstitial" material is greater than calculated $4CaO.Al_2O_3.Fe_2O_3$ for low Al_2O_3/Fe_2O_3 ratios and approximately equal for high ratios.

Qualitative and quantitative microscopic analyses indicate that the crystalline compounds present are not pure, but contain limited amounts of material in solid solution.

Glass is present in all the samples studied.

A comparison of observed heats of solution with those calculated from chemical analysis and from microscopic analysis shows a fairly close correspondence, but it is pointed out that the assumptions on which the calculations by both methods are based are inexact.

The authors are indebted to Dalton G. Miller, senior drainage engineer, United States Department of Agriculture, for his kindness in obtaining samples of clinker from the manufacturers, to G. W. Ward, of the Portland Cement Association Fellowship at the National Bureau of Standards, for his many helpful suggestions, and especially to William Lerch, of the same organization, for generous cooperation in furnishing pure materials and in determining glass contents of many of the samples.

VII. REFERENCES

[1] P. H. Bates and A. A. Klein. Tech. Pap. BS **8** (1917) T78.
[2] Hubert Woods, H. H. Steinour and H. R. Starke. Ind. Eng. Chem. **24,** 1207 (1932).
[3] Wm. Lerch and R. H. Bogue. BS J. Research **12,** 645 (1934) RP684.
[4] B. Tavasci. Giorn. Chim. Ind. Applicata **16,** 538 (1934).
[5] H. Inlsey. J. Research NBS **17,** 353 (1936) RP917.
[6] J. A. Swenson and E. P. Flint, J. Research NBS **17,** 261 (1936) RP910.
[7] Wm. Lerch and R. H. Bogue. Ind. Eng. Chem., Anal. Ed. **2,** 296 (1930).
[8] C. K. Wentworth. J. Geol. **31,** 228 (1923).
[9] A. L. Day and E. S. Shepherd. J. Am. Chem. Soc. **28,** 1089 (1906).
[10] Wm. Lerch. Private communication.
[11] E. S. Shepherd and G. A. Rankin. Am. J. Sci. **28,** 293 (1909).
[12] H. Insley and H. F. McMurdie. J. Research NBS **20,** 173 (1938) RP1074.
[13] F. B. Hornibrook, G. L. Kalousek and C. H. Jumper. J. Research NBS **16,** 487 (1936) RP887.
[14] E. S. Newman and L. S. Wells. J. Research NBS **20,** 825 (1938) RP1107.
[15] Wm. Lerch and L. T. Brownmiller. J. Research NBS **18,** 609 (1937) RP997.
[16] R. H. Bogue. Ind. Eng. Chem., Anal. Ed. **1,** 192 (1929).
[17] L. A. Dahl, Rock Products **32,** 23, 50 (1929).
[18] L. T. Brownmiller. Am. J. Sci. **35,** 241 (1938).
[19] F. M. Lea and T. W. Parker. Bldg. Research Tech. Pap. No. 16, Dept. Sci. Ind. Research (England) (1935).
[20] H. F. McMurdie. J. Research NBS **18,** 475 (1937) RP987.

WASHINGTON, July 28, 1938.

U. S. DEPARTMENT OF COMMERCE NATIONAL BUREAU OF STANDARDS

RESEARCH PAPER RP1136

Part of Journal of Research of the National Bureau of Standards, Volume 21, September 1938

PRODUCTION OF ACCURATE ONE-SECOND TIME INTERVALS

By William D. George

ABSTRACT

This paper describes the technique wherewith a highly accurate frequency of 1 cycle per second is obtained for broadcasting from the Bureau's radio station WWV. Multivibrators are used in obtaining lower frequencies from a radio-frequency standard. Observations are given concerning the nature of short-time instabilities occurring in controlled multivibrators. The measuring technique is described whereby the accuracy between successive time intervals or cycles is checked to better than one part in a million. It is pointed out that the arrangement can be used for supplying extremely short pulses accurately spaced in time. The frequency of 1 c/s is added as a modulation on standard radio frequencies, which are broadcast each Tuesday and Friday.

CONTENTS

	Page
I. Introduction	367
II. Methods of obtaining accurate time intervals	367
III. Short-time variations in the output of controlled multivibrators	368
IV. Description of operation and results	371
V. Additional uses of apparatus	373

I. INTRODUCTION

Standard radio frequencies have been broadcast for 15 years by the National Bureau of Standards from its radio station WWV. Since April 1935 a standard audio frequency, 1000 c/s, as a modulation on the standard radio frequencies, has been included in certain of the broadcasts. To make the broadcasts still more useful, a highly accurate frequency of 1 c/s, supplied as a modulation on the standard radio frequency, is now included in certain of the broadcasts. This makes available by radio standard time intervals of 1 sec. These are not time signals, in that no attempt is made to set them in phase with standard time, but they are useful for certain work requiring an accurately known time rate. This paper is devoted to a description of the method and equipment for production of the standard time intervals.

II. METHODS OF OBTAINING ACCURATE TIME INTERVALS

The quartz-crystal oscillator, when operated under the most favorable conditions, is recognized as the most precise marker of time

87595—38——8

intervals. Pendulums and tuning forks could possibly be operated with comparable precision; however, greater difficulty would probably be experienced in doing so.

Ordinarily standard piezo oscillators operate at frequencies near 100 kc/s, and lower frequencies are obtained by means of multivibrators. Frequencies down to about 1,000 c/s are commonly so obtained.

Frequencies below 1,000 c/s are usually obtained by having a 1000-cycle synchronous motor rotate a beam of light, or rotate a generator having the desired number of poles, or operate reduction gears and contractors. With these arrangements, the primary sources of errors in the time interval between successive cycles are the hunting of the synchronous motor and mechanical imperfections. For high accuracy, ordinary mechanical contactors are unsatisfactory. Time intervals obtained from a 1000-cycle synchronous motor may differ by almost 1/2000 sec.

In the present investigation, multivibrators were constructed for stepping down in frequency from 1,000 c/s to 1 c/s in three 10-to-1 stages. The time intervals between successive pulses in the 1-cycle stage were observed to be equal within a few parts in 10^5. The variation was reduced by using separate power supplies for the 10-cycle and 1-cycle stages.

A special circuit arrangement was devised whereby time intervals of 1 sec accurate to better than one part in 10^6 were obtained. These seconds pulses were made to have a special wave shape suitable for reception on ordinary radio equipment; they were made short so as not to interfere with radio-frequency measurements which were being made on the carrier frequency. The pulses consisted of 5 cycles of a 1,000-cycle wave.

III. SHORT-TIME VARIATIONS IN THE OUTPUT OF CONTROLLED MULTIVIBRATORS

The length of successive half cycles in the output frequency of a controlled multivibrator may not be the same because of changes in any of the following parameters: filament emission, circuit constants, plate voltage, or control voltage. However, the statistical average of the output frequency, over a large number of cycles, may be the same as the controlling frequency divided by the frequency division integer. Measurements were made on a balanced multivibrator operating from 1,000 c/s to 100 c/s. The magnitude of phase shift caused by a 10-percent change in different circuit parameters is given in table 1.

TABLE 1.—*Phase shift caused by a 10-percent change in circuit parameters*

10-percent increase made in—	Phase shift	Equivalent phase shift
	Radians	*μ sec*
Filament voltage	−0.0018	−3
Circuit capacity	−.0735	−117
Circuit resistance	−.0646	−103
Plate voltage	−.0130	−21
1,000-cycle control voltage	+.0075	+12

The shifts caused by changes in circuit constants or filament voltage are of little importance because these shifts are likely to occur slowly if good condensers and resistors are used. Rapid variations in plate and control voltages are responsible for practically all random variations (from cycle to cycle) in the output. As they are in opposite directions, the effect can be largely eliminated by operating all the multivibrator equipment from the same power supply and designing the control-voltage input amplifier so that its output voltage will change a relatively large amount with changes in direct plate voltage.

Figures 1 and 2 are curves showing the results of numerous measurements on a balanced multivibrator having a controlled output

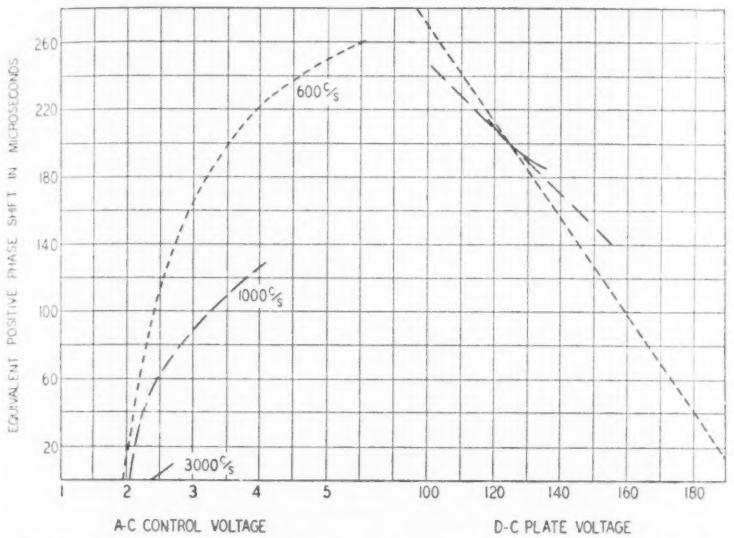

FIGURE 1.—*Experimental observations of phase shift in a balanced multivibrator having a controlled frequency of 100 cycles per second.*

frequency of 100 c/s. The variations caused by changes in plate voltage or control voltage are given for different values of plate voltage, different ratios of frequency division and different values of R/C. It is seen that some advantage was gained in operating the multivibrator at a higher plate voltage, a low R/C ratio, and a small frequency-division. However, these advantages were not very great. Where the uncontrolled frequency was lower than 100 c/s, and E_p was 75 v or greater, the phase shifts were in opposite directions for changes in control voltage and d-c plate voltage.

The phase shift was measured by comparing the output of the multivibrator with the output of a piezo oscillator having a frequency of 200 kc/s or multiples thereof, directly on a cathode-ray oscillograph screen. Advantage was taken of the sharp rise in voltage at the beginning of each half cycle of the frequency obtained from the multivibrator. Figure 3 illustrates the type of oscillograph patterns obtained. Horizontal deflection was obtained, in this case, with a standard-frequency voltage of 1000 kc/s along with the regular sweep frequency of 100 c/s. Vertical deflection was the output of the 100-

cycle multivibrator. Changing the control voltage and plate voltage on the multivibrator caused the visible 1000-kc wave to move. The phase shift was obtained by counting the number of cycles moving past a mark on the oscillograph screen and noting the direction. A movement of 1 cycle corresponded to a change in phase of 0.0006 radian, equivalent to 1 μs. By observing such patterns over a long period of time the magnitude of random variations was seen to be considerably less than one part in 10^6 in the final circuit arrangement. An attempt

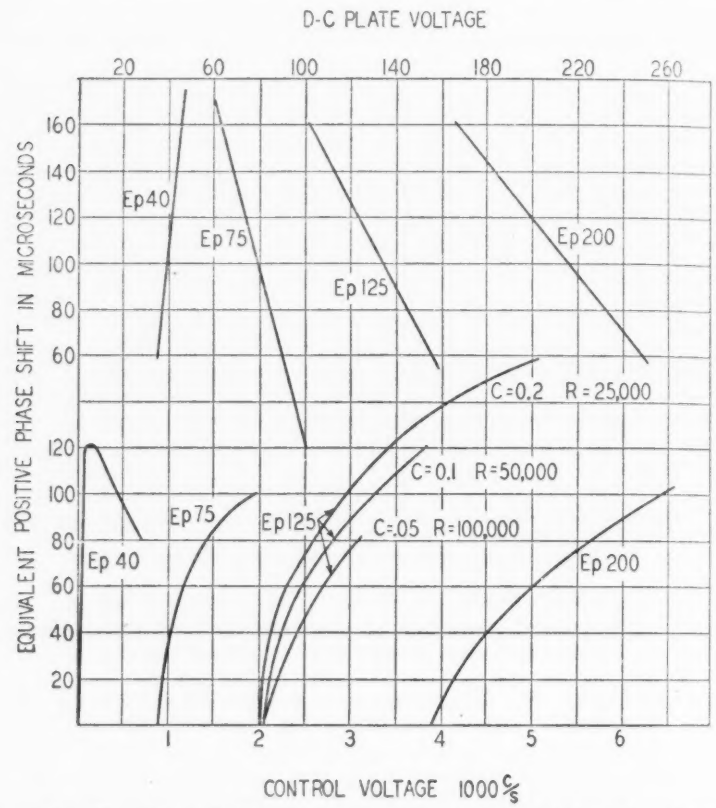

FIGURE 2.—*Experimental observations of phase shift in a balanced multivibrator having a controlled frequency of 100 cycles per second.*

was made to measure the time required for the rapid increase in voltage at the beginning of each half cycle in the multivibrator. With the circuit constants used in the 100-cycle multivibrator (see fig. 4), this rise in voltage took place in much less than 1 μs. The 3-inch cathode-ray oscillograph used was adjusted for maximum brilliancy and no trace of a line was visible at the beginning of a half cycle. In order to obtain figure 3 this rate of change in voltage was decreased by adding a resistor in series with the vertical deflection plates of the oscillograph.

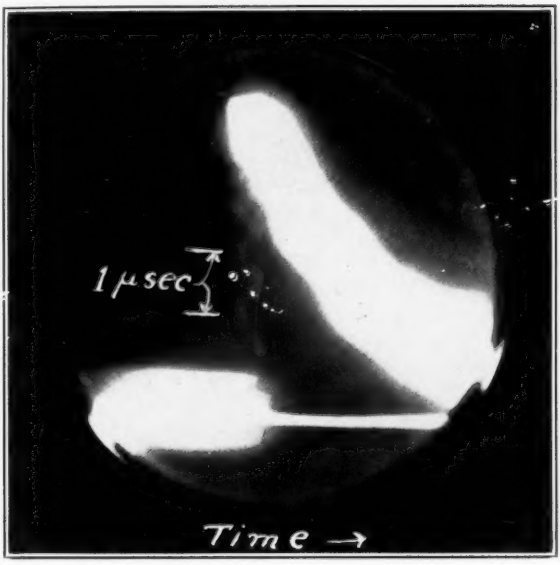

FIGURE 3.—*Oscillograph pattern for measuring phase shift.*

IV. DESCRIPTION OF OPERATION AND RESULTS

A schematic diagram of the apparatus is given in figure 4. Figure 5 shows photographs of oscillograms obtained. The approximtely rectangular wave shape in the multivibrator was amplified with two saturated amplifiers in tandem to obtain a very close approximation to a rectangular wave shape. That is, the output voltage from the fourth tube was present at nearly constant amplitude for 1/200 sec and was off for 1/200 sec. This voltage was used to apply a high bias to and cut off the first push-pull amplifier which amplified the 1,000 c/s; therefore the output of this amplifier consisted of groups of 5 cycles of the 1,000-cycle wave separated by blank spaces of 1/200 sec. A second push-pull amplifier passed this output; however, its plate voltage was applied only once per second. The voltage was applied during a 1/200 sec blank space and removed during the succeeding 1/200 sec blank space. This resulted in an output once per sec of 5 cycles of the 1,000-cycle wave.

To turn on the output amplifier once per sec several arrangements were tried, a relay operated from a multivibrator at 1 c/s, a thyratron operated from a 1-cycle multivibrator, and a synchronous motor operated from an available 300-cycle source and driving a seconds contactor. The synchronous motor arrangement proved most desirable and was used. The motor revolved 5 times per second and on its shaft was a commutator which closed for approximately 1/200 sec for each revolution; a second contactor in series with this (driven by gears), closed once per second. The commutator brush was arranged for adjustment of phase or time of turning on the output amplifier. A variation of $\pm 1/400$ sec in the closing and opening of this contactor was permissible without affecting the accuracy of the seconds pulse, because it closed and opened during the time no input voltage was on the output amplifier.

Figure 5 (a) shows the output wave shape when the groups of waves were occurring 100 times per second; the 1,000 c/s was left on continuously for a short time during this exposure to indicate distortion if present. Figure 5 (c) is the wave form after passing through the speech input equipment of the radio transmitter. Figure 5 (e) shows the pulse frequency greatly amplified and with a standard frequency of 400 kc/s applied to the horizontal deflecting plates of the oscillograph in addition to the sweep frequency. The wave forms shown in the foregoing photograph were similar in all respects, when the groups of 5 cycles were occurring once per second. Oscillograms similar to figure 5 (e) showed the time interval between pulses to be accurate to better than one part in 10^6. Figure 5 (b) is a photograph of the seconds pulses from the equipment, and figure 5 (d) the pulses from a radio receiving set. The latter are 5-minute time exposures with the oscillograph base line covered.

Since these pulses are transmitted it is important that no random phase shifts occur in the transmitting equipment which would destroy their accuracy. High-level modulation is used with transformer coupling in the audio amplifier; a shift occurs for changes in line voltage and for different settings of the attenuator on the speech input amplifier. The attenuator setting is not changed during a broadcast and is ordinarily returned to the previous point for a later broadcast. The variations in line voltage encountered at the transmitter shift the phase less than one part in 10^5.

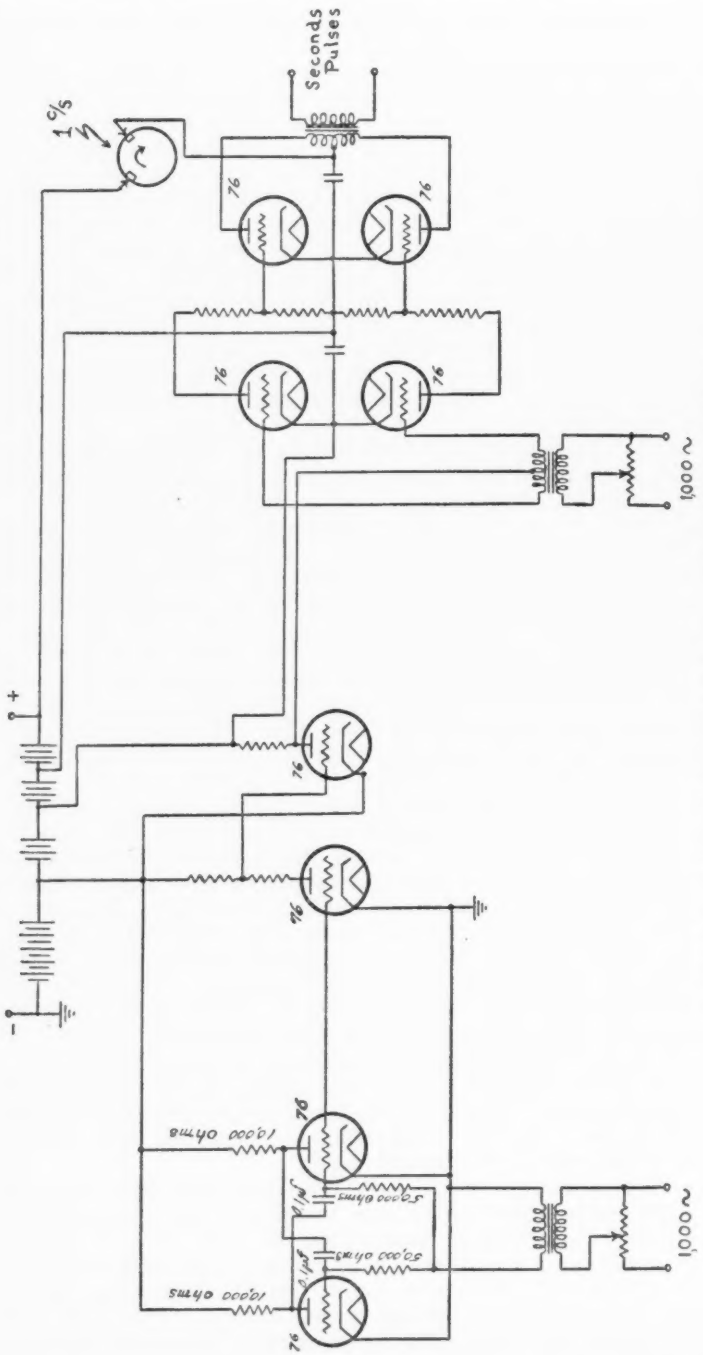

FIGURE 4.—*Schematic diagram of equipment giving seconds pulses.*

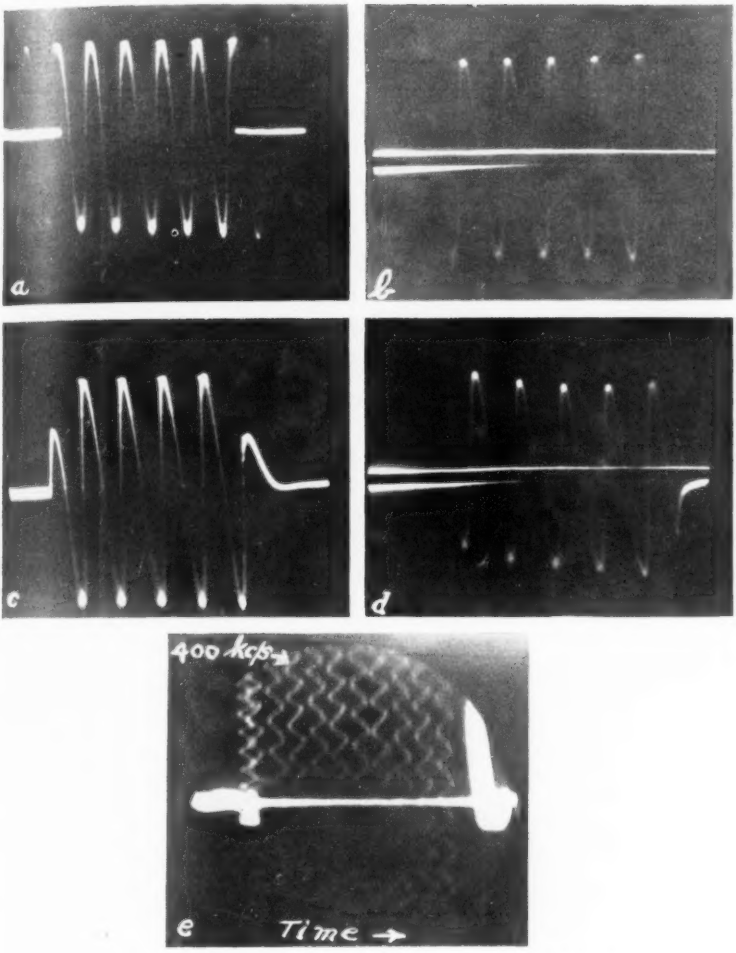

FIGURE 5.—*Wave forms from equipment for seconds pulses.*

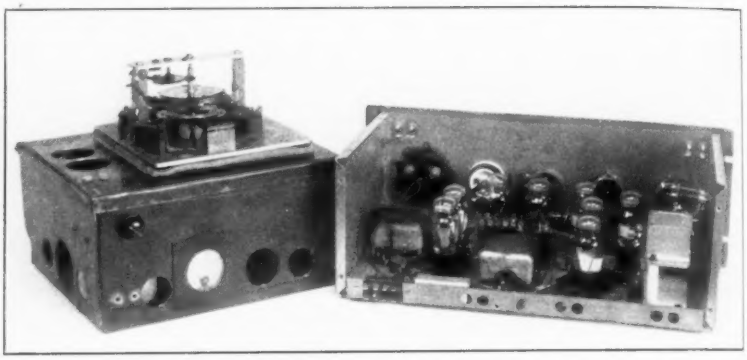

FIGURE 6.—*Equipment for seconds pulses.*

Figure 6 shows the equipment. It is supplied with 1,000 c/s and 300 c/s from other multivibrators.

V. ADDITIONAL USES OF APPARATUS

This system could be used to supply shorter pulses, for example, 5 cycles of a 1,000-kc frequency once per second or even 1 cycle of such a frequency. By using two sets of equipment it would not be difficult to adjust the output pulses to exact synchronism and thereby have a reliable source of seconds pulses over a long period of time. This would be useful in studying the long-time variations of radio-frequency standards with high accuracy. By selecting the proper division numbers for the numerous multivibrators used in such equipment, accurate time intervals of almost any length can be obtained. The method of measuring phase shift could be used with ordinary wave forms in measuring minute changes in phase caused by some changes in a circuit arrangement. A multivibrator could be controlled by the output frequency, and its output compared against a multiple frequency of the input to the device being measured.

WASHINGTON, JULY 9, 1938.

○